PROFILING THE METABOLOME IN PATHOGENIC YEASTS

VARIOUS ASPECTS OF PROFILING THE METABOLOME IN HUMAN PATHOGENIC YEASTS USING GAS CHROMATOGRAPHY-MASS SPECTROMETRY

By

ROVENA TEY, Hon. B.Sc.

A Thesis

Submitted to the School of Graduate Studies

In Partial Fulfillment of the Requirements

For the Degree

Master of Science

McMaster University

MASTER OF SCIENCE (2004) **McMaster University**
(Biology) **Hamilton, Ontario**

TITLE:	Various aspects of profiling the metabolome in human pathogenic yeasts using gas chromatography-mass spectrometry
AUTHOR:	Rovena Tey, Hon. B.Sc. (McMaster University)
SUPERVISOR:	Dr. Jianping Xu
COMMITTEE MEMBERS:	Dr. Brian McCarry Dr. Elizabeth Weretilnyk
NUMBER OF PAGES:	xvii, 156

ABSTRACT

Human pathogenic yeasts of the genus Candida and *Cryptococcus neoformans* are responsible for about 10% of hospital-acquired infections. In addition, drug-resistant yeasts are rapidly emerging with the use of anti-fungal drugs. Common drugs such as Fluconazole and Amphotericin B target the ergosterol pathway in yeast. Learning about other metabolic differences in yeasts may also give a new understanding to their role as pathogens. Metabolomics is a field of study about the large spectrum of metabolites necessary for the growth and survival of an organism. Gas chromatography-mass spectrometry (GC-MS) was used to analyze the metabolome of different yeasts in three different studies. The first study was a targeted analysis of the ergosterol pathway in *Candida albicans* and a double drug-resistant mutant was found to have several changes in its sterol composition while Fluconazole-resistant strains were similar to the wild-type. In the second study, a comprehensive analysis of the polar and lipid metabolite profiles of six pathogenic yeasts revealed that lipid profiles were more conserved than polar profiles, thereby better reflecting their taxonomical relationship according to 26S rRNA sequences. However, there were several potential species-specific metabolites and short regions in the metabolite profiles with enough peak differentiation that could be used to rapidly distinguish between these yeasts by

visual inspection. In the third study, the metabolic phenotypes of three strains of *Cryptococcus neoformans* were analysed to determine the extent of contribution of the metabolite phenotypes from two parents to their hybrid offspring. While the lipid metabolite phenotypes of all strains resembled each other, the polar metabolite phenotype of the hybrid offspring strongly resembled one parent but not the other.

ACKNOWLEDGEMENTS

I wish to express immense gratitude and thanks to my supervisor, Dr. Jianping Xu for the chance to work in his laboratory and all his guidance during my pursuit of this wonderful project for my M.Sc. studies at McMaster University. I am also very grateful for the many opportunities to attend conferences to further enrich my scientific research. Secondly, I wish to thank my committee members, Dr. Brian McCarry and Dr. Elizabeth Weretilnyk who made my project possible by allowing me to use their equipment, primarily the GC-MS. I also thank Dr. Peter Summers for helpful suggestions with the GC-MS. I am very thankful to my fiancé, David Guevara for all his advice and assistance in matters concerning the GC-MS, for the numerous times that he has simply stayed with me during all those late-working nights in the lab, for editing the drafts of this manuscript and mostly, for all his love. Getting through the writing process of this thesis would also not have been possible without all the encouragement, love and support of my family, my mom, Nayani Wijetunga, my dad, Kang Wai Tey, my brother, Jasper Tey and my dearest friend, Rakhi Mathur. I also appreciate the efforts of my mom and dad for taking care of my food and sustenance on a weekly basis for the last two months during the intense write-up of this manuscript. I would like to thank all the many members of the Xu lab, both past and present for all their help and suggestions. Finally, I would like to thank this institution, McMaster University for all my wonderful memories here in the last six and a half years during my undergraduate and graduate schooling.

TABLE OF CONTENTS

List of Abbreviations

ABC	–	ATP-binding cassette
AmB	–	Amphotericin B
CA	–	*Candida albicans*
CG	–	*Candida glabrata*
CK	–	*Candida krusei*
CN-A	–	*Cryptococcus neoformans*, serotype A
CN-D	–	*Cryptococcus neoformans*, serotype D
Conc	–	concentration
CP	–	*Candida parapsilosis*
CT	–	*Candida tropicalis*
ddH_2O	–	distilled and de-ionized water
DNA	–	deoxyribonucleic acid
EDTA	–	ethylene diamine tetraacetic acid
ESI-MS	–	electrospray ionization mass spectrometry
FAB-MS	–	fast atom bombardment mass spectrometry
FAME	–	fatty acid methyl esters
Fig.	–	Figure
FLU	–	Fluconazole
FT-IR	–	Fourier transform infrared spectroscopy
GC	–	gas chromatogram
GC-MS	–	gas chromatography-mass spectrometry
Gen.	–	generation
GLC	–	gas liquid chromatography
IR	–	infrared
ITR	–	Itraconazole
KET	–	Ketoconazole

LC-MS	–	liquid chromatography-mass spectrometry
MAT	–	mating type
MIC	–	minimum inhibitory concentration
MGA	–	MetaGeneAlyse
MSTFA	–	N-methyl-N-trimethylsilyl-trifluoroacetamide
MS	–	mass spectrum
MW	–	molecular weight
m/z	–	mass to charge ratio
NCCLS	–	National Committee for Clinical Laboratory Standards
ND	–	not detected
NIST	–	National Institute of Standards and Technology
NMR	–	nuclear magnetic resonance
NPA	–	normalized peak area
OD	–	optical density
PBS	–	phosphate buffered saline
PCR	–	polymerase chain reaction
PFGE	–	pulse field gel electrophoresis
pH	–	per Hydrogen
RE	–	restriction enzyme
rRNA	–	ribosomal ribonucleic acid
rpmi1640	–	Roswell Park Memorial Institute 1640 medium
rpm	–	revolutions per minute
RT	–	retention time
SDS	–	sodium dodecyl sulphate
sp.	–	species
TE	–	Tris-Ethylene diamine tetraacetic acid
TMS	–	trimethylsilyl
var	–	variety
YEPD	–	yeast extract peptone dextrose

List of Tables

Chapter 3

List of Figures

Chapter 2

Chapter 3

MAIN INTRODUCTION

Human pathogenic yeasts that have the greatest medical significance today are the ascomycetes of the Candida genus and the basidiomycete *Cryptococcus neoformans*. These yeasts are opportunistic pathogens that can cause life-threatening infections. They are already responsible for one-tenth of nosocomial infections and the widespread use of drugs for anti-fungal treatments are causing drug-resistant strains to rapidly emerge (Tey, R. et al., 2003). All these reasons define the significance of studying these organisms.

Metabolomics is a new field of study about the entire complement of small molecules (called metabolites) required for the growth and survival of an organism (Fiehn, O., 2001). Metabolites encompass the starting products, intermediates and end products of the complex but regulated network of biochemical and energy yielding reactions in an organism. The entire pool of cellular metabolites is known as the metabolome. The metabolome closely reflects the functional effects of genetic and physiological changes that are occurring in an organism in a given time (Oliver, S., 2002). In other words, the metabolome is the closest equivalent to an organism's phenotype. There are many ways to study metabolomics but some of the best methods are coupled to mass spectrometry. In this thesis, gas chromatography-mass spectrometry (GC-MS) was the method of choice because it is rapid as well as highly sensitive and

reproducible. There is a small spectrum of strategies that can be employed when studying metabolites in an organism (Fiehn, O., 2001) but this can be summarized to two basic approaches. One is a targeted approach and this can be restricted to the analysis of specific classes of compounds or intermediates that are part of a biochemical pathway of interest. The other is a comprehensive analysis of all the metabolites in a profile where the pattern of peaks may give rise to a characteristic fingerprint for a biological system under a given set of conditions in a given time.

In this thesis, various aspects of profiling the metabolome in human pathogenic yeasts using GC-MS were demonstrated. Altogether, there were three studies, each dedicated to a separate chapter. In the first study (Chapter 1), GC-MS was used to carry out a targeted analysis on the ergosterol pathway to study the impact of Fluconazole and Amphotericin B resistance on the fitness and sterol composition in *C. albicans*. Fluconazole and Amphotericin B are two of the most commonly used anti-fungal drugs and both target the ergosterol pathway. The second study (Chapter 2) was a comprehensive analysis of both the polar and lipid metabolite profiles of six pathogenic yeasts (*Candida albicans, C. glabrata, C. parapsilosis, C. tropicalis, C. krusei* and *Cryptococcus neoformans*) to determine if metabolomic data would reflect their taxonomical relationship. At the same time, this approach served to evaluate the usefulness of GC-MS as a tool for the identification and classification of these yeasts. In the third study (Chapter 3), the polar and lipid metabolic profiles were examined in

three strains of *C. neoformans* to determine the level of contribution from the metabolite phenotypes of haploid serotype A and D parent strains to their diploid hybrid serotype AD offspring. In doing so, this would contribute towards a better understanding of sexual reproduction in *C. neoformans*.

CHAPTER 1

A targeted analysis of the ergosterol pathway in drug-resistant *Candida albicans* using gas chromatography-mass spectrometry (GC-MS)

1.1 ABSTRACT

C. albicans is an opportunistic human pathogen and the widespread use of anti-fungal agents to treat infections are causing drug-resistant strains to continually emerge. Fluconazole and Amphotericin B are the most commonly used anti-fungal drugs and both target the ergosterol pathway. In this study, the main goal was to study the impact of drug-resistance on fitness and the sterol composition of *C. albicans*. Various drug-resistant mutants were generated experimentally, their relative fitness was assayed and their sterol compositions were examined with a targeted approach using gas chromatography-mass spectrometry. All strains were also tested for mutations in the *erg11* gene, the Fluconazole target. A previously isolated clinical *C. albicans* strain that was

Fluconazole-resistant (TW16) contained a mutation in the *erg11* gene but its sterol composition was not very different from the wild-type and its relative fitness was not compromised. Other Fluconazole-resistant strains from this study had similar fitness and sterol profiles as the TW16 strain but did not contain mutations in the region of the *erg11* gene tested. Finally, there was a Fluconazole and Amphotericin B double drug-resistant mutant of *C. albicans* (TWAF) that contained a different mutation in the *erg11* gene from the TW16 strain and had a sterol profile that was drastically altered from that of the wild-type and other Fluconazole-resistant strains. This mutant was severely reduced in relative fitness and this could be explained by the lack of ergosterol in the double mutant because it is a sterol that is absolutely essential for fungal growth. In addition, seven novel peaks were detected in this double mutant that could be aberrant fungal sterols that were compensating for the normal function of ergosterol, thus allowing this drug-resistant *C. albicans* to survive.

1.2 INTRODUCTION

1.2.1 *Candida albicans* and anti-fungal drug resistance

Candida albicans is a predominantly asexually reproducing fungus that belongs to the division of yeasts called Ascomycota. Its distribution in nature is mainly localized to reservoirs that are closely associated with warm-blooded animals. While *C. albicans* is a commensal in 18% of the healthy human population (Tey, R. et al., 2003), it is more prevalent as an opportunistic

pathogen that is the leading cause of candidiasis and infections associated with immuno-compromised or HIV-positive individuals (Coleman, D., et al., 1993). Over the last 15 years, the number of nosocomial infections caused by *C. albicans* has risen considerably on a global scale (Sobel, J., 2000; Tey, R. et al., 2003). Furthermore, with the widespread and recurrent use of various anti-fungal agents to treat infections, drug-resistant *C. albicans* are continually re-emerging at a very rapid rate and anti-fungal treatment failure is not uncommon (Munoz, P. et al., 2002; Nolte, F. et al., 1997). This poses a severe threat to public health and brings on the urgency to design even more successful patient therapies for anti-fungal infections.

1.2.2 Anti-fungal drugs

There are many drugs that are available for anti-fungal therapy. Fluconazole (FLU) and Amphotericin B (AmB) are two of the most commonly used drugs for treating *C. albicans* infections. Both drugs target the ergosterol biosynthesis pathway in *C. albicans*, although at different sites (Fig 1.1). The ergosterol pathway serves as an excellent drug target because ergosterol is absent in humans, yet it is essential for the survival of *C. albicans*. In yeasts, ergosterol ensures the integrity of the cell membrane by maintaining fluidity (Mishra, P. et al., 1992).

Fluconazole (Fig. 1.2 A) belongs to the family of drugs known as the azoles that all target the enzyme 14α-lanosterol demethylase (encoded by the *erg11* gene, formerly known as the *erg16* gene) to inhibit the production of ergosterol

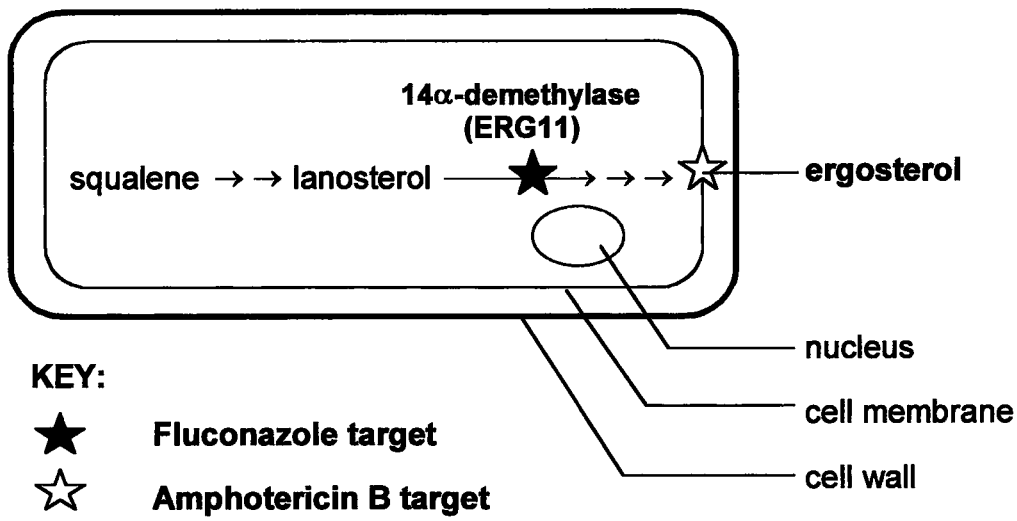

Fig 1.1 An illustration of a typical yeast cell showing the targets for Fluconazole and Amphotericin B. Fluconazole targets the *erg11* gene product, which is the 14α-demethylase enzyme to inhibit ergosterol production. Amphotericin B binds to ergosterol itself and alters membrane permeability.

A

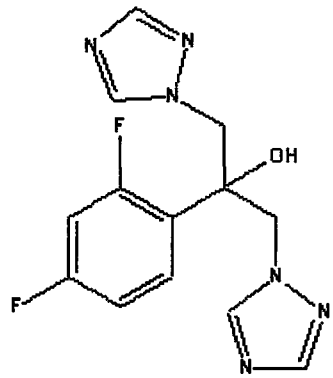

FLUCONAZOLE

B

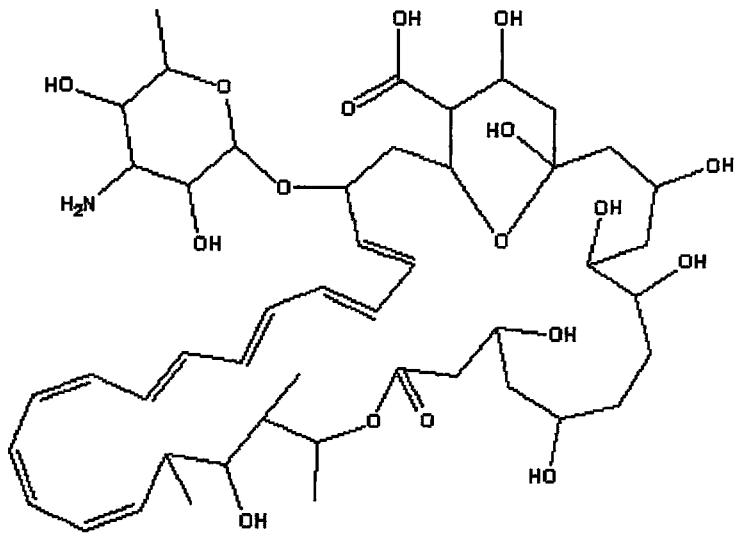

AMPHOTERICIN B

Fig 1.2 The structures of two of the most common anti-fungal drugs used to treat *C. albicans* infections are (A) Fluconazole and (B) Amphotericin B.

and retard fungal growth (Georgopapadakou and Walsh, 1996). This enzyme normally catalyzes a reaction that removes a methyl group on the 14^{th} carbon of lanosterol and converts it to 4,4-dimethylcholesta-8,14,24-trien-3β-ol (Figs. 1.4 and 1.5). Fluconazole is a fungistatic drug, in that it only inhibits growth and therefore does not kill the fungal cell.

Amphotericin B (Fig. 1.2 B) is a broad-spectrum fungicide that belongs to a group of drugs called the polyenes. Its amphipathic nature allows this drug to intercalate membrane phospholipids and bind to ergosterol, resulting in the disruption of membrane potentials. The increase in membrane permeability promotes the leakage of electrolytes from the cytoplasm, eventually resulting in cell death (Brajtburg, J. et al., 1990; Georgopapadakou and Walsh, 1996). A less common alternative mechanism of action for Amphotericin B is its ability to induce oxidative damage to the cell (Sokol-Anderson, M. et al., 1986).

1.2.3 Interactions between Fluconazole and Amphotericin B in *C. albicans*

With the rise in incidence of clinical failure to anti-fungal drug mono-therapy, the next obvious approach is to try combination therapy with more than one drug. However, before such therapy can be approved for use, it has to be thoroughly tested first and the interactions between different drugs must be well understood.

There are two possible ways that one drug may interact with another: antagonistically or synergistically. If two drugs are antagonistic, one drug hinders the action of the other and vice-versa, thus allowing cells to survive at a higher concentration in the presence of both drugs than when each drug is present

alone. In a therapeutic perspective, this means that each drug reduces the efficacy of the other drug when they are administered together. In the opposite scenario, two drugs could be synergistic or have an additive effect when it comes to cell inhibition or cell killing. Then cells would be more susceptible when both drugs are present together rather than when each drug is by itself. In this case, when both drugs are administered simultaneously, each drug enhances the action of the other and improves the treatment. Aside from antagonistic and synergistic interactions, the only remaining possibility is for there to be no interaction between two drugs.

The interactions between Fluconazole and Amphotericin B are seemingly complex in *C. albicans*. The majority of studies suggest that Fluconazole and Amphotericin B are antagonistic drugs in *C. albicans* (Lewis, R. et al., 1998; Louie, A. et al., 2001; Vazquez, J. et al., 1998). However, other studies on the same species have demonstrated that Fluconazole and Amphotericin B lack antagonism (Scheven and Schwegler, 1995) and may even act in synergy instead (Sugar, A. et al., 1995). At this point, this issue still remains unresolved with respect to *C. albicans*.

1.2.4 Fluconazole resistance mechanisms in *C. albicans*

Fluconazole-resistant *C. albicans* are most commonly isolated from the oral cavities of patients and HIV-positive individuals (Tey, R. et al., 2003). There are many known FLU-resistant mechanisms in *C. albicans* that range from the overexpression of efflux pumps to mutations in genes involved in ergosterol

biosynthesis. The efflux pumps that rid the fungal cell of Fluconazole come in the form of ABC (ATP-binding cassette) transporter proteins such as CDR1 (Albertson, G. et al., 1996, Sanglard, D. et al., 1995; White, T., 1997a) and CDR2 (Sanglard, D. et al., 1997) and a major facilitator, MDR1 (Albertson, G. et al., 1996; Sanglard, D. et al. 1995; White, T., 1997a). The most common genetic alteration associated with FLU-resistance in *C. albicans* occurs in the primary target of Fluconazole itself encoded by the *erg11* (formerly *erg16*) gene. Several clinical isolates that exhibit FLU-resistance have been found to contain a variety of point mutations in the *erg11* gene (Loeffler, J. et al., 1997; White, T., 1997b). Point mutations in the *erg11* gene have also been detected in laboratory-generated azole-resistant strains (Lamb, D. et al., 1997). In addition, there have been reports of FLU-resistant *C. albicans* with mutations in other *erg* genes. The *erg3* gene encodes Δ-^{5,6}-desaturase and acts towards the end of the ergosterol pathway. It normally converts episterol to ergosta-5,7,24(28)-trienol by introducing a double bond at the 5th carbon in the B ring (Figs. 1.4 and 1.5). Mutations in *erg3* in *C. albicans* cause the accumulation of ergostaenol and ergostadienol derivatives that do not lead to synthesis of ergosterol (Kelly, S. et al., 1997). Clinical strains that have been isolated with defects in the *erg3* gene are cross-resistant to both Fluconazole and Amphotericin B (Kelly, S. et al., 1997; Nolte, F. et al., 1997).

1.2.5 Amphotericin B resistance mechanisms in *C. albicans*

Amphotericin B-resistant *C. albicans* are almost exclusively isolated from patients with bloodstream infections (Tey, R. et al., 2003). Resistance to Amphotericin B is primarily associated with structural changes in the cell membrane. In *C. albicans*, the predominant mechanism of AmB-resistance is the structural alteration of ergosterol (Georgopapadakou and Walsh, 1996). Alternatively, there could be a reduction in the number of ergosterol molecules available for binding the drug in AmB-resistant *C. albicans* (Georgopapadakou and Walsh, 1996). Both these mechanisms reduce or prevent Amphotericin B binding to the ergosterol target. The composition of membrane phospholipids and other sterols may also vary in resistant strains (Neely and Ghannoum, 2000). There is also evidence for many Candida species including *C. albicans* that drug-sensitive strains pre-exposed to Fluconazole can become more tolerant to Amphotericin B when consecutively exposed to Amphotericin B (Vazquez, J. et al., 1998).

1.2.6 Yeast sterols and the ergosterol pathway

The majority of anti-fungal drugs on the market have been designed to target sterols, mainly because they are key components of the yeast cell membrane and therefore important for growth-dependent functions. Sterols are large molecules that constitute a tetracyclic carbon ring system (Fig. 1.3) with three 6-membered rings (designated A, B, C) and one 5-membered ring (designated D) fused together. Usually, there is a hydroxyl group at the 3rd

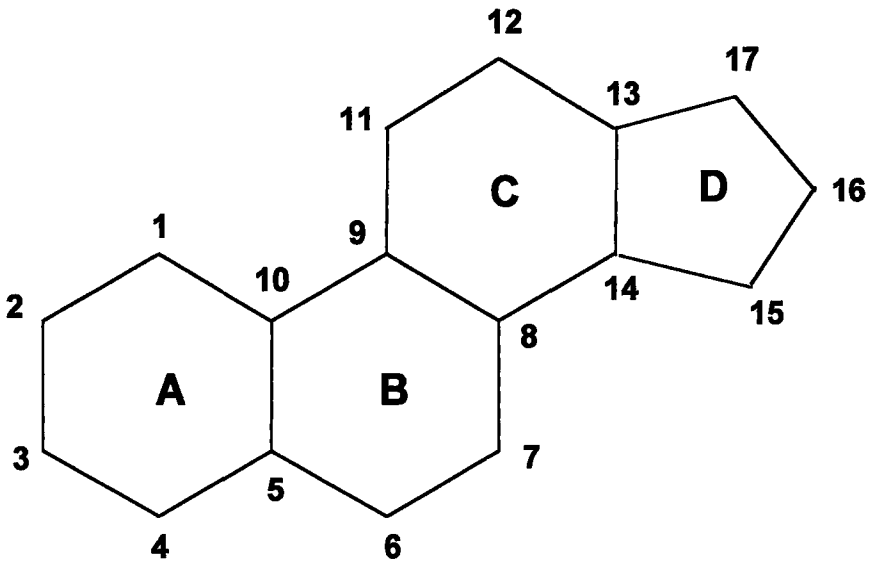

Fig. 1.3 The general molecular structure of a sterol is a tetracyclic ring system that consists of three 6-membered rings (A, B, C) and one 5-membered ring (D). Carbon atoms in a sterol molecule are conventionally numbered as shown.

carbon position and methyl groups at the 10^{th} and 13^{th} carbons of the tetracyclic skeleton. Sterols belong to the class of lipids known as the neutral lipids. Yeast sterols can be in free form or as esters with fatty acids, where sterol-esters make up a higher proportion of the total sterol composition (Mishra and Prasad, 1990). Free sterols tend to have an active role in membrane functions while sterol-esters are a form whereby excess sterols can be stored. Intermediates in sterol biosynthetic pathways also predominate as sterol-esters.

It has been reported that total sterols (sterol-esters plus free sterols) in *C. albicans* make up about 1.5% of its fresh weight (Mishra, P. et al., 1992). Ergosterol is the major sterol in ascomycetes and basidiomycetes. It is analogous to cholesterol in animals and sitosterol, stigmasterol and campesterol in plants (Hartmann, M., 1998). It has a function in maintaining fluidity and permeability in the cell membrane, along with other developmental and growth-related functions. In all living organisms, sterols are derived from acetyl-CoA building blocks and share the same biosynthesis pathway until squalene (Fig. 1.4). This pathway differentiates post-squalene where in fungi it leads to the synthesis of ergosterol (Fig. 1.5).

Due to its implication in anti-fungal drug resistance, yeast sterols are very useful to study. Some recent techniques that have been employed to study yeast sterols include a spectrophotometric method developed by Arthington-Skaggs et al. (1999), liquid chromatography-mass spectrometry (LC-MS) (Heimark, L. et al., 2002) and gas chromatography-mass spectrometry (GC-MS)

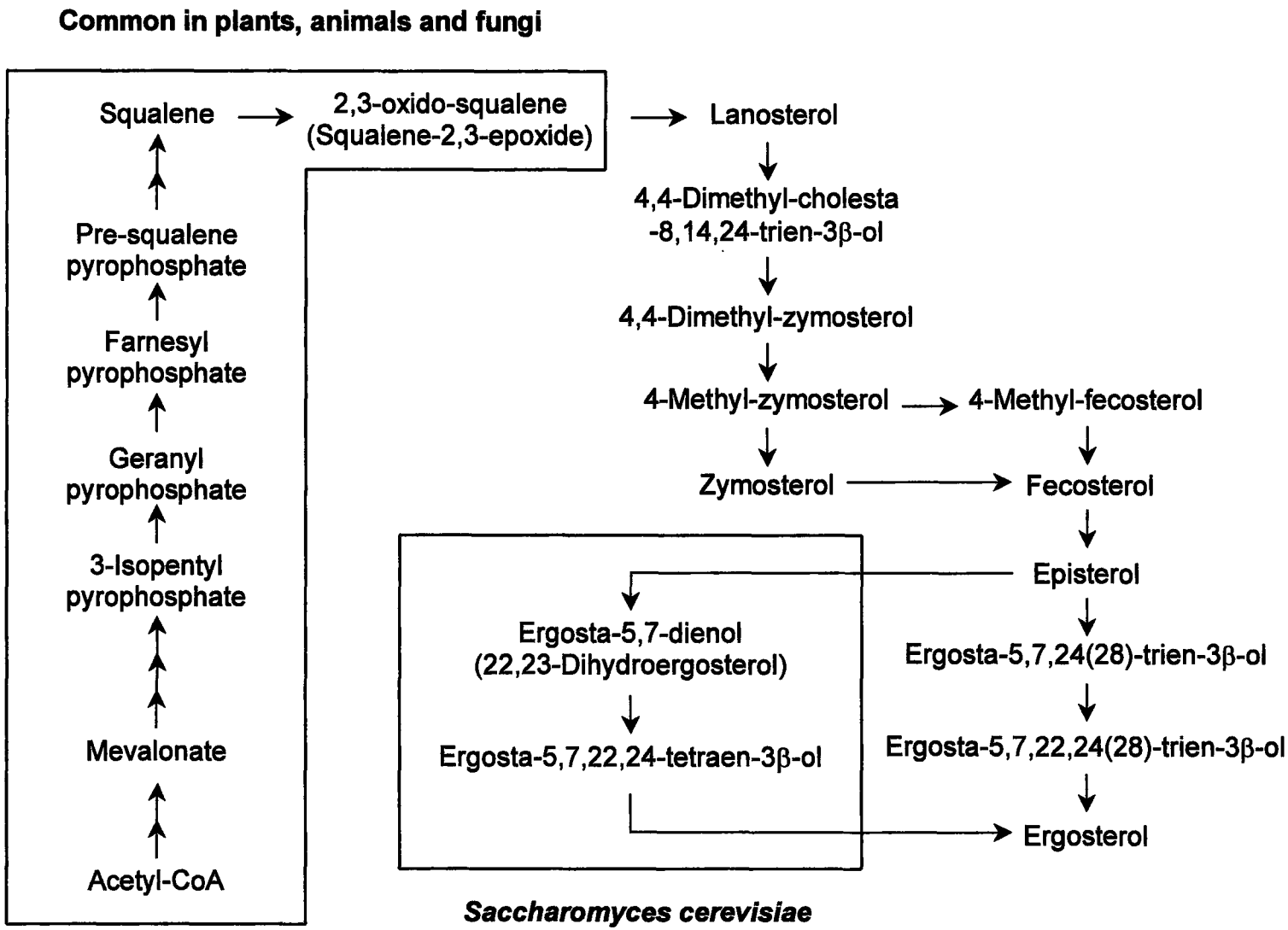

Fig. 1.4 The complete ergosterol biosynthesis pathway starting from acetyl-CoA (Ratledge and Evans, 1989)

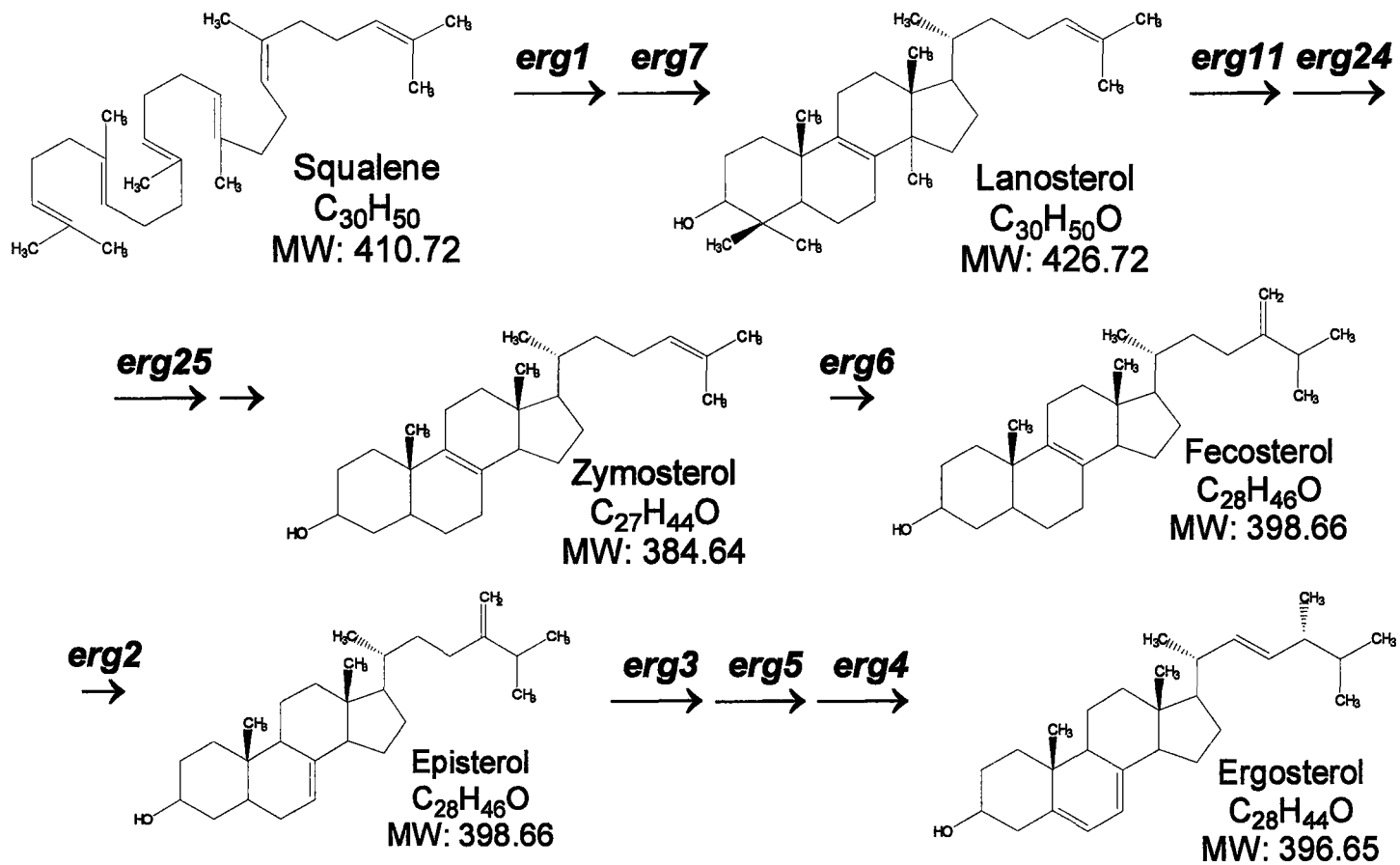

Fig 1.5 The ergosterol biosynthesis pathway post-squalene is where changes are most likely to occur in drug-resistant *C. albicans* because it contains various anti-fungal drug targets. (Units for MW or molecular weight are in g/mol)

(Le Fur, Y. et al., 1999, Howell, S. et al., 1990; Sanglard, D et al., 2003). Although, absorbance spectrometry is a quick and easy approach, it was only designed to quantify ergosterol (Arthington-Skaggs, B. et al., 1999) and as a result, would not be very helpful to study other yeast sterols. LC-MS and GC-MS are better methods to use because in a single run, they can provide a more comprehensive output on the quantity and composition of sterols, along with many other yeast metabolites that may be detected. Gas chromatography coupled to electron-impact quadrupole mass spectrometry has been reported as a rapid, comprehensive yet highly sensitive and reproducible approach to study the impact of metabolism as a result of genetic or environmental perturbations (Weckwerth, W., 2003).

1.2.7 Analysis of yeast sterols using gas chromatography-mass spectrometry (GC-MS)

Much of the previous work done on yeast sterols has been in the baker's yeast, *Saccharomyces cerevisiae* in efforts to enhance its performance in the food and brewery industries. Not as much attention has been focused on sterol metabolism in *C. albicans*, particularly with respect to drug-resistance and using GC-MS. There were only two studies that were relevant (Howell, S. et al., 1990; Sanglard, D et al., 2003). When Howell et al. (1990) examined the sterol composition of a group five sensitive and three azole-resistant *C. albicans* clinical strains by GC-MS, it was found that most of the strains, including the azole-resistant ones were not different from the wild-type. There was one unusual

exception where a sensitive strain contained ergosterol but was lacking most of the other sterols in the ergosterol pathway that were detected in the wild-type (Howell, S. et al., 1990). The second study was published late last year, on drug-resistant mutants of *C. albicans* that were constructed by targeted mutagenesis of the *erg3* and *erg11* genes (Sanglard, D. et al., 2003). One FLU-resistant and three cross-resistant mutants to AmB + FLU were constructed and their sterol composition was different from each other and the wild-type. All drug-resistant mutants from that study lacked zymosterol and ergosterol (Sanglard, D. et al., 2003).

1.2.8 Objectives of this study

In this study, the main goal was to study the impact of drug-resistance on fitness and the sterol composition of *C. albicans*. To address this issue, the first objective was to generate FLU or AmB-resistant mutant strains of *C. albicans* by experimental evolution of a wild-type progenitor strain. Secondly, these drug-resistant mutants would be tested to identify any mutations in the *erg11* gene, the azole target. The third objective was to determine if anti-fungal resistance was associated with a fitness cost to the organism. Finally, drug-resistant mutants would be examined by a targeted analysis of the ergosterol pathway using gas chromatography-mass spectrometry (GC-MS) to identify any differences in sterol metabolism. The findings of this study should also allow for a better understanding of the implication of changes in the ergosterol pathway on the normal growth and survival of *C. albicans*.

1.3 MATERIALS AND METHODS

1.3.1 Chemicals, reagents, culture media and enzymes

All chemicals were purchased from Sigma (Oakville, ON, Canada), BDH (Toronto, ON, Canada) and Fisher Scientific (Whitby, ON, Canada). Organic solvents and acids were purchased from Caledon Laboratories (Georgetown, ON, Canada), EM Science (Darmstadt, Germany), BDH (Toronto, ON, Canada), ACP (Montreal, PQ, Canada) and Fisher (Whitby, ON, Canada). Ingredients for culturing media were purchased from BD Biosciences (Mississauga, ON, Canada). Lyticase and lysing enzymes for yeast cell disruption were from Sigma (Oakville, ON, Canada). Restriction enzymes were supplied by Roche (Laval, PQ, Canada), PCR reagents, *Taq* polymerase, DNA ladders and loading dye came from MBI Fermentas (Burlington, ON, Canada). Agarose for making gels was obtained from Bio-shop (Burlington, ON, Canada). N-methyl-N-trimethylsilyl-trifluoroacetamide (MSTFA) for derivatizing samples for GC-MS analysis was obtained from Pierce (Brockville, ON, Canada). Sterol standards (farnesol, squalene, ergosterol and lanosterol) and internal standards (ribitol and 5β-cholesten-3α-ol) were obtained from Sigma-Aldrich-Fluka (Oakville, ON, Canada) while zymosterol was purchased from Steraloids (Newport, RI, USA). The anti-fungal drugs, Amphotericin B, Fungizone® was manufactured by Bristol-Myers Squibb (Montreal, PQ, Canada) and Fluconazole, Diflucan® from Pfizer Inc. (Kirkland, PQ, Canada).

1.3.2 *Candida albicans* strain background, culture and storage conditions

All drug-resistant mutants of *C. albicans* used in this study were of the TW1 strain background. The TW1 strain originated from the oral cavity of a 30 year old male hospital patient with AIDS in San Antonio (TX, USA) at the beginning of his Fluconazole therapy for recurrent candidiasis (Redding, S. et al., 1994). With therapy progressing to higher and higher doses of Fluconazole at every recurrence of infection, FLU-resistance eventually developed in *C. albicans* isolates from this patient. *C. albicans* strains were isolated from this patient at every infectious episode over 2 years until the patient's death (strains TW1 to 16). The transition point from FLU-sensitive to FLU-resistant occurred somewhere between the 12th (TW12) and 13th (TW13) isolate from this patient (White, T., 1997a). The TW16 strain was found to be of the same genetic background as the TW1 strain through electrophoretic karyotyping or DNA sub-typing with pulse-field gel electrophoresis (PFGE) (Redding, S. et al., 1994). Therefore, it is most likely that the TW1 strain evolved over time to become FLU-resistant. This makes the TW1 strain a good candidate as a progenitor to generate potential *in vitro* drug-resistant mutants through experimental evolution.

Four strains from the series above were used in this study, TW1, TW12, TW13 and TW16. There were also six drug-resistant *C. albicans* mutant strains (TWF1, TWF2, TWF3, TWF4, TWF5 and TWAF) that were generated through experimental evolution of the TW1 progenitor strain *in vitro*, described in the next section. All strains were cultured on YEPD (1% yeast extract, 2% peptone, 2%

dextrose) agar plates or YEPD broth (pH 7) and grown at 37 °C. Strains were stored at –70 °C in 20% glycerol-YEPD in 2-ml screw-capped polypropylene tubes.

1.3.3 Experimental evolution of drug-resistant mutants *in vitro*

The TW1 progenitor strain was allowed to propagate in 14-ml polypropylene round-bottomed culture tubes containing 5 ml of YEPD (rich medium) liquid broth plus gradually increasing concentrations of drug (FLU or AmB separately), in replicates of 6 tubes per drug. The Fluconazole stock solution was in 0.9% NaCl (physiological saline) while Amphotericin B was dissolved in sterile ddH_2O. To generate FLU-resistant mutants, the TW1 strain was first cultured in a tube containing YEPD liquid plus 32 μg/ml FLU (low concentration) and allowed to grow up to stationary phase on a roller-drum (New Brunswick Scientific model TC7, Edison, NJ, USA) turning at 40 rpm while incubating at 37 °C (Precision Scientific incubator model 805, Winchester, VA, USA). Once cultures appeared turbid, indicating growth to stationary phase, a 50 μl inoculum was transferred to a new tube containing freshly prepared YEPD plus 64 μg/ml FLU and allowed to grow up under the same conditions. This process of cell transfer was repeated 2 more times, increasing the FLU concentration to 128 μg/ml and a final transfer to a very high FLU concentration of 256 μg/ml. A similar method was employed to generate AmB-resistant mutants by serially transferring the TW1 progenitor strain into culture tubes containing YEPD plus gradually increasing concentrations (2 to

4 to 8 to 16 to 32 μg/ml) of AmB. For every replicate, 50 μl of cell culture was taken at each transfer point for storage at –70 °C in 20% glycerol-YEPD in 2-ml screw-capped polypropylene tubes.

1.3.4 Growth curves

Growth curves were generated for eight *C. albicans* strains, TW1, TW16, TWAF and TWF1 to F5 in rpmi-1640 medium. An overnight grown liquid culture of each strain was sub-cultured into fresh rpmi-1640 (pH 7) liquid in Erlenmeyer flasks at a 1:250 dilution. These flask cultures were grown in a 37 °C incubator, shaking at 200 rpm (innova 4300, New Brunswick Scientific, Edison, NJ, USA). Cell growth was monitored over time by absorbance spectrometry in a UV-Visible spectrophotometer (Biochrom 2100pro, Cambridge, UK). The optical density (OD) was monitored at a wavelength of 600 nm. Once cell cultures reached early exponential phase (OD600 approx. 0.01), 1 ml was sampled at regular intervals of 2 hrs (4 hrs for TWAF) until cells reached stationary phase where the next few samples were taken at 5 or 6 hr intervals. Absorbance was set to zero using ddH_2O before the absorbance of cell cultures were measured. To measure absorbance, 1 ml of cell culture was transferred into a disposable polystyrene cuvette with a path length of 1 cm. Once the absorbance of cell cultures approached a value of 1 (late exponential phase), it was diluted (10 μl cell culture + 990 μl ddH_2O) and mixed well before its absorbance was measured to ensure that Beer's law (Absorbance = molar absorptivity × path length × concentration)

would not be violated. In other words, at high concentrations of the absorbing species (i.e., cell culture), concentration is no longer linearly related to absorbance. For each strain, a growth curve of OD600 vs. time (hrs) was generated from this data using Microsoft Excel. Generation times were calculated from exponential phase data using the following two formulas:

(i) $N = N_0 2^n$

N = final cell number or absorbance
N_0 = initial cell number or absorbance
n = number of generations

(ii) $g = t/n$

g = generation time
t = time of growth in minutes

1.3.5 MIC and fitness measurements of drug-resistant mutants

Two different methods were used to test the minimum inhibitory concentration or MIC of Amphotericin B (Bristol-Myers Squibb, Montreal, PQ, Canada) and Fluconazole (Pfizer, Kirkland, PQ, Canada) for the drug-resistant *C. albicans* mutants in this study: (i) National Committee for Clinical Laboratory Standards (NCCLS) micro-broth dilution method (1997) and (ii) colony size (Xu, J. et al., 1998) method. Strains were considered resistant or susceptible according to interpretive breakpoints that are commonly used at present for both FLU (Rex, J. et al., 1997) and AmB (Klepser, M., 2001). *C. albicans* was considered FLU-resistant if its MIC $\geq$ 64 μg/ml and AmB-resistant if its MIC $\geq$ 8 μg/ml. All strains were tested for their susceptibilities to both FLU and AmB in an effort to detect any cross-resistant mutants.

Briefly, the NCCLS micro-dilution method for *C. albicans* involved inoculating 2.4×10^3 cells into a final volume of 200 μl of rpmi1640 liquid medium

(pH 7) plus gradually increasing concentrations of drug in polystyrene micro-titre plates with round-bottom wells (refer to key in Fig. 1.6). The MIC of each strain to FLU and AmB were tested separately in different micro-titre plates. An OD600 of 0.01 is equivalent to 3×10^5 yeast cells/ml (Treco and Winston, 1997). These plates were consequently incubated at 37 °C for 48 hrs before the turbidity of the medium was qualitatively assessed to determine the MIC of the strain. The MIC on FLU was the drug concentration where turbidity of the cell culture was 20% that of the control that contains no drug, while the MIC on AmB was the drug concentration of the optically clear tube.

The colony size method was based on streaking a strain to obtain isolated colonies on YEPD-agar plates with gradually increasing drug concentrations, similar to the NCCLS method. The plates were incubated at 37 °C for 48 hrs before colony sizes were measured under a compound light microscope (Leitz-Wetzlar SM-LUX, Germany) with an ocular micrometer. Similar to the NCCLS micro-broth dilution method, the MIC on FLU was the concentration where growth was reduced by 80% compared to the drug-free control, while the MIC on AmB was the point where growth had completely ceased.

Using data from the MIC determination of the drug-resistant mutants by the colony size method, fitness curves were generated for all mutants and compared to the fitness of the TW1 progenitor on all concentrations of FLU or AmB. Mean colony sizes of the strains measured on different concentrations of drug on YEPD-agar plates were used as an indicator of growth or fitness.

		FLUCONAZOLE (μg/ml)											
		0	0.25	0.5	1	2	4	8	16	32	64	128	256
Strains	1	O	O	O	O	O	O	O	O	O	O	O	O
	2	O	O	O	O	O	O	O	O	O	O	O	O
	3	O	O	O	O	O	O	O	O	O	O	O	O
	4	O	O	O	O	O	O	O	O	O	O	O	O
	5	O	O	O	O	O	O	O	O	O	O	O	O
	6	O	O	O	O	O	O	O	O	O	O	O	O
	7	O	O	O	O	O	O	O	O	O	O	O	O
	8	O	O	O	O	O	O	O	O	O	O	O	O
		0	0.03	0.06	0.12	0.25	0.5	1	2	4	8	16	32
		AMPHOTERICIN B (μg/ml)											

Fig. 1.6 The layout of the micro-titre plate showing the FLU or AmB concentration in rpmi1640 media in each well when testing for the MIC. The MIC on each drug was tested on separate plates.

1.3.6 Interactions between AmB and FLU in the double drug-resistant strain

An assay was conducted to determine if there were any antagonistic or synergistic interactions between Amphotericin B and Fluconazole in the AmB + FLU-resistant strain, TWAF and TW1. This procedure was based on the micro-dilution MIC testing method proposed by the NCCLS, where 2.4×10^3 cells were inoculated into 200 µl of rpmi1640 (pH 7) media plus varying concentrations of both drugs (see key in Fig. 1.7) in polystyrene micro-titre plates with round-bottom wells. Micro-titre plates were then incubated at 37 °C for 50 hrs, afterwhich their absorbance was measured using a micro-titre reader (Bio-tek Instruments, EL-340 Bio Kinetics reader, Winooski, VT, USA) at OD570, setting absorbance to zero with ddH_2O to determine the cell density in each well.

1.3.7 DNA extraction, PCR and restriction enzyme digests of *erg11*

DNA was extracted with a yeast mini-prep protocol described by Xu et al. (2000) and also in Appendix A.1. In summary, cells were collected from an overnight grown culture on YEPD-agar at 37 °C and suspended in sterile ddH_2O in microfuge tubes. Tubes were vortexed, then centrifuged at 13000 rpm for 2 mins (Hettich mikro20, Tuttlingen, Germany) to obtain a cell pellet and the supernatant was discarded. Yeast cell walls were lysed with a protoplasting buffer made with lyticase and lysing enzyme (see end of Appendix A.1) by incubating at 37 °C for 2 hrs. Protoplasts were discarded. Then, cell membranes were solubilized with a lysing buffer made with EDTA and 1% SDS

AMPHOTERICIN B (μg/ml)	FLUCONAZOLE (μg/ml)											
	0	0.25	0.5	1	2	4	8	16	32	64	128	256
0	O	O	O	O	O	O	O	O	O	O	O	O
0.03	O	O	O	O	O	O	O	O	O	O	O	O
0.06	O	O	O	O	O	O	O	O	O	O	O	O
0.12	O	O	O	O	O	O	O	O	O	O	O	O
0.25	O	O	O	O	O	O	O	O	O	O	O	O
0.5	O	O	O	O	O	O	O	O	O	O	O	O
1	O	O	O	O	O	O	O	O	O	O	O	O
2	O	O	O	O	O	O	O	O	O	O	O	O
4	O	O	O	O	O	O	O	O	O	O	O	O
8	O	O	O	O	O	O	O	O	O	O	O	O
16	O	O	O	O	O	O	O	O	O	O	O	O
32	O	O	O	O	O	O	O	O	O	O	O	O

Fig. 1.7 The layout of the micro-titre plate showing the drug concentrations in rpmi1640 media in each well when testing for antagonistic or synergistic interactions between AmB and FLU.

detergent (see end of Appendix A.1), incubating at 65 °C for 30 mins. Proteins were removed with 24:1 chloroform:iso-amyl alcohol and then DNA was precipitated with ice cold iso-propanol. Tubes were centrifuged at 13000 rpm for 2 mins to obtain the DNA pellet and the supernatant was discarded. The pellet was washed with 70% ethanol, air-dried overnight, then re-dissolved in 1X TE (10mM Tris-Cl, 1mM EDTA) buffer (pH 8) and stored at –20 °C until further use. Before this, 5 μl of DNA was checked by electrophoresis on a gel made with 1% agarose dissolved in 1X TAE (40 mM Tris acetate, 2 mM EDTA) buffer (pH 8.5) at 100 V for 1 hr (Gel boxes from: Continental Lab Products, San Diego, CA, USA; Powerpac 3000 from: Bio-rad, Mississauga, ON, Canada; Gel imaging machine from: Alpha-Innotech Fluorchem 8000, San Leandro, CA, USA).

A highly mutable region of the *erg11* gene, called the "region 7" was first amplified by PCR followed by digestion with three restriction enzymes (White, T., 1997b). The forward and reverse PCR primer sequences were 5'-GGGAAAGTT TCTAAAGGGG-3' and 5'-GTTAATCCAACTAAGTAAC-3' respectively and they were synthesized by Sigma (Oakville, ON, Canada). The PCR was carried out in a thermal cycler (i-Cycler, Bio-rad, Mississauga, ON, Canada) with the following temperature program: (i) initial denaturation at 95 °C for 4 mins, (ii) forty cycles of amplification with denaturation at 95 °C for 30 sec, annealing at 50 °C for 30 sec and extension at 72 °C for 1 min, (iii) final extension at 72 °C for 7 mins, after which 5 μl of PCR product was checked by electrophoresis on a 1% agarose gel at 100 V for 1 hr.

The PCR product from each strain was subsequently digested with 3 different enzymes *Acc*I, *Mun*I and *Afl*II (Roche, Laval, PQ, Canada) in separate reactions, incubating at 37 °C for 12 hrs. Restriction enzyme digestion patterns (presence or absence of restriction sites) were compared between the TW1 strain and the drug-resistant mutants by banding patterns on a 1% agarose gel run at 80 V for 3 hrs.

1.3.8 Preparation of yeast cells for GC-MS analysis

Before a yeast strain could be analyzed for its sterols by GC-MS, it was first grown to stationary phase in Erlenmeyer flask cultures at 37 °C in an incubator shaker at 200 rpm (innova 4300, New Brunswick Scientific, Edison, NJ, USA). Cells were harvested by centrifuging at 10000 rpm for 15 mins (JLA-16.250 rotor, Beckman Coulter Avanti J-25, Fullerton, CA, USA) and the supernatant was discarded. Cell pellets were then washed 3 times with 1X PBS buffer (pH 7.3) (see end of Appendix A.2) followed by 3 times with sterile ddH_2O, centrifuging after every wash at 4000 rpm for 15 mins (S40 rotor, Jouan B4i, Winchester, VA, USA) to discard the supernatant. Cells were then re-suspended in sterile ddH_2O and aliquoted into sterile, pre-weighed 2-ml screw-capped polypropylene storage tubes. Cell suspensions in storage tubes were centrifuged at 13000 rpm for 2 mins (Hettich mikro20, Tuttlingen, Germany), supernatant was discarded and pellet weights were adjusted to 600 mg (fresh weight) in each tube. Cell samples were then flash frozen with liquid nitrogen (–196 °C) and then stored at –70 °C

until further analysis. For sterol analysis, cells were retrieved from the –70 °C freezer and thawed on ice. It was then transferred to a 15-ml screw-capped polypropylene tube and broken by vortexing (Vortex Genie 2 model G-560, Fisher, Whitby, ON, Canada) at a speed setting of 8 with glass beads of 0.45 - 0.55 mm in diameter (Sigma, Oakville, ON, Canada) for five intervals of 1 min with 2 mins of resting time on ice between intervals. This bead grinding procedure was modified from Dunn and Wobbe (1997). After this, cellular proteins and enzymes were deactivated by incubating tubes for 15 mins at 70 °C in a water bath (Fisher Iso-temp 205, Whitby, ON, Canada). The lipid phase was then extracted twice with chloroform and saponified with 33% methanolic KOH on a dry heating block (Fisher Iso-temp Economical, Whitby, ON, Canada) at 45 °C for 2.5 hrs. The lipid phase was saponified to remove esters bound to sterols so that all the sterols analysed would be in a same free form. At this point, lipid extracts were kept at –20 °C in 4 ml glass Kimble® vials until ready for running on the GC-MS. A detailed procedure for harvesting, bead-grinding and phase separation can be found in Appendix A.2, A.3 and A.4 respectively.

When ready to analyze by GC-MS, saponified lipid extracts were equilibrated to room temperature and then 500 μl was transferred to a 1 ml conical thick-walled glass reaction vial (Chromatographic Specialties, Brockville, ON, Canada) together with 5 μl of 5β-cholestan-3α-ol (0.1 mg/ml dissolved in chloroform), the internal standard. They were blown to dryness under a stream of N_2 gas (Meyer N-evap Organomation model 111, Berlin, MA, USA) with an

airflow pressure of 20 psi and the bottom of the tubes suspended in a water bath set at 40 °C. Then samples were re-dissolved in 20 μl pyridine and metabolites were derivatized with 30 μl of N-methyl-N-trimethylsilyl-trifluoroacetamide (MSTFA) by incubating for 30 mins in a dry heating block (Fisher Iso-temp Economical, Whitby, ON, Canada) set at 37 °C. When metabolites are derivatized, labile hydrogens are replaced with a trimethylsilyl (TMS) group so that they become volatile and amenable for GC-MS analysis. Using a robot (Gerstel MPS2 Multi-purpose sampler, Gerstel, Baltimore, MD, USA), samples were diluted 1:1 with hexane in GC auto-sampler vials before 1 μl was injected into the GC-MS for analysis. A detailed protocol of the derivatization process can be found in Appendix A.5. All strains were analyzed on the GC-MS in duplicate.

The sterol profiles generated by various *C. albicans* strains would then be compared with that of authentic sterol standards where possible to make definitive identifications of the sterols. The only commercially available standards were farnesol, squalene, lanosterol, ergosterol (Sigma, Oakville, ON, Canada) and zymosterol (Steraloids, Newport, RI, USA). For those intermediates that were not commercially available, mass spectra would be compared with those already published for putative identification of sterols. Commercially available libraries of mass spectra from the National Institute of Standards and Technology (NIST) and Fiehn (Fiehn, O. et al., 2000) libraries were also used for putative identifications of compounds.

1.3.9 GC-MS instrument and temperature program

The gas chromatography–mass spectrometry (GC-MS) system was composed of a Gerstel Multipurpose sampler (MPS2) (Gerstel Inc., Baltimore, MD, USA), a Trace GC gas chromatograph, and a Trace DSQ quadrupole mass spectrometer (Thermo-Finnigan, Mississauga, ON, Canada). Gas chromatography was performed on a 30 m DB17MS polysiloxane column coated with 50% methyl and 50% phenyl groups, with a 0.25 mm internal diameter and a 0.25 µm film thickness (Agilent Technologies, Mississauga, ON, Canada) coupled to an intermediate polarity fused silica guard column 5 m in length with a 0.53 mm diameter (Supelco, Bellefonte, PA, USA). The ion source was set to 200 °C. Helium was used as the carrier gas at a flow rate of 1 mL min^{-1}. The temperature program was as follows: the oven temperature was isocratic at 50 °C for 2.5 min and was increased to 70 °C at a rate of 7.5 °C min^{-1}. The oven temperature was increased at 5 °C min^{-1} to 310 °C, and was held for 1 min at 310 °C. The oven was then cooled down to 50 °C before injection of the next sample. Mass spectra were recorded at 0.9 scans per sec with a scanning range of 50 to 700 m/z. The MS detector was turned on at 6 min. Both chromatograms and mass spectra were evaluated using the Xcalibur program version 1.3 (Thermo-Finnigan, Mississauga, ON, Canada). Peaks were identified by comparison with authentic standards and comparisons to the NIST MS search library version 2.0 and Fiehn library (www.mpimp-golm.mpg.de/mms-library/index-e.html) (Fiehn, O. et al., 2000).

1.3.10 GC-MS data analysis

Peak areas or the area under peaks were obtained from the Xcalibur program and then exported to Microsoft Excel for further analysis. All peak areas were normalized with the internal standard (5β-cholestan-3α-ol) to generate a value known as the normalized peak area (NPA) for each peak. In this study, the NPA was calculated by dividing the area of a peak by the area of the internal standard. The internal standard is a compound that is not found in an organism and can therefore be used for this purpose. Peaks from different gas chromatograms were aligned manually by their retention time (RT) and mass spectra (MS) for the comparison of lipid profiles between different strains of *C. albicans*.

1.4 RESULTS

1.4.1 Six drug-resistant *C. albicans* were generated from experimental evolution

Altogether, six drug-resistant strains of *C. albicans* were generated from the TW1 progenitor by experimental evolution *in vitro*. Five strains, TWF1, TWF2, TWF3, TWF4 and TWF5 were FLU-resistant and they were generated from selection on gradually increasing concentrations of Fluconazole in YEPD liquid media. One drug-resistant mutant, TWAF was generated from selection on Amphotericin B in YEPD liquid. The TWAF strain also happened to be resistant to Fluconazole. These strains were determined to be drug-resistant according to

their MIC or minimum inhibitory concentration measurements by the NCCLS micro-broth dilution method and standardized interpretive breakpoints (Rex, J. et al., 1997; Klepser, M., 2001). The MIC values for all strains determined by the NCCLS method are presented in Table 1.1. The MIC to Fluconazole and Amphotericin B were also determined by the colony size method (Xu, J. et al., 1998). The FLU MIC values from both methods (Table 1.2) were correlated and therefore compatible for interpretation using the standard breakpoints. This is consistent with the results reported by Xu et al. (1998). On the other hand, AmB MIC values from both methods (Table 1.2) were different, although they followed the same trends. Since the standard approved method for MIC testing is the NCCLS method, only those MIC values were used to interpret resistance to AmB for the strains in this study.

1.4.2 Fitness of *C. albicans* drug-resistant strains

It was interesting to compare the relative fitness of the drug-resistant mutants to the progenitor strain to determine the extent of any trade-off between drug-resistance and survival. Colony size measurements of these *C. albicans* strains on drug-free YEPD-agar plates revealed that the AmB + FLU-resistant double mutant, TWAF was significantly ($p = 10^{-11}$, T-test) decreased in fitness compared to the wild-type. On average, colonies of the TWAF strain were 50% the size of the TW1 progenitor when there was no drug. In reference to Fig. 1.8 B, TWAF decreased in fitness at very low concentrations (0.12 - 0.25 μg/ml) of AmB and then peaked in fitness at 0.5 μg/ml AmB onwards until 16 μg/ml. After

Table 1.1 MIC values, anti-fungal drug-susceptibilities and generation times for the *C. albicans* strains used in this study

Candida albicans Strain	Gen. Time (mins)	MIC AmB (μg/ml)		MIC FLU (μg/ml)		Description of strains and their susceptibility to anti-fungal drugs
		NCCLS	Literature[a]	NCCLS	Literature[a]	
TW 1	66	0.5	0.12	4	0.25	original progenitor strain from AIDS patient before anti-fungal treatment, FLU^S and AmB^S
TW12	–	–	0.12	–	16	12^{th} isolate from AIDS patient, FLU^{SDD} and AmB^S
TW13	–	–	0.12	–	16, 128[b]	13^{th} isolate from AIDS patient, FLU^R but AmB^S
TW 16	66	0.25	0.12	> 256	> 128	FLU^R mutant from AIDS patient; AmB^S; also reported as ITR^R and KET^R (White, T., 1997)
TW F1	75	0.12	–	> 256	–	*in vitro* FLU^R mutant selected on FLU; AmB^S.
TW F2	70	0.12	–	> 256	–	*in vitro* FLU^R mutant selected on FLU; AmB^S
TW F3	68	0.12	–	> 256	–	*in vitro* FLU^R mutant selected on FLU; AmB^S
TW F4	70	0.12	–	> 256	–	*in vitro* FLU^R mutant selected on FLU; AmB^S
TW F5	77	0.12	–	> 256	–	*in vitro* FLU^R mutant selected on FLU; AmB^S
TW AF	254	8	–	> 256	–	*in vitro* AmB^R and FLU^R mutant, selected on AmB

[a] Reference: White, T. (1997a)

[b] MIC from NCCLS macro-dilution method

Table 1.2 Comparison of MIC values determined by the NCCLS micro-dilution and colony size methods.

C. albicans Strain	MIC AmB (μg/ml)		MIC FLU (μg/ml)	
	NCCLS	Colony Size	NCCLS	Colony Size
TW 1	0.5	2	4	2
TW 16	0.25	2	> 256	> 256
TW F1	0.12	4	> 256	> 256
TW F2	0.12	4	> 256	> 256
TW F3	0.12	4	> 256	> 256
TW F4	0.12	4	> 256	> 256
TW F5	0.12	4	> 256	> 256
TW AF	8	> 32	> 256	> 256

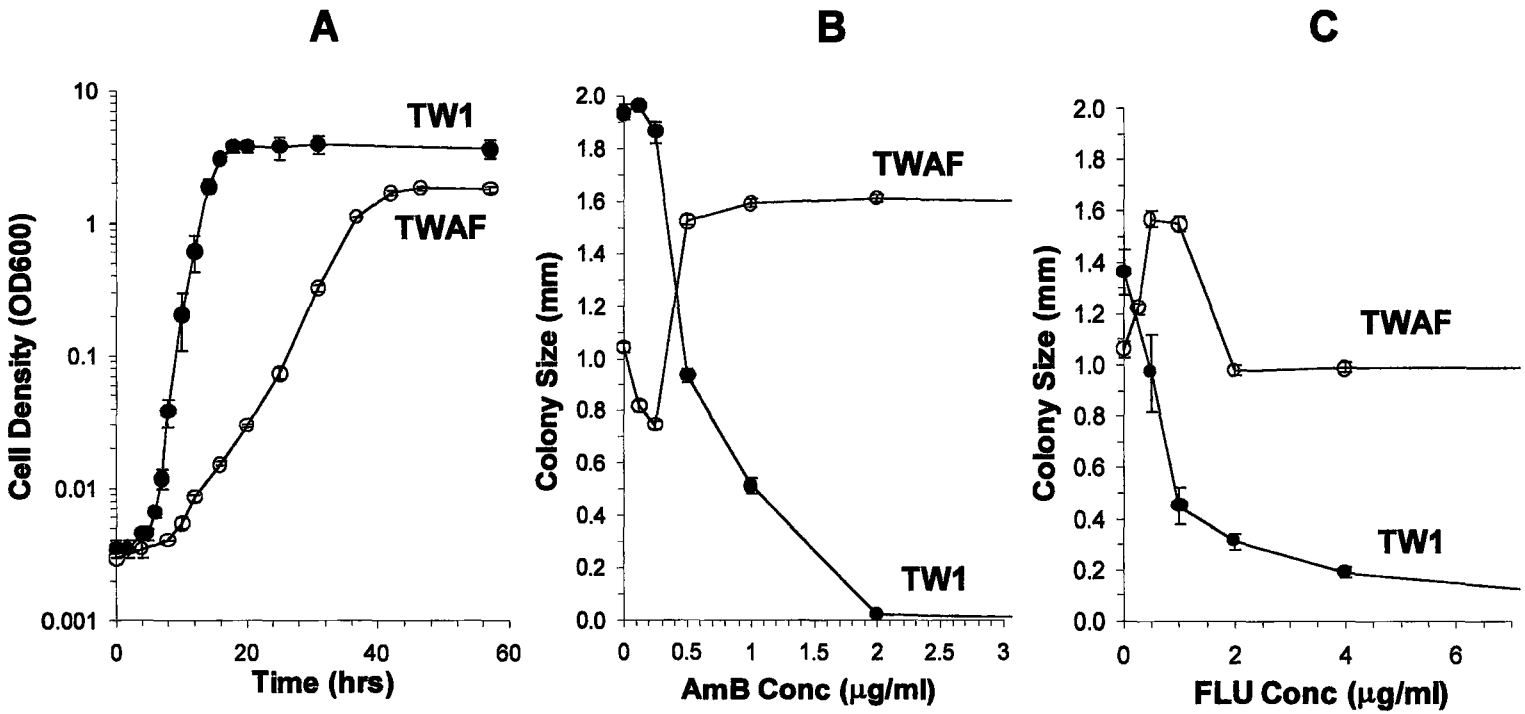

Fig. 1.8 (A) Growth curves of TW1 and TWAF on rpmi1640 liquid media show that the TWAF double mutant grows at a slower rate than the TW1 wild-type strain. (B) Colony sizes of TW1 and TWAF on different concentrations of AmB+YEPD-agar and (C) Colony sizes of TW1 and TWAF on different concentrations of FLU+YEPD-agar.

this, its colony size sharply dropped at 32 μg/ml AmB to the same level of fitness as when the AmB concentration was 0.12 μg/ml (not shown). On Fluconazole (Fig. 1.8 C), the TWAF strain had its peak fitness at very low concentrations (0.5 - 1 μg/ml) before its fitness fell to about the same level as when no drug was present and it was constantly maintained until the FLU concentration was 128 μg/ml. The peak level of fitness of the TWAF strain on AmB (Fig. 1.8 B) and FLU (Fig. 1.8 C) was about the same ($p = 0.75$, T-test). The double mutant, TWAF also had a significantly ($p = 2 \times 10^{-7}$, T-test) longer doubling time at 254 mins compared to the TW1 progenitor at 66 mins in rpmi1640 media (see Fig. 1.8 A). Therefore, despite a clear fitness advantage over the original TW1 strain when the AmB or FLU concentration is high, the TWAF AmB + FLU-resistant mutant has a fitness deficit in an environment where drugs are not present.

In contrast, the TW16 FLU-resistant mutant did not show a reduction in fitness compared to the wild-type TW1. The average generation time of both strains was exactly the same at 66 mins ($p = 0.98$, T-test) (Fig. 1.9). Although the five *in-vitro* generated FLU-resistant strains, TWF1 to F5 had generation times that were slightly longer than the original TW1 strain, ranging from 68 - 77 mins (Fig. 1.9), each of these times were not significantly different ($p > 0.2$, T-test) from that of the wild-type. On the other hand, the mean colony sizes of these strains were decreased by 27 - 40% ($p \leq 10^{-9}$, T-test) relative to the TW1 strain in the absence of drug, indicating that there may be some reduction in fitness (Fig. 1.10). Therefore, it is unclear if these FLU-resistant strains incurred

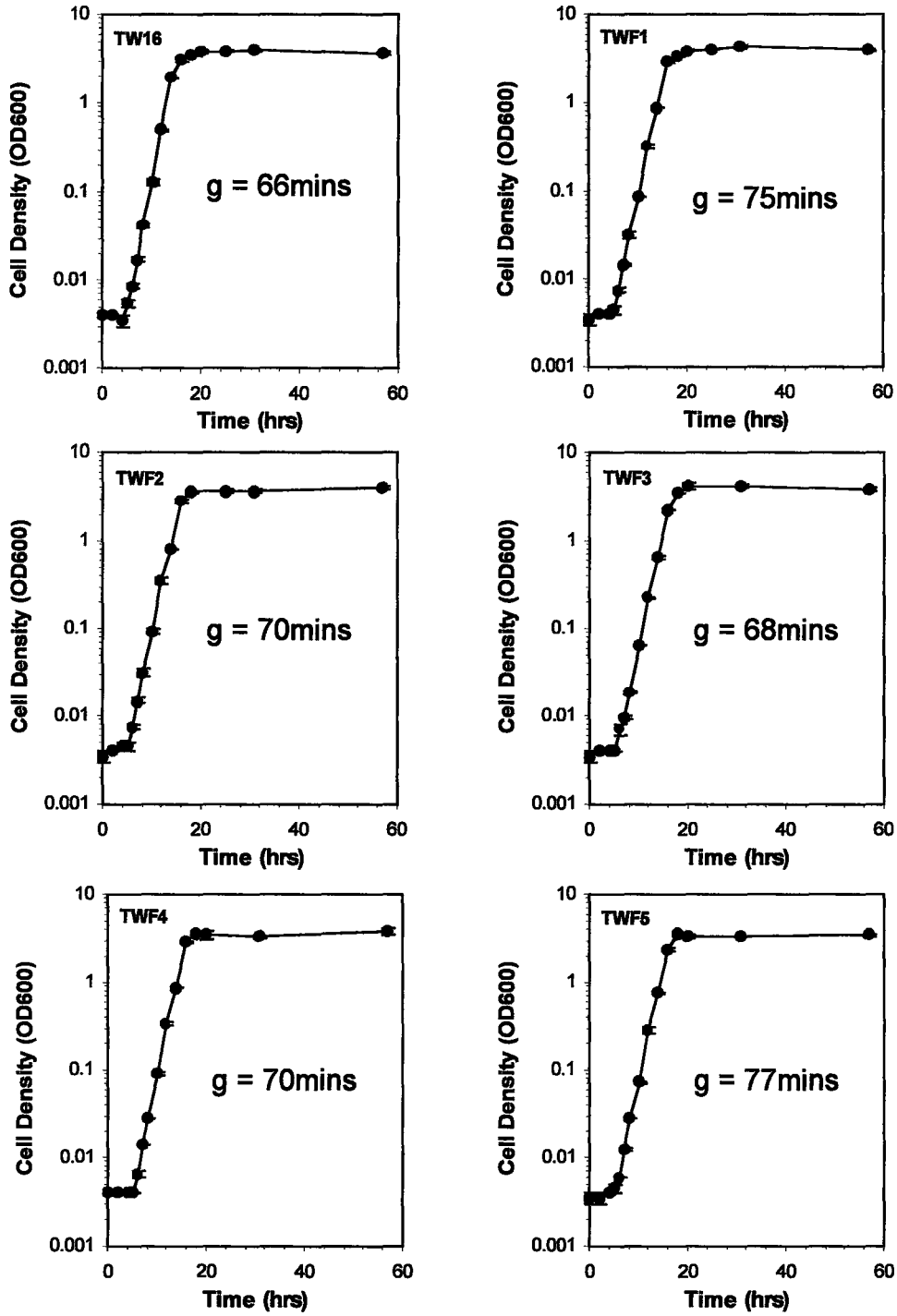

Fig. 1.9 Growth curves of the other *C. albicans* strains: TW16, TWF1, TWF2, TWF3, TWF4 and TWF5 on rpmi1640 media indicate that they all grow at similar rates, comparable with the TW1 wild-type strain.

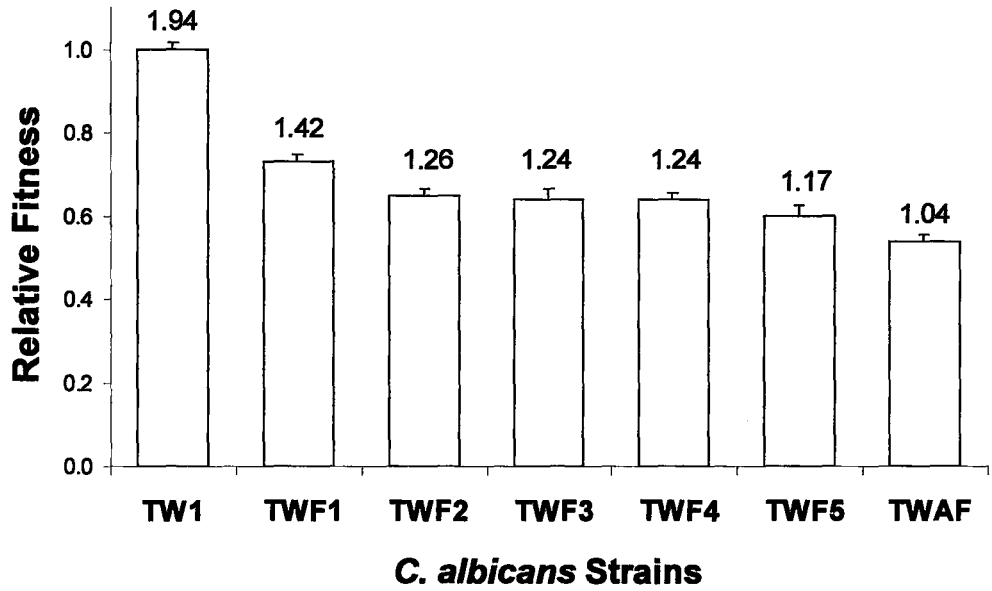

Fig. 1.10 Relative fitness of *in vitro* drug-resistant *C. albicans* mutants based on colony size measurements on drug-free YEPD-agar. Numbers above the bars are mean colony sizes. (Units for colony sizes are mm)

a significant deficit in fitness due to the conflicting results from two different methods. Generation times for TW12 and TW13 are not available because growth curves were not generated for them.

1.4.3 The interaction between Fluconazole and Amphotericin B in *C. albicans* may be antagonistic

The absorbance measurements generated from the micro-titre reader for the AmB and FLU interaction tests in the *C. albicans* strains TW1, TWAF and TW16 are presented in Table 1.3 A, B and C respectively. The results for the drug interaction tests for TW1, TWAF and TW16 were somewhat different. In reference to Table 1.3 A, the AmB MIC of the TW1 strain increased 2-fold as the concentration of FLU increased. For the same wild-type strain, as the concentration of AmB increased, the MIC of FLU also increased in a step-wise manner until reaching 16 μg/ml FLU (Table 1.3 A). This shows that AmB and FLU may interact antagonistically because the MIC in the presence of both drugs was higher than the MIC on FLU and the MIC on AmB separately.

For the TWAF double mutant (Table 1.3 B), the MIC of AmB did not change in the presence of both drugs relative to the controls with only one drug present and the MIC of FLU also did not appear to change. This suggests the lack on interaction between FLU and AmB in the double mutant. Finally, for the TW16 azole-resistant strain (Table 1.3 C), the AmB MIC increased 2-fold when the FLU concentration increased, similar to the TW1 strain. This increase in AmB remained constant until the FLU concentration was 128 μg/ml but increased

Table1.3 Absorbance measurements (OD570) of microtitre plates after 50 hrs of incubation at 37 °C showing interactions between Fluconazole and Amphotericin B for *C. albicans* strains: (A) TW1, (B) TWAF and (C) TW16

A

AmB (μg/ml) \ FLU (μg/ml)	TW1	0	0.25	0.5	1	2	4	8	16	32	64	128	256
	0	0.459	0.135	0.117	0.084	0.067	0.061	0.065	0.070	0.065	0.064	0.075	0.120
	0.03	0.406	0.137	0.123	0.091	0.088	0.070	0.083	0.073	0.066	0.061	0.082	0.107
	0.06	0.394	0.133	0.123	0.099	0.104	0.090	0.081	0.065	0.064	0.090	0.094	0.080
	0.12	0.498	0.122	0.114	0.087	0.088	0.105	0.063	0.087	0.086	0.069	0.063	0.083
	0.25	0.776	0.156	0.115	0.106	0.091	0.090	0.133	0.109	0.080	0.069	0.072	0.083
	0.50	0.019	0.226	0.141	0.113	0.116	0.087	0.093	0.139	0.087	0.082	0.088	0.000
	1	0.001	0.001	0.000	0.001	0.002	0.076	0.000	0.044	0.016	0.014	0.023	0.000
	2	0.003	0.002	0.000	0.001	0.000	0.004	0.000	0.003	0.001	0.000	0.004	0.002
	4	0.000	0.000	0.000	0.000	0.002	0.000	0.000	0.000	0.000	0.000	0.000	0.000
	8	0.000	0.000	0.000	0.000	0.000	0.001	0.000	0.000	0.000	0.000	0.000	0.000
	16	0.000	0.001	0.000	0.000	0.000	0.001	0.000	0.000	0.000	0.000	0.002	0.005
	32	0.001	0.002	0.003	0.001	0.003	0.003	0.001	0.001	0.001	0.000	0.004	0.017

B

AmB (μg/ml) \ FLU (μg/ml)	TWAF	0	0.25	0.5	1	2	4	8	16	32	64	128	256
	0	0.078	0.095	0.081	0.105	0.097	0.099	0.101	0.097	0.096	0.087	0.087	0.086
	0.03	0.099	0.086	0.082	0.070	0.075	0.083	0.089	0.085	0.100	0.098	0.091	0.072
	0.06	0.098	0.071	0.070	0.067	0.073	0.075	0.074	0.094	0.102	0.085	0.094	0.070
	0.12	0.093	0.071	0.076	0.064	0.082	0.118	0.138	0.090	0.082	0.095	0.094	0.084
	0.25	0.121	0.080	0.078	0.074	0.102	0.127	0.104	0.109	0.103	0.120	0.093	0.070
	0.50	0.121	0.098	0.073	0.097	0.104	0.091	0.125	0.097	0.119	0.100	0.093	0.100
	1	0.160	0.106	0.101	0.092	0.113	0.099	0.110	0.116	0.135	0.122	0.105	0.132
	2	0.126	0.122	0.114	0.118	0.111	0.110	0.124	0.118	0.111	0.098	0.090	0.065
	4	0.005	0.002	0.002	0.002	0.008	0.004	0.002	0.003	0.002	0.002	0.002	0.004
	8	0.001	0.002	0.006	0.004	0.009	0.007	0.004	0.003	0.000	0.000	0.008	0.007
	16	0.002	0.003	0.005	0.005	0.010	0.004	0.005	0.021	0.021	0.023	0.023	0.009
	32	0.006	0.006	0.006	0.009	0.010	0.009	0.008	0.007	0.010	0.021	0.014	0.024

Table 1.3 continued

C

		FLU (μg/ml)											
	TW16	**0**	**0.25**	**0.5**	**1**	**2**	**4**	**8**	**16**	**32**	**64**	**128**	**256**
AmB (μg/ml)	**0**	1.001	0.958	0.942	0.929	0.904	0.917	0.979	0.922	0.873	0.454	0.191	0.333
	0.03	0.925	0.937	0.890	0.943	0.921	0.891	0.927	0.905	0.812	0.465	0.181	0.293
	0.06	0.807	0.727	0.710	0.754	0.743	0.780	0.823	0.809	0.799	0.366	0.164	0.273
	0.12	0.260	0.424	0.423	0.591	0.589	0.567	0.621	0.579	0.317	0.278	0.151	0.262
	0.25	0.340	0.230	0.259	0.331	0.278	0.238	0.216	0.304	0.344	0.186	0.184	0.253
	0.50	0.051	0.286	0.243	0.334	0.256	0.233	0.166	0.116	0.152	0.279	0.313	0.213
	1	0.000	0.001	0.001	0.004	0.007	0.005	0.004	0.009	0.016	0.003	0.000	0.217
	2	0.001	0.002	0.000	0.004	0.005	0.006	0.004	0.005	0.001	0.000	0.000	0.002
	4	0.000	0.003	0.000	0.001	0.003	0.001	0.067	0.028	0.000	0.000	0.000	0.000
	8	0.002	0.000	0.003	0.002	0.004	0.004	0.002	0.045	0.001	0.000	0.000	0.001
	16	0.000	0.002	0.003	0.003	0.007	0.004	0.003	0.001	0.007	0.008	0.021	0.007
	32	0.004	0.030	0.007	0.009	0.019	0.008	0.009	0.010	0.006	0.010	0.006	0.000

another 2-fold at the highest concentration of FLU (256 μg/ml) tested. The FLU MIC remained constant for the TW16 strain. Therefore, there may be a slight degree of antagonism between AmB and FLU in the TW16 strain.

1.4.4 Restriction enzyme analysis on the *erg11* gene

A region of the *erg11* gene previously shown to contain point mutations in the TW16 FLU-resistant mutant (White, T., 1997b) was also analyzed in all the *in vitro* mutants generated by experimental evolution from the same TW1 progenitor strain. It was previously shown that the TW16 mutant strain lost all three restriction sites (*Acc*I, *Afl*II and *Mun*I) on both strands of its DNA, thus becoming homozygous for the absence of all sites (White, T., 1997b). In the analysis for this study, the digest with the *Mun*I enzyme, revealed a different electrophoretic pattern between the wild-type, TW1 and TWAF AmB + FLU-resistant strain (Fig. 1.11). The TWAF strain gained an *Mun*I restriction site absent in the original TW1 strain, such that it would now be homozygous for the presence of this restriction site. There were no differences between TW1 and the TWAF double mutant in their restriction digest pattern for the *Acc*I and *Afl*II enzymes. Although the *erg11* gene from the TWAF strain was not sequenced, the addition of one restriction enzyme site in a small region suggests that there might only be a point mutation in this gene. The other FLU-resistant strains, TWF1 to TWF5 did not differ from the TW1 wild-type with their restriction digest banding patterns with all three enzymes, *Acc*I, *Afl*II and *Mun*I (Fig. 1.11). An interpretation of the RE banding pattern on the agarose gel for all drug-resistant mutants is illustrated in

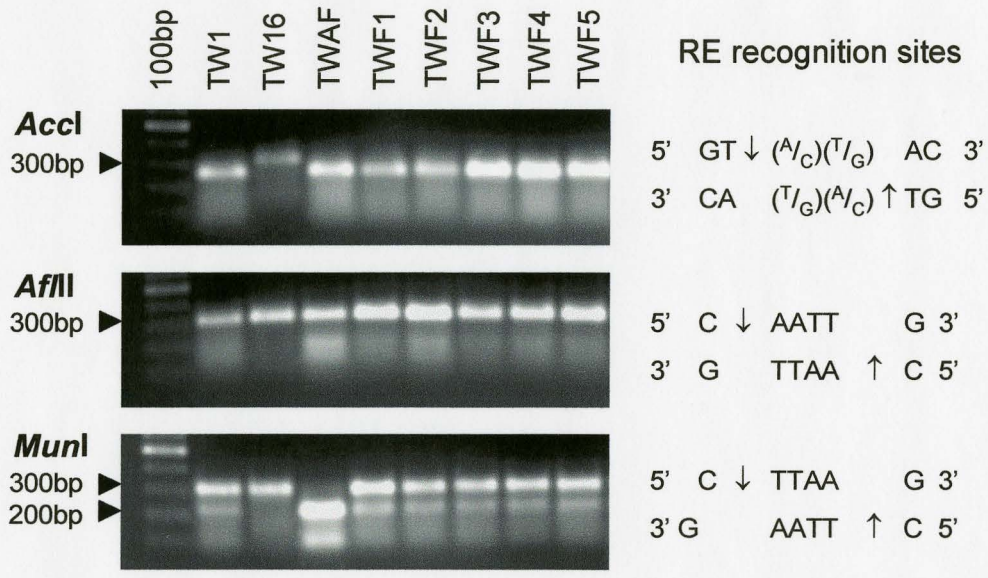

Fig. 1.11 Agarose gel photo showing restriction digest banding patterns of *Acc*I, *Afl*II and *Mun*I for the set of drug-resistant mutants generated from the TW1 strain. The DNA sequences that the restriction enzymes recognize are also shown.

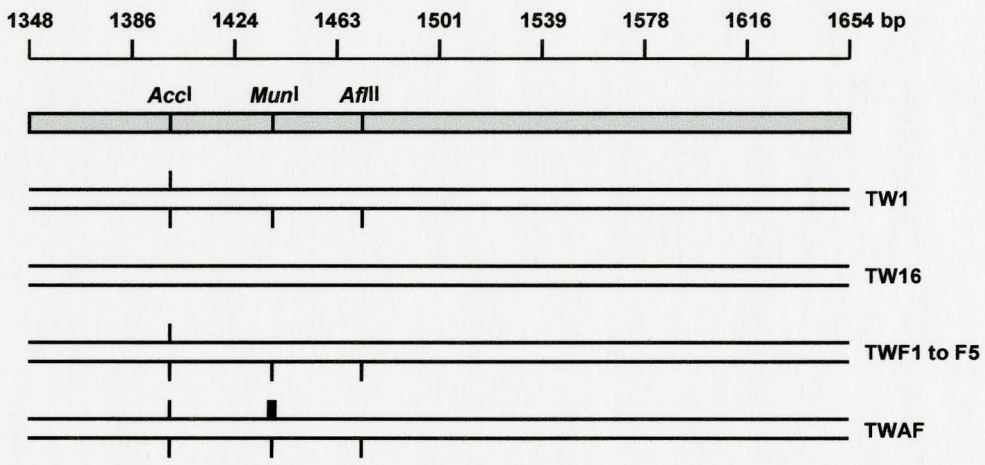

Fig. 1.12 Genetic map of the PCR-amplified "region 7" of the *erg11* gene of *C. albicans* from position 1348 to 1654 bp, showing 3 restriction sites (*Acc*I, *Mun*I and *Afl*II). All restriction sites were deleted on both DNA strands of the TW16 azole-resistant *in vivo* mutant. The *in vitro* FLU-resistant mutants, TWF1 to F5 all had the same pattern of restriction sites as the TW1 wild-type. The TWAF AmB + FLU-resistant mutant gained an additional *Mun*I site (in bold), previously absent in the original TW1 strain.

Fig. 1.12 as a map of the PCR-amplified region with relative positions of the restriction sites.

1.4.5 GC-MS lipid profiles revealed differences in the sterol composition of the double mutant compared to the wild-type

The region most likely to contain sterols (retention times 40 - 53 mins) in the lipid profiles of the *C. albicans* strains were analyzed and peak abundances are listed in Appendix B.1. The peaks and their abundances identified with authentic standards are summarized in Table 1.4. Gas chromatograms for *C. albicans* strains, TW1, TWAF, TW12, TW13 and TW16 are in Fig 1.13 and gas chromatograms for strains TWF3, TWF4 and TWF5 are in Fig. 1.14. The major differences in the sterol composition among the strains were observed between the AmB + FLU-resistant double mutant, TWAF and the TW1 wild-type. There were both qualitative and quantitative differences. Firstly, ergosterol, the major sterol in yeasts and zymosterol were not detected in the TWAF double mutant (Fig. 1.13). Secondly, lanosterol was increased 14-fold ($p = 0.01$, T-test) in TWAF compared to TW1 (Table 1.4). The level of lanosterol in the TWAF strain was significantly higher than all other strains ($p = 1.2 \times 10^{-5}$, ANOVA). Thirdly, 7 novel peaks were detected in the double mutant that were absent in the TW1 progenitor. The identities of these novel peaks are currently unknown due to the lack of commercially available authentic standards. The mass spectra of all these unknown peaks are found in Appendix C.1 to C.7. A summary of the key ions in the mass spectrum of each unknown peak is presented in Table 1.5. The

Table 1.4 Summary of compounds in the ergosterol pathway that were identified with authentic standards for the *C. albicans* strains.

Compound	Mean normalized peak areas (NPA) ± SE							
	TW1	TWAF	TW16	TW12	TW13	TWF3	TWF4	TWF5
Farnesol	0.175 ± 0.04	0.211 ± 0.03	0.023 ± 0.005	0.091 ± 0.02	0.028 ± 0.0006	0.046 ± 0.01	0.023 ± 0.005	0.053 ± 0.005
Squalene	0.096 ± 0.0004	0.102 ± 0.02	0.369 ± 0.05	0.246 ± 0.04	0.108 ± 0.06	0.039 ± 0.01	0.075 ± 0.02	0.052 ± 0.0009
Zymosterol	0.695 ± 0.13	ND[a]	0.344 ± 0.06	0.334 ± 0.02	0.326 ± 0.13	0.226 ± 0.006	0.112 ± 0.02	0.187 ± 0.05
Ergosterol	0.975 ± 0.14	ND	0.387 ± 0.04	0.533 ± 0.18	0.961 ± 0.75	0.169 ± 0.07	0.168 ± 0.06	0.415 ± 0.16
Lanosterol	0.094 ± 0.01	1.279 ± 0.18	0.067 ± 0.008	0.050 ± 0.01	0.095 ± 0.05	0.038 ± 0.05	0.035 ± 0.008	0.044 ± 0.001

[a] ND means not detected

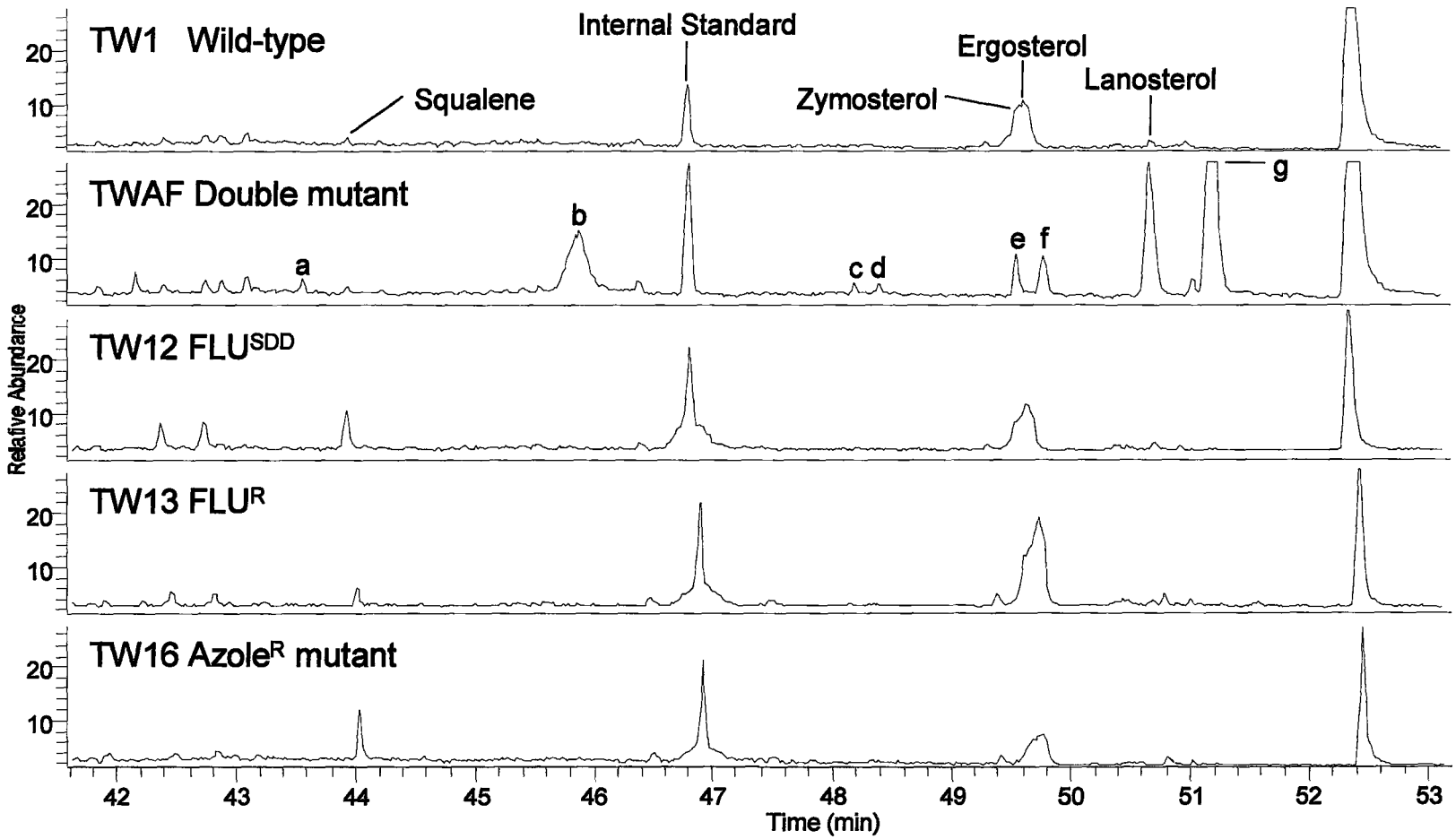

Fig. 1.13 Gas chromatograms showing the sterol profiles of *C. albicans* strains TW1, TWAF, TW12, TW13 and TW16. The double mutant has a very distinct sterol composition compared to wild-type but all other strains resemble the wild-type. (a-g, novel peaks)

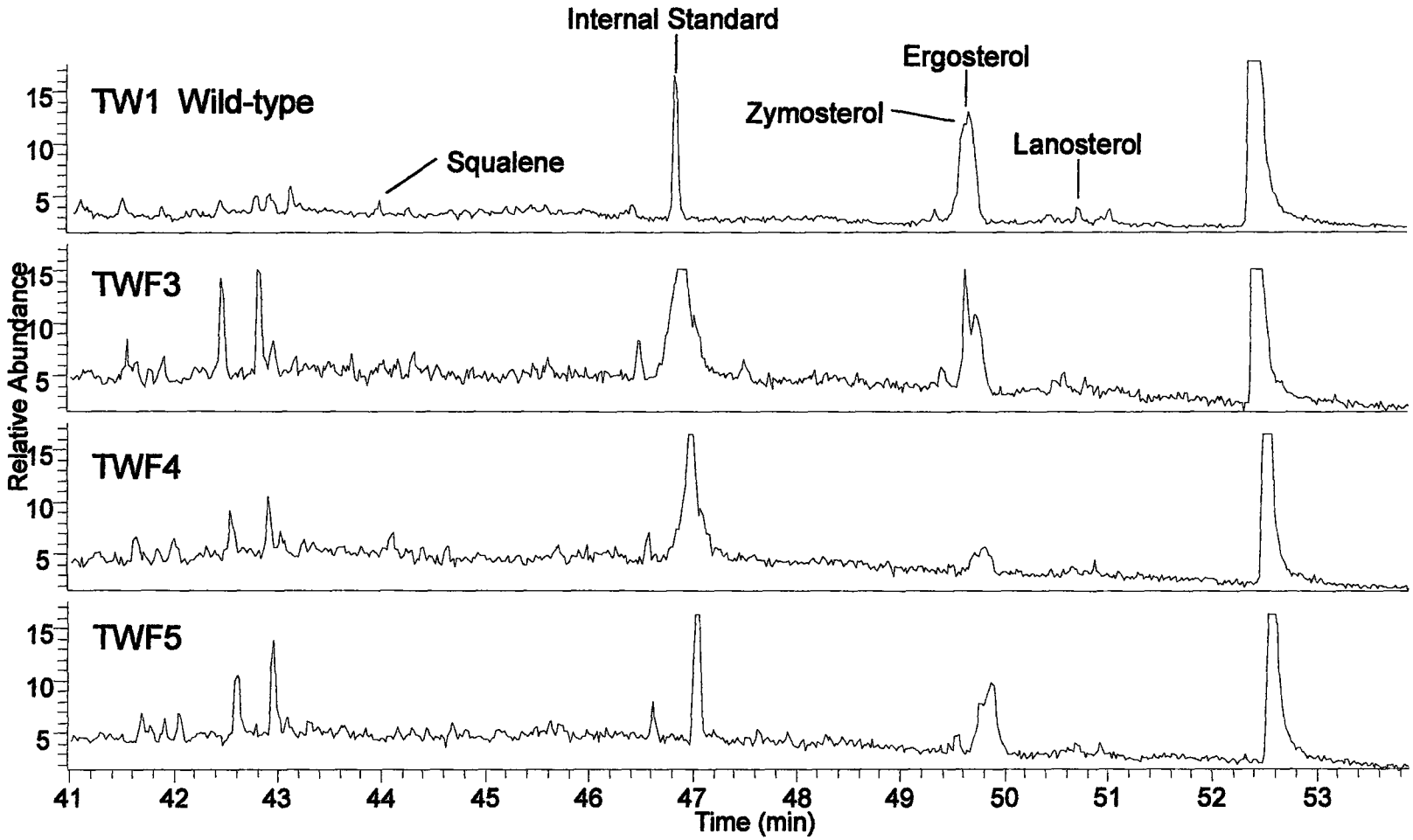

Fig. 1.14 Gas chromatograms showing the sterol profiles of *C. albicans* strains TW1 (wild-type) and *in vitro* FLU-resistant mutants TWF3, TWF4 and TWF5.

Table 1.5 Major mass ions and their abundance in the novel peaks detected in the *C. albicans* TWAF double drug-resistant mutant

Peak[a]	RT (mins)	Major mass ions, m/z > 200 (% Abundance)
a	43.56	212 (100), 225 (47), 242 (68), 256 (79), 282 (27), 312 (38), 357 (38), 391 (38), 399 (22), 457 (14), 467 (14)
b	45.88	206 (46), 254 (22), 317 (100), 330 (17), 382 (19)
c	48.19	207 (100), 253 (42), 366 (20), 408 (20), 433 (15)
d	48.38	212 (100), 221 (70), 240 (91), 259 (72), 265 (72), 259, 374, 314 (51), 316 (77), 373 (56), 374 (86), 392 (32), 420 (27)
e	49.54	204 (100), 205 (89), 217 (51), 226 (29), 230 (17), 247 (17), 275 (24), 317 (30), 369 (10), 431 (10)
f	49.78	213 (61), 226 (61), 286 (100), 293 (48), 302 (30), 378 (67), 404 (24), 466 (15), 481 (15)
g	51.19	216 (47), 229 (84), 242 (100), 255 (32), 281 (17), 284 (19), 324 (8), 332 (8), 365 (5), 408 (39), 470 (1)

[a] refer to Fig. 1.13 for peak positions

mass spectra of these peaks were compared to previously published mass spectra of fungal sterols and only peak "g" at RT 51.19 mins shared 5 major ions (229, 255, 281, 365 and 470) with episterol (Le Fur, Y. et. al., 1999) and 3 ions (229, 255 and 470) with fecosterol (Howell, S. et. al., 1990). However, there were other dominant ions (e.g. 409) that were characteristic for peak "g" that were absent in the published spectra. The levels of the other peaks identified with standards (farnesol and squalene) were not significantly different between the double mutant and the wild-type ($p = 0.3$, T-test).

For all the *in vivo* isolates of *C. albicans* from the AIDS patient, including the azole-resistant TW16 strain, their GC-MS lipid profiles resembled that of the original TW1 strain (Fig. 1.13). Of the FLU-resistant *in vitro* mutants, TWF1 to F5, only TWF3-F5 were analyzed by GC-MS and their profiles also resembled the wild-type profile (Fig. 1.14). Ergosterol and lanosterol levels in all these strains were not significantly different from each other ($p = 0.4$ and 0.3 respectively, ANOVA). Zymosterol was also present in all these strains but its abundance was significantly higher in the wild-type ($p = 0.02$, ANOVA). The farnesol level in the wild-type strain was also higher than the other strains. The squalene level in the TW16 azole-resistant strain was 3.8-fold higher than the wild-type and this was a significant difference ($p = 0.01$, T-test). There were two peaks that were detected in all these strains that were absent in the wild-type (RT 40.30 and 40.84 mins, see Appendix B.1) but they have not been identified.

1.5 DISCUSSION AND CONCLUSIONS

In this study, it was clearly shown that the double drug-resistant mutant underwent the most severe decrease in fitness with respect to the wild-type. FLU-resistant *in vitro* mutants may also have a slight reduction in fitness while the *in vivo* FLU-resistant mutant did not incur any loss in fitness relative to the wild-type. Acquiring multiple drug-resistance must then occur at a trade-off of functions related to growth and survival of an organism. It is common for drug-resistance to cause a reduction in fitness under conditions where drugs are absent. This has been observed not only in fungi but in bacteria as well. In *Mycobacterium tuberculosis*, a drug-susceptible and a multi-drug-resistant strain from the same background were isolated from two patients who were also siblings and their fitness was assayed (Davies, A. et al., 2000). The drug-resistant strain sustained a fitness deficit when propagated on drug-free media in the lab (Davies, A. et al., 2000). Similarly in yeast, many experimentally evolved azole-resistant mutants of *C. albicans* were found to be greatly lowered in relative fitness, where fitness was measured by generation time of growth in drug-free media (Cowen, L. et al., 2000). There were only two mutants from that study that did not experience any fitness loss and in fact had shorter doubling times compared to the ancestral progenitor strain (Cowen, L. et al., 2000).

The contradiction with regards to the fitness cost for the five FLU-resistant *in vitro* mutants cannot be attributed to the use of different media in the colony size method (YEPD) and growth curve assay (rpmi1640). This is because a

study by Cowan et al. (2000) showed that the growth rates of eleven different *C. albicans* mutant strains were correlated in rpmi1640 and YEPD media. The TW16 azole-resistant strain was not reduced in fitness. Therefore, drug-resistance does not always come at a cost to the organism and it must be specific to the strain and environment.

In this study, the interaction between AmB and FLU appeared to be antagonistic in the wild-type strain and azole-resistant *in vivo* mutant. This result is in agreement with the majority of studies in the past that have reported antagonistic interactions between FLU and AmB in *C. albicans* (Lewis, R. et al., 1998; Louie, A. et al., 2001; Vazquez, J. et al., 1998). Scheven and Schwegler (1995) found that although many azoles were antagonistic with Amphotericin B, there was no such antagonism between Fluconazole and Amphotericin B in particular. It was also suggested that azole-AmB interactions could be dependent on the lipophilicity of azoles because many azoles are lipid soluble while Fluconazole is not (Scheven and Schwegler, 1995). In this study, it was also determined that there was no interaction between FLU and AmB in the double drug-resistant mutant. Therefore, the interaction between AmB and FLU is still a complex issue but it appears to be strain specific. There may also be other underlying factors, not yet apparent that may influence the interactive abilities of two drugs.

As sterols serve as the principal target in *C. albicans* for many anti-fungal drugs, the development of drug-resistance should logically be associated with

changes in the sterols. In this study, both the TW16 and TWAF strains contained mutations in the azole target, the *erg11* gene, although each strain had a different mutation (Fig. 1.12). The sterol composition of the TWAF double mutant was consistent with a mutation in the *erg11* gene. In reference to the ergosterol pathway (Fig. 1.5), lanosterol levels were significantly increased while zymosterol was absent, pointing to potential genetic mutations in the steps of the ergosterol pathway between lanosterol and zymosterol to which *erg11* is one of those genes. In recognizing this, the sterol composition of the TW16 azole-resistant strain may not seem to correspond to a mutation in the *erg11* gene because it resembled the wild-type. However, it was previously found that the TW16 azole-resistant mutant was associated with increased levels of mRNA for the *erg11* gene without gene amplification as well as genes encoding efflux pumps, compared to wild-type (White, T., 1997a). The over expression of the *erg11* gene may explain why lanosterol levels were not elevated in the TW16 strain despite having a mutation in *erg11*. Since the TWAF and TW16 strains have a different sterol composition, it can be inferred that the *erg11* gene mutation in both strains are of a different nature and the mechanism of drug-resistance in the double mutant is different from the azole-resistant mutant.

The FLU-resistant mutants that were generated by experimental evolution, TWF3, TWF4 and TWF5 also resembled the wild-type strain in their sterol composition, similar to the TW16 azole-resistant mutant. However, they were different from the TW16 strain because they did not contain any mutation in the

erg11 gene region that was tested. Therefore, it is still unclear from this analysis how the TWF3, TWF4 and TWF5 strains acquired FLU-resistance. It is possible that the *erg11* gene in these strains could still have mutations, but in other regions of the gene that were not tested. Alternatively, FLU-resistance may have occurred by mechanisms unrelated to the ergosterol pathway, such as efflux pumps and drug transporter channels.

The principal sterol in yeasts, ergosterol is essential for growth-related functions and survival. The presence of ergosterol in the azole-resistant TW16 mutant as well as the TWF3, TWF4 and TWF5 FLU-resistant strains explains why their fitness did not decline in the absence of drugs. However, the AmB + FLU-resistant mutant was still able to grow without ergosterol. Therefore something else was compensating for the normal function of ergosterol in the cell membrane of the TWAF strain. It is most likely that these molecules would still be sterols that may be only slightly altered from the structure of ergosterol. Some of the 7 novel peaks detected in the GC profile of the TWAF strain may very well correspond to aberrant sterols that are taking over the function of ergosterol and therefore, it would be very useful to identify them in future work. In a recent study by Sanglard et al. (2003), GC-MS analysis of *erg3/erg3* mutants were found to accumulate 14α-demethylated sterols, including ergosta-7,22-dienol and ergosta-7-enol, as well as fecosterol and episterol. *C. albicans erg11/erg11* mutants contained 14α-methylated sterols such as eburicol, lanosterol, 4,14-dimethylzymosterol and 14a-methylfecosterol (Sanglard, D. et

al., 2003). In both *erg3/erg3* and *erg11/erg11* mutants, zymosterol and ergosterol were absent, resembling the TWAF double drug-resistant strain in this study.

CHAPTER 2

Profiling the metabolome in six pathogenic yeasts using gas chromatography-mass spectrometry (GC-MS)

2.1 ABSTRACT

Metabolomics is the comprehensive study of the metabolites that are necessary for maintaining cellular functions and sustaining the growth of an organism. The metabolome is considered the closest equivalent to an organism's phenotype. The objective of this study was to determine if metabolomic data would reflect the taxonomical relationship of six pathogenic yeasts. Five ascomycetes (*Candida albicans, C. glabrata, C. parapsilosis, C. tropicalis* and *C. krusei*) and one basidiomycete (*Cryptococcus neoformans*) were used in this study and their metabolites were analyzed using gas chromatography-mass spectrometry. Overall, lipid metabolite profiles were more conserved than polar metabolite profiles. Therefore lipid metabolites were better correlated to the taxonomical relationship between these yeasts according to their 26S rRNA sequences. In addition, numerous potential species-specific

metabolites were detected in both polar and lipid profiles of the yeast species in this study. While metabolite profiles among these yeast species looked very similar overall, there were short regions in their polar and lipid gas chromatograms that showed enough peak differentiation for a rapid way to identify and distinguish between these yeast species by visual inspection.

2.2 INTRODUCTION

2.2.1 Candida species

Yeasts of the Candida genus are ascomycetes and many of its species are frequently associated with human infections, although some are associated with environmental reservoirs. Candida sp. tend to reproduce asexually in nature by budding. However, *C. albicans* is capable of reproducing sexually (Magee and Magee, 2000; Hull, C. et al., 2000) and there is evidence of a sexual cycle in *C. glabrata* (Wong, S. et al., 2003). Candida sp. are morphologically very similar under the microscope in that they all produce blastoconidia and pseudohyphae (Larone, D., 1995). Species within the Candida genus vary from each other with respect to colony morphologies on different agar medium and their patterns of fermenting different carbohydrates (Larone, D., 1995).

2.2.2 *Cryptococcus neoformans*

Cryptococcus neoformans is one of the best studied basidiomycetes due to its medical significance. *C. neoformans* can cause life-threatening infections in

immuno-compromised and AIDS patients (Tey, R. et al., 2003) and fatal meningitis (Gottfredsson and Perfect, 2000). The features that make *C. neoformans* distinct from Candida sp. are their morphologies. There are two reproductive cycles in *C. neoformans*: sexual and asexual. It is an encapsulated yeast and does not have very well developed pseudohyphae as Candida sp. (Larone, D., 1995). They also differ in their carbohydrate assimilation patterns (Larone, D., 1995). Within *C. neoformans* itself, there are 3 different varieties or 4 different haploid serotypes that differ from each other according to their ecology, geography, genetic, biochemical and physiological characteristics. The serotype A strains are of the variety *grubii*, strains of serotypes B and C belong to the variety *gattii* while serotype D strains are of the variety *neoformans*. *C. neoformans var. gattii* (serotypes B and C) has been isolated from trees in both tropical (Ellis, and Pfeiffer, 1990) and semi-tropical (Fraser, J. et al., 2003) climates. *C. neoformans var. grubii* (serotype A) *and var. neoformans* (serotype D) are associated with bird droppings worldwide (Swine-Desgain, D., 1974; Garcia-Hermoso, D. et al., 1997).

2.2.3 Metabolomics

Metabolomics is the comprehensive study of the large number of metabolites and intermediates that are necessary for maintaining cellular functions and sustaining the growth and survival of an organism (Fiehn, O., 2001). The entire pool of cellular metabolites in an organism is known as the metabolome. Metabolites are the building blocks of biochemical pathways and

energy yielding reactions that may aggregate to form complex networks that are strictly regulated. Metabolites can be divided into two groups based on their hydrophobicities: polar and lipid. Polar metabolites are hydrophilic or water-soluble and include compounds such as sugars, amino acids and organic acids. Lipid metabolites are mostly hydrophobic and include phospholipids, fatty acids and sterols. From the hierarchy that begins with the genome, transcriptome and then the proteome, the metabolome is the most downstream and it resonates the greatest effects of genetic and physiological changes that are occurring in an organism in a given time (Oliver, S., 2002). Therefore the metabolome is the closest equivalent to an organism's phenotype.

Metabolomics can be studied by many methods such as nuclear magnetic resonance (NMR), electrospray ionization mass spectrometry (ESI-MS), Fourier transform infrared spectroscopy (FT-IR) (Raamsdonk, L. et al., 2001), liquid chromatography-mass spectrometry (LC-MS) and gas chromatography-mass spectrometry (GC-MS) (Fiehn, O. et al., 2000). The output of these methods is what is referred to as the metabolite profile and it is only a portion of the entire composition of metabolites in an organism. No one technique can provide a complete analysis of the entire metabolome. The range of metabolites that are present in a single profile is largely dependent on the detection limits of the instrument used as well as the concentration of cell extract analyzed.

NMR is a valuable method for elucidating the structure of compounds because peaks in an NMR profile provides information about the number and

types of atoms within a molecule (Vaidyanathan and Goodacre, 2003). However, NMR is limited by its lack of sensitivity and would not be the best method to study metabolomics. This can be improved with mass spectral methods that allow the analysis of a greater number of metabolites in a single profile. FT-IR can also provide a metabolic fingerprint of a biological sample. It is a rapid technique based on absorbance, where chemical bonds and different functional groups of molecules correspond to different wavelengths of light (Ellis, D. et al., 2003). A disadvantage with FT-IR is that water has a very high infrared (IR) absorbance and this can prove problematic when interpreting the IR spectrum of a sample. ESI-MS allows for the analysis of non-volatile compounds and is a soft-ionization technique that produces minimal mass spectral fragmentation (Vaidyanathan and Goodacre, 2003). Although commonly used in biomolecular analysis, fragmentation by soft-ionization is not very reproducible. Alike ESI-MS, the LC-MS method require samples to be in the liquid phase. LC-MS is similar to GC-MS but requires a large sample size for analysis.

GC-MS was chosen for metabolite analysis because it has many advantages of being a rapid, sensitive and comprehensive yet highly reproducible. It is also a relatively inexpensive mass spectral method. GC-MS also has an excellent resolving power for better deconvolution of peaks (Weckwerth and Fiehn, 2002). At present, GC-MS is considered the "gold standard" for studying metabolomics (Fiehn, O. et al., 2000).

2.2.4 Identification and taxonomic classification of yeasts

Traditional ways for classifying and identifying yeasts have involved the analysis of their physiology, morphology, ecology and reproduction but these methods were not comprehensive enough and sometimes inaccurate. Over the last 30 years, modern molecular methods such as electrophoretic karyotyping (Monod, M. et al., 1990), randomly amplified polymorphic DNA (RAPD) (Virioni and Matsiota-Bernard, 2001) and PCR-fingerprinting (Meyer, W. et al., 1997) have considerably improved on these traditional procedures. The preferred method for yeasts is to divide them into taxonomic groups based on 18S or 26S ribosomal RNA gene sequences (Hendriks, L. et al., 1991; Valente, P. et al., 1999; Kurtzman and Robnett, 1998). For rapid identification of yeasts, commercial kits (API AUX 20C, bioMérieux Vitek, Lyon, France) that are based on the assimilation of carbohydrates and other metabolites are used. Metabolomic methods that have been used in the past to infer taxonomic relationships between yeasts are NMR (Himmelreich, U. et al., 2003) and fast atom bombardment mass spectrometry (FAB-MS) (Abdi, M. et al., 1999). FAB-MS is another soft-ionization method similar to ESI-MS described in the previous section.

2.2.5 Objectives of this study

In this study, the aim was to determine if metabolomic data would reflect the taxonomical relationship of six human pathogenic yeasts. If it does, then this might be an alternative method to apply as a taxonomic tool for the identification

and classification of yeasts. To explore this topic, the medically significant yeasts, *C. albicans, C. glabrata, C. parapsilosis, C. tropicalis, C. krusei* and *C. neoformans* were subjected to metabolite profiling of both the polar and lipid phase by GC-MS.

2.3 MATERIALS AND METHODS

2.3.1 Chemicals, reagents and media

All the chemicals used in this study were purchased from Sigma (Oakville, ON, Canada) and BDH (Toronto, ON, Canada) and Fisher Scientific (Whitby, ON, Canada). Organic solvents and acids were obtained from Caledon Laboratories (Georgetown, ON, Canada), EM Science (Darmstadt, Germany), BDH (Toronto, ON, Canada), ACP (Montreal, PQ, Canada) and Fisher (Whitby, ON, Canada). Ingredients to make culturing media were purchased from BD Biosciences (Mississauga, ON, Canada). N-methyl-N-trimethylsilyl-trifluoro acetamide (MSTFA) for derivatizing samples for GC-MS analysis was obtained from Pierce (Brockville, ON, Canada). Internal standards, ribitol and 5β-cholestan-3α-ol were obtained from Sigma (Oakville, ON, Canada).

2.3.2 Yeast species and strains used in this study

Six yeast species were used in this study. They were five ascomycetes of the Candida genus: *C. albicans, C. glabrata, C. parapsilosis, C. tropicalis* and *C. krusei* and one basidiomycete, *Cryptococcus neoformans*. All the strains used

Table 2.1 Strains used for the metabolite profiling of pathogenic yeasts.

Strain names of yeast species					
Candida albicans	*Candida glabrata*	*Candida parapsilosis*	*Candida tropicalis*	*Candida krusei*	*Cryptococcus neoformans*
TW1	AU186	AU119	AU232	AU257	H99[a]
TW12	AU187	AU120	AU233	AU258	ATCC34883[b]
	AU231	AU181	AU256	AU275	JEC20[c]

[a] *C. neoformans var. grubii* (serotype A)
[b] *C. neoformans var. gattii* (serotype C)
[c] *C. neoformans var. neoformans* (serotype D)

are listed in Table 2.1. There were three strains of each species, except for *C. albicans* where there were two. For *C. neoformans*, the three strains were each of a different variety (*var. grubii, gattii* and *neoformans*). All strains were cultured on YEPD-agar plates or YEPD broth and grown at 37 °C, except for the *C. neoformans var. gattii,* serotype C strain that was grown at 30 °C. Strains were stored at –70 °C in 20% glycerol-YEPD.

2.3.3 Determining the phylogenetic relationship between yeasts

Partial 26S rRNA sequences were used to determine the phylogenetic relationship between yeasts and their sequences were obtained from the NCBI GenBank (www.ncbi.nlm.nih.gov/entrez/query.fcgi?db=Nucleotide&itool=toolbar). The nucleotide sequence accession numbers for *C. albicans, C. glabrata, C. parapsilosis, C. tropicalis, C. krusei* and *C. neoformans* are AY497673, AY497670, AY497686, AY497695, AY497686 and F335984 respectively. A phylogenetic tree was constructed using the unweighted pair group method with arithmetic mean (UPGMA), using the computer program PAUP4d64 (Swofford, D., 2001).

2.3.4 Preparation of cells for GC-MS analysis

For GC-MS analysis, all strains were grown to stationary phase in Erlenmeyer flask cultures at 37 °C in an incubator shaker at 200 rpm (innova 4300, New Brunswick Scientific, Edison, NJ, USA) except for the *C. neoformans var. gattii,* serotype C strain that was grown at 30 °C, also shaking at 200 rpm

(series 25 incubator shaker, New Brunswick Scientific, Edison, NJ, USA). Cells were harvested and disrupted for metabolite analysis by the same method described in Chapter 1 (please see 1.3.8). After cellular proteins and enzymes were deactivated for 15 mins in a 70 °C water bath (Fisher Iso-temp 205, Whitby, ON, Canada), each sample was separated into two phases (polar and lipid) by a series of extraction steps. The polar phase was extracted with a 1:1 solution of methanol:water, while the lipid phase was extracted twice with chloroform. The lipid phase was then saponified with 33% methanolic KOH on a dry heating block (Fisher Iso-temp Economical, Whitby, ON, Canada) at 45 °C for 2.5 hrs. After this, polar and saponified lipid extracts were stored at –20 °C until ready for running on the GC-MS. A detailed procedure for harvesting, bead-grinding and phase separation can be found in Appendix A.2, A.3 and A.4 respectively.

When samples were ready to be run on the GC-MS, polar and lipid extracts were defrosted to room temperature and then an aliquot was transferred into separate 1-ml conical thick-walled glass reaction vials (Chromatographic Specialties, Brockville, ON, Canada) together with an internal standard. Ribitol (2 mg/ml, dissolved in ddH_2O) and 5β-cholestan-3α-ol (0.1 mg/ml, dissolved in chloroform) were used as internal standards for the polar and lipid phases, respectively. For the polar phase, 230 μl of extract and 4.31 μl of ribitol were blown to dryness under a stream of N_2 gas (Meyer N-evap Organomation model 111, Berline, MA, USA) with an airflow pressure of 20 psi and the bottom of the tubes suspended in a water bath set at 40 °C. Then 50 μl of 20 mg/ml

methoxyamine dissolved in pyridine was added to the reaction vial and allowed to incubate for 1.5 hrs at 30 °C. Methoxyamine was added to protect carbonyl moieties in sugars from forming cyclic derivatives that would make the metabolite profiles more complicated. In other words, this would allow sugars to occur in one form. After this, the polar metabolites were derivatized with 80 μl of N-methyl-N-trimethylsilyl-trifluoroacetamide (MSTFA) for 30 mins at 37 °C in a dry heating block (Fisher Iso-temp Economical, Whitby, ON, Canada). Derivatized polar samples were diluted 25X with hexane in GC auto-sampler vials (Chromatographic specialties, Brockville, ON, Canada) by a robot (Gerstel MPS2 Multi-purpose sampler, Gerstel, Baltimore, MD, USA) before 1 μl was injected into the GC-MS instrument for analysis. The lipid phase was treated similarly with the omission of the methoxyamine step. Saponified lipid extracts (500 μl) plus 5 μl of 5β-cholestan-3α-ol were blown down to dryness with N_2 gas, then re-dissolved in 20 μl pyridine and derivatized with 30 μl MSTFA. Derivatized lipid samples were diluted 1:1 with hexane and 1 μl was injected into the GC-MS instrument for analysis. A detailed protocol for the derivatization step is found in Appendix A.5. All yeast strains were analyzed by GC-MS in duplicate. A summary of the entire process, from harvesting cells to injecting samples in the GC-MS is illustrated in a flow chart (Fig. 2.1).

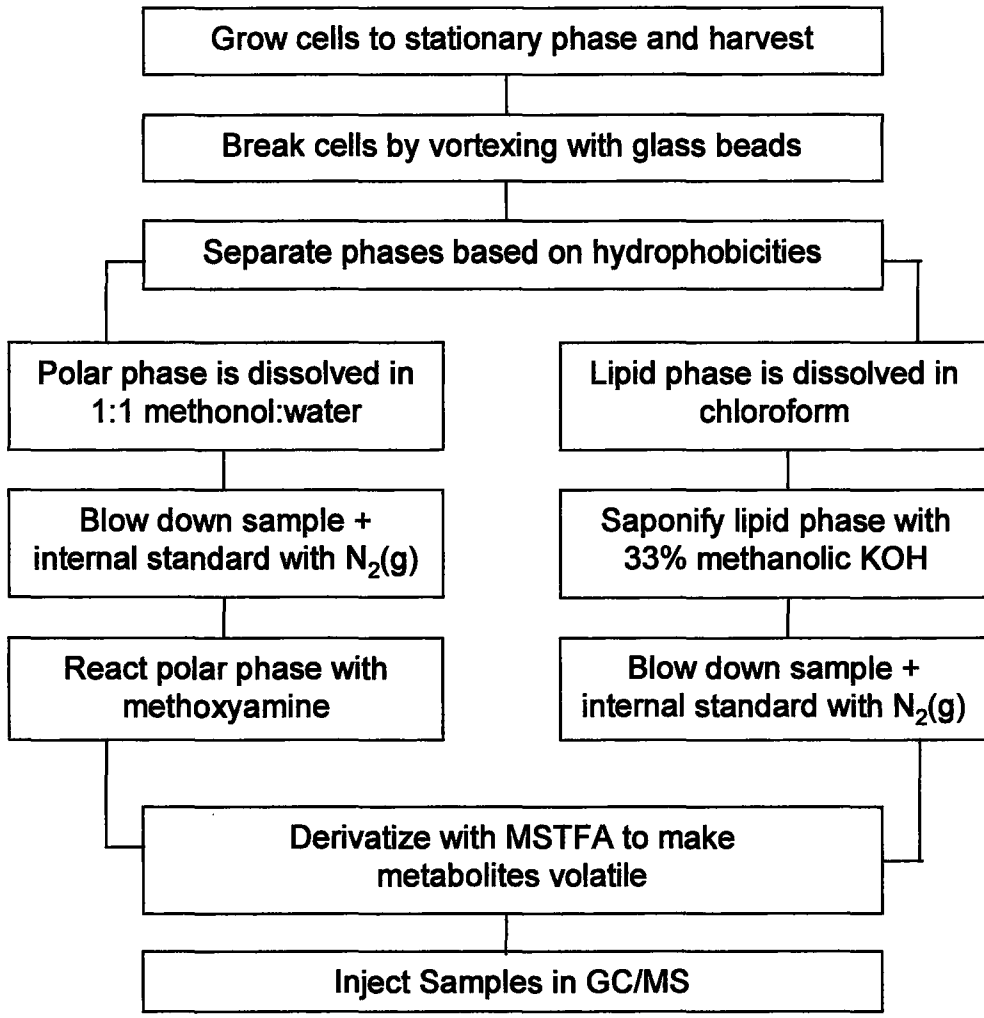

Fig. 2.1 Summary of the procedure used for preparing yeast cells for GC/MS analysis.

2.3.5 GC-MS instrument and temperature program

The GC-MS instrument and temperature program in this study was the same as that used in Chapter 1. Please refer to the Materials and Methods section (1.3.9) for those details. In summary, the gas chromatography-mass spectrometry (GC-MS) system was composed of a Gerstel Multipurpose sampler (MPS2) (Gerstel Inc., Baltimore, MD, USA), a Trace GC gas chromatograph, and a Trace DSQ quadrupole mass spectrometer (Thermo-Finnigan, Mississauga, ON, Canada). The temperature program was as follows: the oven temperature was isocratic at 50 °C for 2.5 min and was increased to 70 °C at a rate of 7.5 °C min^{-1}. The oven temperature was increased at 5 °C min^{-1} to 310 °C, and was held for 1 min at 310 °C. The oven was then cooled down to 50 °C before injection of the next sample.

Peaks in the gas chromatograms were tentatively identified by comparisons of their mass spectra with the National Institute of Standards and Technology (NIST) MS search library version 2.0 and Fiehn library (www.mpimp-golm.mpg.de/mms-library/index-e.html) (Fiehn, O. et al., 2000).

2.3.6 GC-MS data analysis

After peak areas (or area under peaks) from each gas chromatogram were extracted from the Xcalibur program, they were exported to Microsoft Excel. Peak areas were standardized with the internal standard: ribitol for the polar phase or 5β-cholestan-3α-ol for the lipid phase to generate a normalized peak

area (NPA) for every peak (described further in 1.3.10). Individual peaks in the metabolite profiles of all species were manually aligned according to their retention times (RT) and mass spectra (MS) so that profiles could be compared to each other. For qualitative analysis of the data, peak values were converted into a binary format where 1 indicated the presence of the peak and 0 meant that the peak was absent. In separate analyses, quantitative and qualitative peak values were clustered hierarchically with a program called MetaGeneAlyse (MGA), version 1.5 (Daub, C. et al., 2003) that is also accessible on the world wide web (http://metagenealyse.mpimp-golm.mpg.de/). This program was used to first normalize metabolite data, then construct Euclidean distance matrices, followed by complete hierarchical clustering of these distances, finally generating a dendrogram where individual clades consisted of peaks that were unique to one or a group of species. Qualitative binary data did not have to be normalized while quantitative data was normalized to the mean of each peak (or each row). Qualitative metabolite data was also used to generate phylogenetic trees with UPGMA.

2.4 RESULTS

2.4.1 Polar metabolite profiles of the six pathogenic yeasts

The polar metabolite profiles of the five Candida yeasts can be visualized in Fig. 2.2. In all polar profiles, most of the visible peaks were distributed from retention times (RT) 6 - 28 mins, with fewer peaks found after a RT of 28 mins.

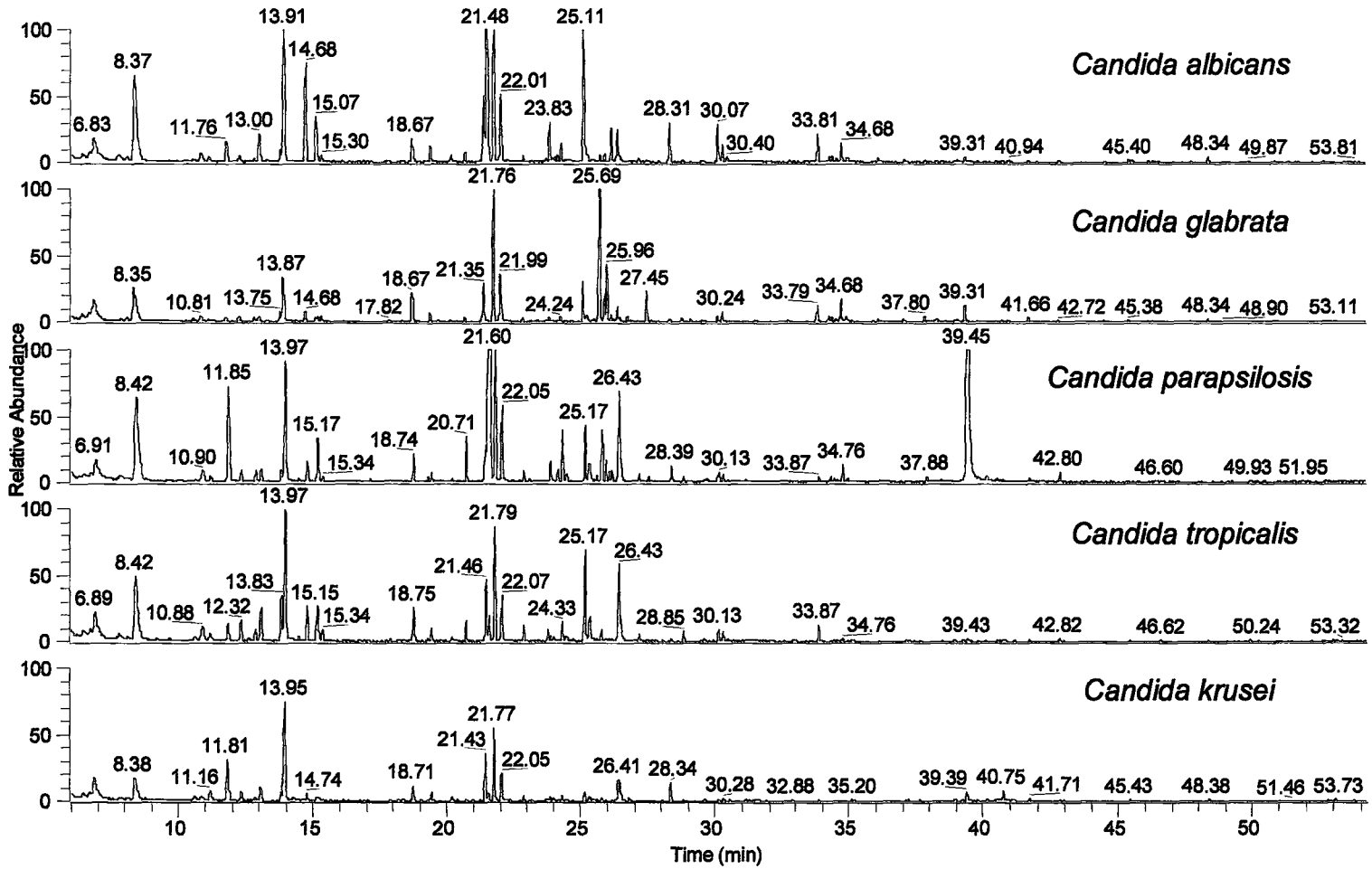

Fig. 2.2 Polar metabolite profiles for representative strains of five Candida sp. (ascomycetes)

The number of peaks detected in the polar metabolite profiles of these yeasts ranged from 89 in *C. krusei* to 120 in *C. parapsilosis* (Table 2.2). Overall, the profiles for all five Candida sp. were very similar, although there were differences with respect to the levels of polar metabolites. By visual inspection, many peaks in the *C. krusei* polar metabolite profile were lower in abundance than respective peaks belonging to the other four Candida sp. One large peak (RT 39.45 mins) stood out in the polar profile of *Candida parapsilosis* that did not appear to be present in the profiles of the other Candida sp. to such a high level. However, that peak was present at similar levels in all three varieties of *C. neoformans* (Fig. 2.3).

The polar metabolite profiles for the different varieties of *C. neoformans* (Fig. 2.3) looked different from each other although strains of the *var. grubii* and *var. gattii* looked more similar to each other than the *var. neoformans* strain. The polar metabolite profiles of the serotype A *C. neoformans var. grubii* and the serotype D *C. neoformans var. neoformans* strains were analyzed more thoroughly and peak differences are summarized in Table 2.3. Overall, there were more peaks detected in the polar metabolite profile of *C. neoformans var. neoformans* than *var. grubii* (Table 2.2). There were also a large number of peaks that were either unique to or significantly increased (45 peaks altogether) in *C. neoformans var. neoformans* and some of them have been identified as members of the citric acid cycle, amino acids and sugar alcohols (Table 2.3).

Table 2.2 Number of potential species-specific polar metabolites in the six pathogenic yeasts.

Yeast Species	Total No. Peaks	No. Unique Peaks[a]
C. albicans	99	5
C. glabrata	103	11
C. parapsilosis	120	16
C. tropicalis	96	3
C. krusei	89	7
C. neoformans var. grubii	68	2
C. neoformans var. neoformans	88	10

[a] Peaks are unique relative to all other species listed in this table

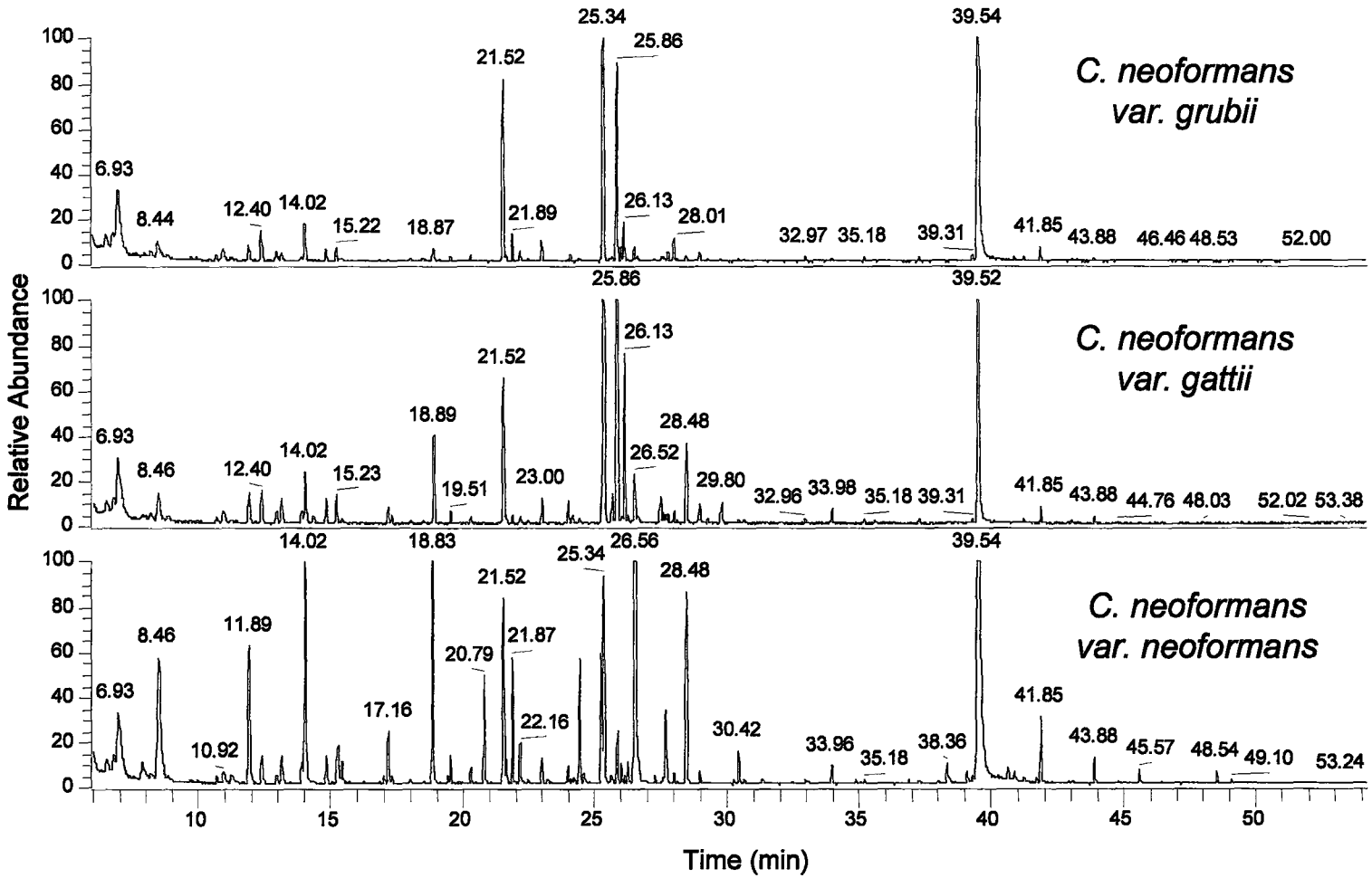

Fig. 2.3 Polar metabolite profiles for representative strains of three varieties of *Cryptococcus neoformans* (basidiomycetes) show that *C. neoformans var. grubii* is more similar to *var gattii* than *var. neoformans*.

Table 2.3 Summary of peak differences between the polar metabolite profiles of the serotype A *C. neoformans var. grubii* and the serotype D *C. neoformans var. neoformans*.

Description of Peaks	No. Peaks	Polar Metabolites Identified[b]
Increased[a] in *C. neoformans var. grubii* (sero. A)	2	none
Increased[a] in *C. neoformans var. neoformans* (sero. D)	20	alanine, glutamine, proline, aspartic acid, ornithine, succinic acid, malic acid, phosphate, glycerol, myo-inositol
Unique in *C. neoformans var. grubii* (sero. A)	7	none
Unique in *C. neoformans var. neoformans* (sero. D)	25	lysine, fumaric acid

[a] Significantly increased ($p < 0.05$)
[b] Putative identifications made with NIST and Fiehn libraries

None of the peaks unique to or increased in *C. neoformans var. grubii* have been identified.

There was also a portion of the polar phase gas chromatogram from RT 23 - 31 mins where there were obvious differences in the pattern of peaks across the six pathogenic yeasts (Fig. 2.4). Within this region, the Candida and Cryptococcus species from this study could be easily distinguished from one another by visual examination. Although, *C. parapsilosis* looked similar to *C. tropicalis*, there were more peaks at a higher abundance in *C. parapsilosis*. Likewise, *C. neoformans var. grubii* and *var. gattii* also looked very similar to each other but peaks were at higher levels in *C. neoformans var. gattii*.

MetaGeneAlyse hierarchical cluster analysis revealed that there were several unique peaks in each species relative to all other species examined in this study. The complete list of aligned peaks in *C. albicans, C. glabrata, C. parapsilosis, C. tropicalis, C. krusei, C. neoformans var. grubii* and *C. neoformans var. neoformans* can be found in Appendices B.2 (qualitative data, binary format) and B.3 (quantitative data, actual peak abundances). Altogether, 185 total peaks were aligned in the polar phase. Of these 185 peaks, 37 or 20% were common to all the yeast species in this analysis. The actual dendrograms generated by the MGA programme from qualitative and quantitative polar metabolite data are in Appendices D.1 and D.2 respectively. The species-specific peaks or peaks unique to each species are summarized in Table 2.2. From this table, it is evident that a large number of peaks were unique to *C.*

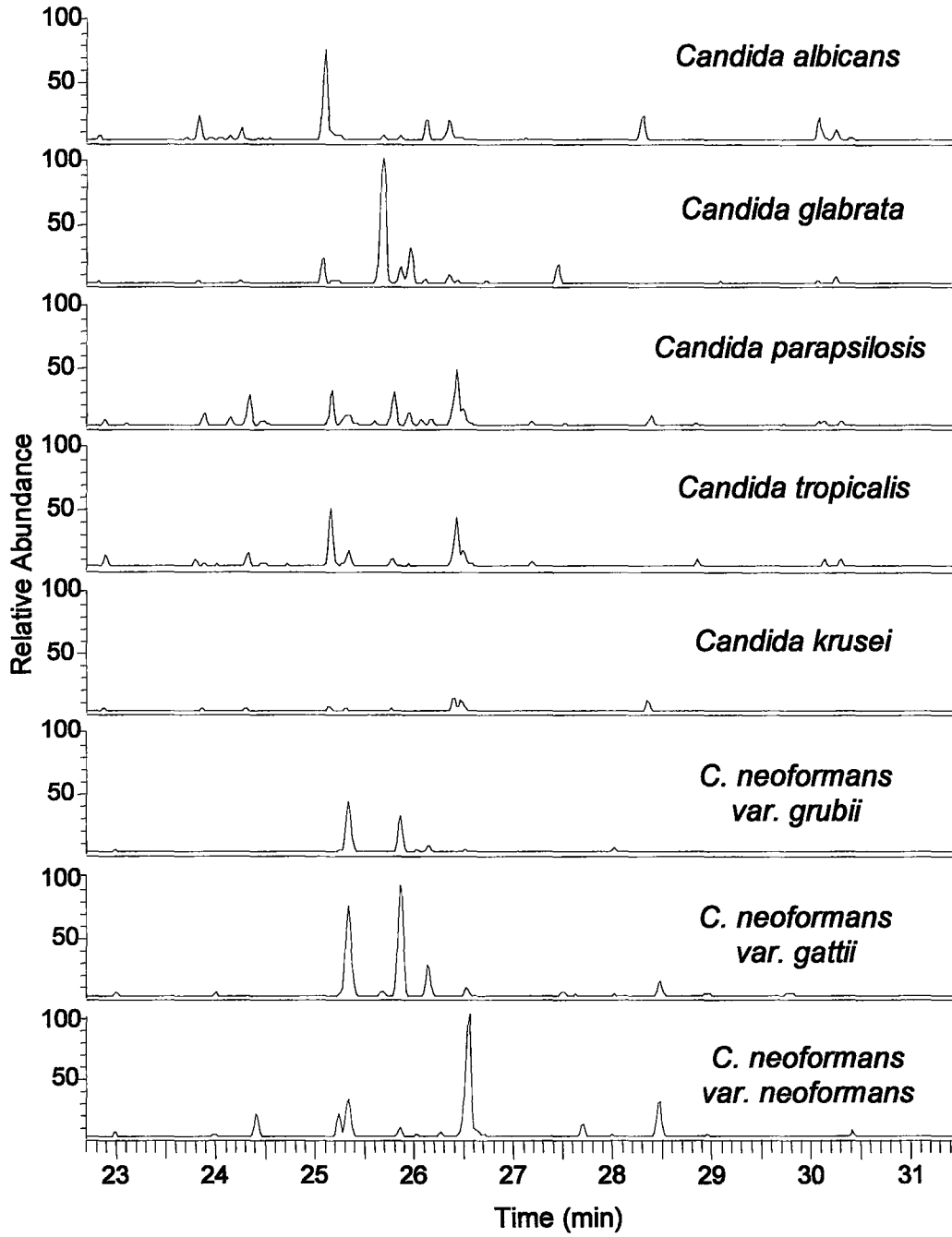

Fig. 2.4 A region in the polar phase gas chromatogram from RT 23 to 31 mins that shows differences between Candida and Cryptococcus yeasts.

parapsilosis (16 peaks), *C. glabrata* (11 peaks) and *C. neoformans var. neoformans* (10 peaks). The majority of these species-specific polar metabolites are unknown. However, in *C. neoformans var. neoformans*, one of those species-specific metabolites was identified as glucose. This will be discussed further in the next section (2.5).

A summary of all the classes of compounds identified in the polar metabolite profiles of all six pathogenic yeasts is presented in Table 2.4. Out of 185 total peaks from the alignment of polar phase data in these yeasts, 26 peaks were found to span five classes of compounds based on their characteristic mass to charge ratios (m/z). There were 14 amino acids, 4 organic acids, 4 phosphorylated compounds, 2 sugar alcohols and 2 sugars. Of these 26 peaks, only 22 were putatively identified using the NIST and Fiehn libraries (Table 2.4).

The quantitative polar metabolite data provided more information about these yeast species. For example, certain peaks were present at elevated levels in one species but not the rest. In reference to Appendix B.3, peaks "p56", "p73" and "p141" were very abundant in *C. parapsilosis* while peaks "p87", "p90", "p91" and "p101" were at high levels in *C. glabrata*. There are also large clades in the dendrogram (Appendix D.3) that represented peaks at similar levels in pairs or groups of species. There were 11 peaks that were at levels greater than the mean in *C. parapsilosis* and *C. neoformans var. neoformans* (serotype D), 8 peaks were similar in *C. parapsilosis* and *C. tropicalis* and another 8 peaks were similar in *C. albicans* and *C. parapsilosis*. There were 2 clades with 12 and 6

Table 2.4 Classes of compounds identified in the aligned polar metabolite profiles of the six pathogenic yeasts

Class of Compound	Characteristic m/z[a]	Total No. Peaks	Polar Metabolites Identified[b]
Amino acids	various	14	alanine, glycine, leucine, iso-leucine, valine, serine, methionine, proline, glutamine, glutamic acid, aspartic acid, phenylalanine, lysine, ornithine
Organic acids	various	4	citric acid, succinic acid, fumaric acid, malic acid
Phosphorylated compounds	243, 299, 315	4	phosphate
Sugar alcohols	103, 205, 217	2	glycerol, myo-inositol
Sugars	117, 129, 191, 204, 205, 217, 319	2	glucose

[a] Obtained from Halket, J. (1993)
[b] Putative identifications made with NIST and Fiehn libraries

peaks each (totaling 18 peaks) where peak levels were higher than the mean in *C. albicans* and *C. glabrata*.

2.4.2 Lipid metabolite profiles of the six pathogenic yeasts

The lipid metabolite profiles of the Candida yeast species are presented in Fig. 2.5. In general, peaks were distributed throughout the lipid phase gas chromatogram, with a group of large peaks that were concentrated from RT 28 - 35 mins in all species. There were more peaks detected in the lipid metabolite profiles than the polar metabolite profiles. The number of peaks in the lipid profiles of these yeast species ranged from 143 to 156 peaks (Table 2.5). Upon visual inspection, the lipid profiles for all five Candida species looked very similar to each other from the beginning of the run until a RT of about 42 mins. After 42 mins, the lipid profiles of *C. parapsilosis* resembled *C. neoformans var. gattii* (Fig. 2.5) more than the other 4 Candida sp. In that same region, the lipid profiles looked very similar among *C. albicans*, *C. glabrata* and *C. krusei*.

By visual examination, the lipid metabolite profiles of the three varieties of *C. neoformans* were also very similar to each other and to the profiles of the Candida sp. (Fig. 2.6). However, the region of the gas chromatogram from RT 40 - 53 mins showed more differences between the *C. neoformans* varieties. The lipid metabolite profiles of *C. neoformans var. grubii* and *C. neoformans var. neoformans* were analyzed in more detail and there were very few differences between them. There were 3 unique peaks and 2 other peaks that were significantly increased in *C. neoformans var. grubii*. In *C. neoformans var.*

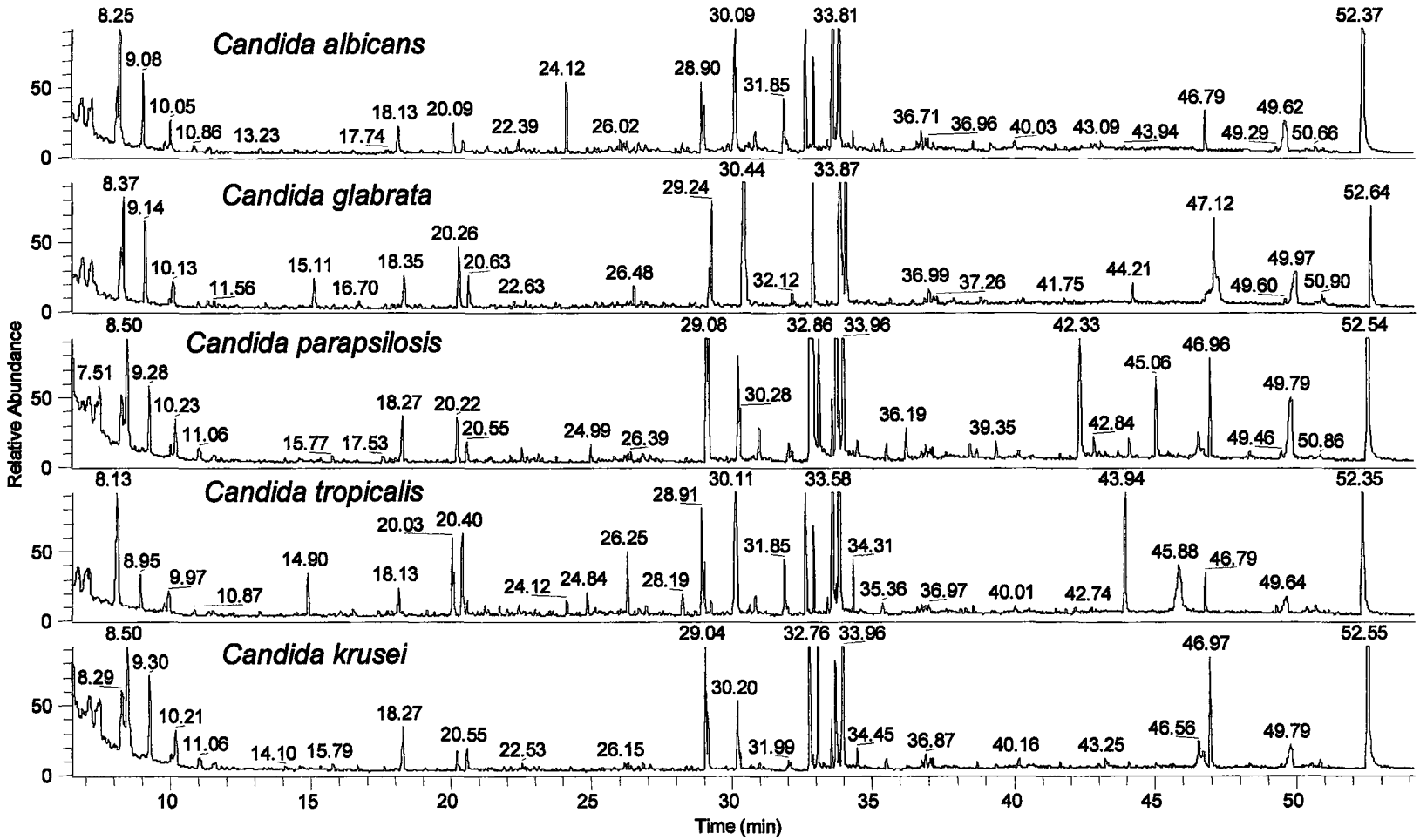

Fig. 2.5 Lipid metabolite profiles for representative strains of five Candida sp. (ascomycetes)

Table 2.5 Number of potential species-specific lipid metabolites in the six pathogenic yeasts.

Yeast Species	Total No. Peaks	No. Unique Peaks[a]
C. albicans	143	0
C. glabrata	147	14
C. parapsilosis	152	0
C. tropicalis	156	5
C. krusei	144	0
C. neoformans var. grubii	153	12

[a] Peaks are unique relative to all other species listed in this table

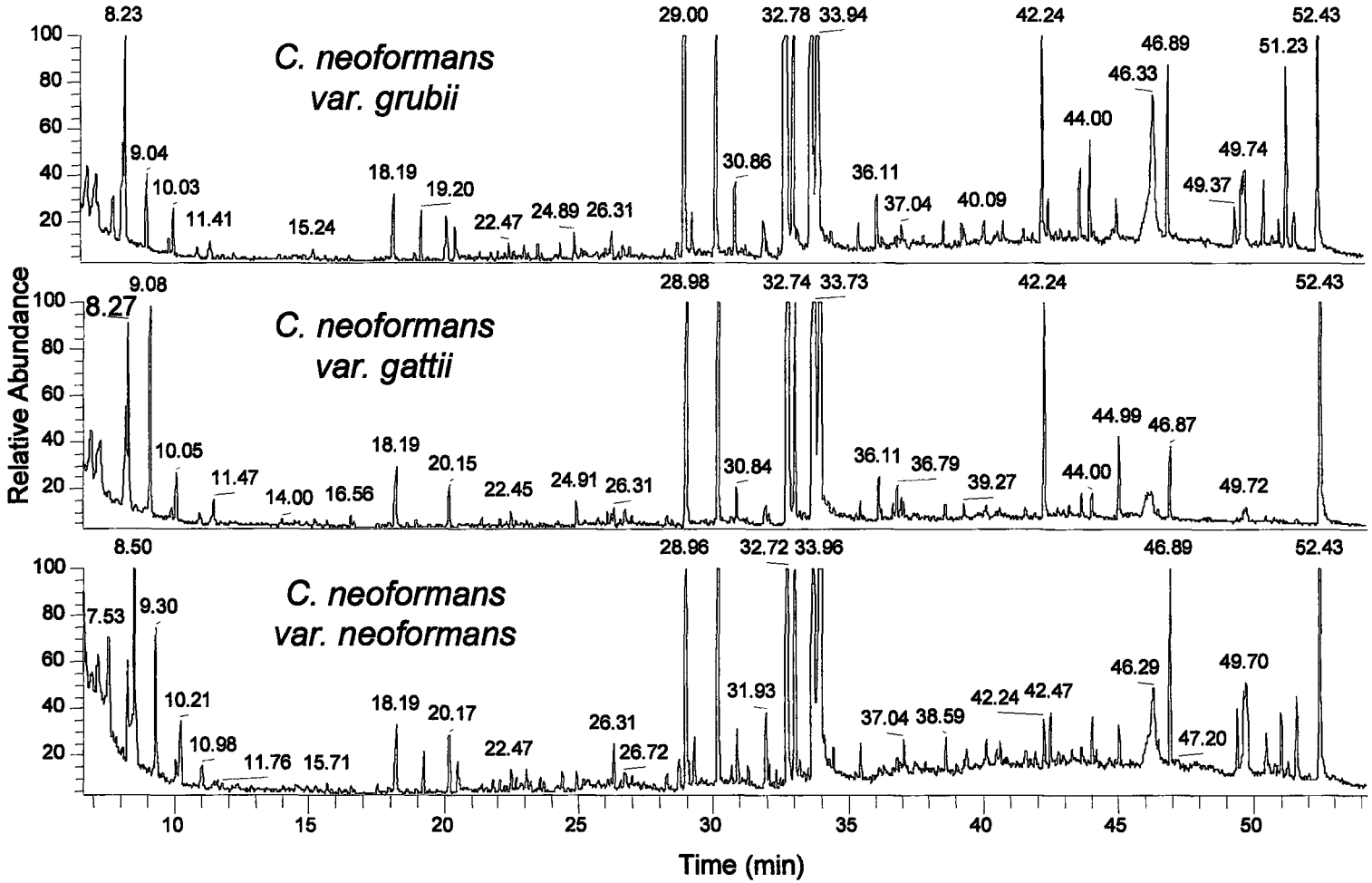

Fig. 2.6 Lipid metabolite profiles for representative strains of three varieties of *Cryptococcus neoformans* (basidiomycetes) look similar.

neoformans, only one peak was significantly increased and there were 2 peaks that were unique (Table 2.6).

Similar to polar phase profiles, there was a short region in the lipid phase gas chromatograms (RT 41 - 52 mins) of the six pathogenic yeasts that showed some peak differentiation (Fig. 2.7). Although *C. parapsilosis* resembled *C. neoformans var. gattii* and *C. albicans,* C. *glabrata* and *C. krusei* resembled each other, they were distinguishable from *C. tropicalis* and the other *C. neoformans* varieties. Comparing the three varieties of *C. neoformans*, the beginning of this region of the gas chromatogram (RT 41 - 45 mins) in *var. grubii* was more similar to *var. gattii.* However, after RT 45 mins the gas chromatogram of *C. neoformans var. grubii* was more similar to that of *var. neoformans.*

Since the lipid metabolite profiles appeared to be fairly conserved by visual inspection, it was not subject to the same extensive analysis as the polar metabolite data. Only qualitative lipid phase data was analysed with the MetaGeneAlyse program for the yeast species *C. albicans, C. glabrata, C. parapsilosis, C. tropicalis, C. krusei* and *C. neoformans var. grubii.* This data is in a tabular format in Appendix B.4 and the dendrogram generated from this data is in Appendix D.3. This analysis revealed that 105 out of 197 aligned peaks or 53% of peaks were shared among these six yeasts. There were also peaks that were unique to a few yeast species and they are summarized in Table 2.5. A large number of unique peaks were detected for *C. glabrata* (14 peaks) and *C.*

Table 2.6 Summary of peak differences between the lipid metabolite profiles of the serotype A *C. neoformans var. grubii* and the serotype D *C. neoformans var. neoformans*.

Description of Peaks	No. Peaks
Increased[a] in *C. neoformans var. grubii* (sero. A)	2
Increased[a] in *C. neoformans var. neoformans* (sero. D)	1
Unique in *C. neoformans var. grubii* (sero. A)	3
Unique in *C. neoformans var. neoformans* (sero. D)	2

[a] Significantly increased ($p < 0.05$)

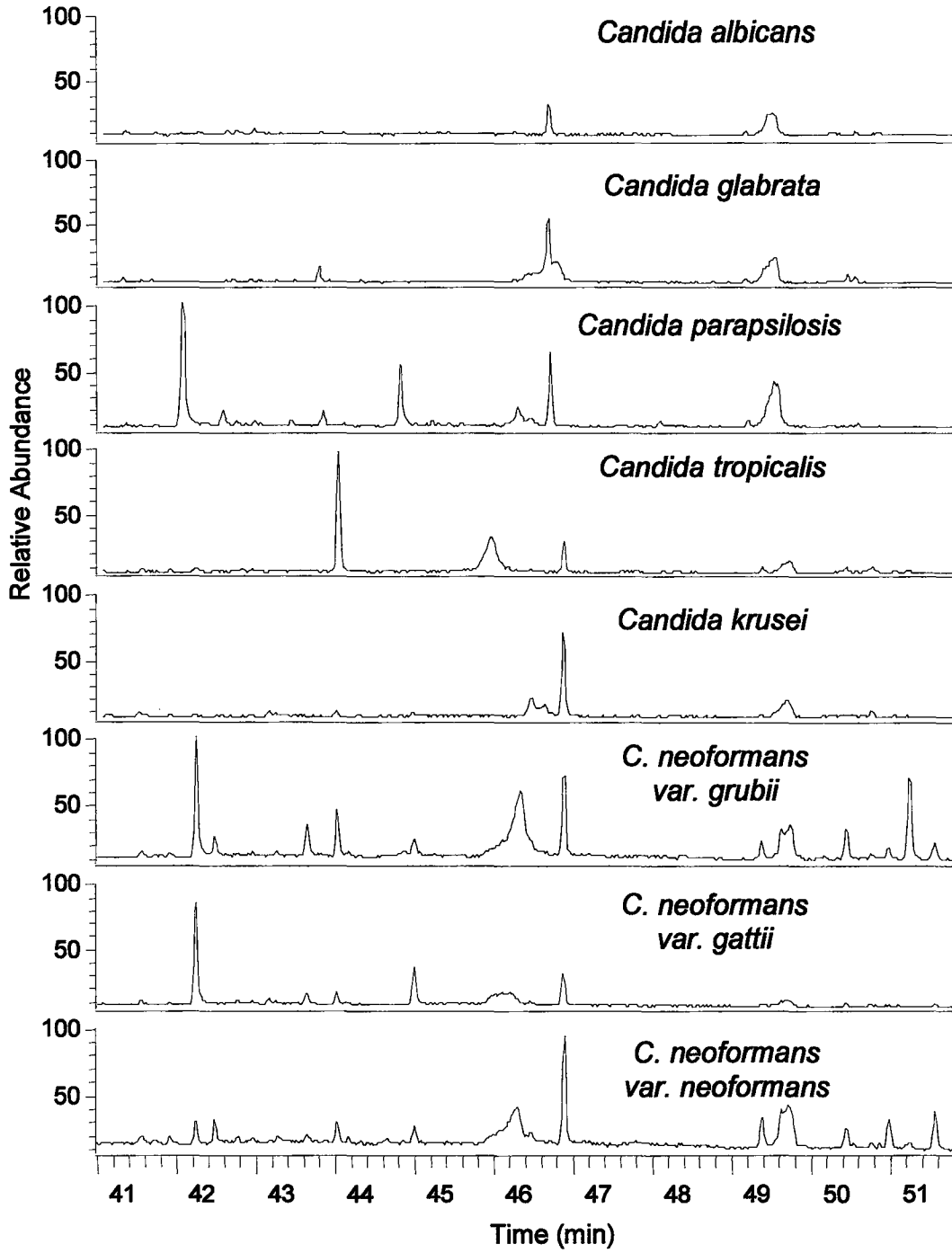

Fig. 2.7 A region in the lipid phase gas chromatogram from RT 41 to 52 mins that shows differences between Candida and Cryptococcus yeasts.

neoformans var. grubii (12 peaks). However, no unique peaks were detected in the lipid profiles of *C. albicans, C. parapsilosis* and *C. krusei.*

2.4.3 Comparison of metabolite data with 26S rRNA sequences for the taxonomical classification of yeasts

The phylogenetic relationship between the pathogenic yeast species from this study was determined using partial sequences of 26S rRNA and the dendrogram constructed using the UPGMA method with qualitative metabolite data for the six yeast species in this study (*C. albicans, C. glabrata, C. parapsilosis, C. tropicalis, C. krusei* and *C. neoformans var. neoformans*). The dendrograms in Fig. 2.8 showed that there was no correlation between polar metabolite data and 26S rRNA sequences. However, the dendrogram constructed with lipid metabolite data was more similar to the dendrogram based on 26S rRNA sequences. Polar metabolites appeared to change more rapidly while there were fewer changes in lipid metabolites between species.

2.5 DISCUSSION AND CONCLUSIONS

It is estimated that in the baker's yeast *Saccharomyces cerevisiae*, there are about 600 low molecular weight metabolites (Raamsdonk, L. et al., 2001). However, this is most likely an underestimation because in other organisms, the metabolome exceeds the number of genes encoding the enzymes that are involved in their biochemical pathways (Schwab, W., 2003). Some of the reasons that contribute to metabolite diversity can occur at many levels of the cell

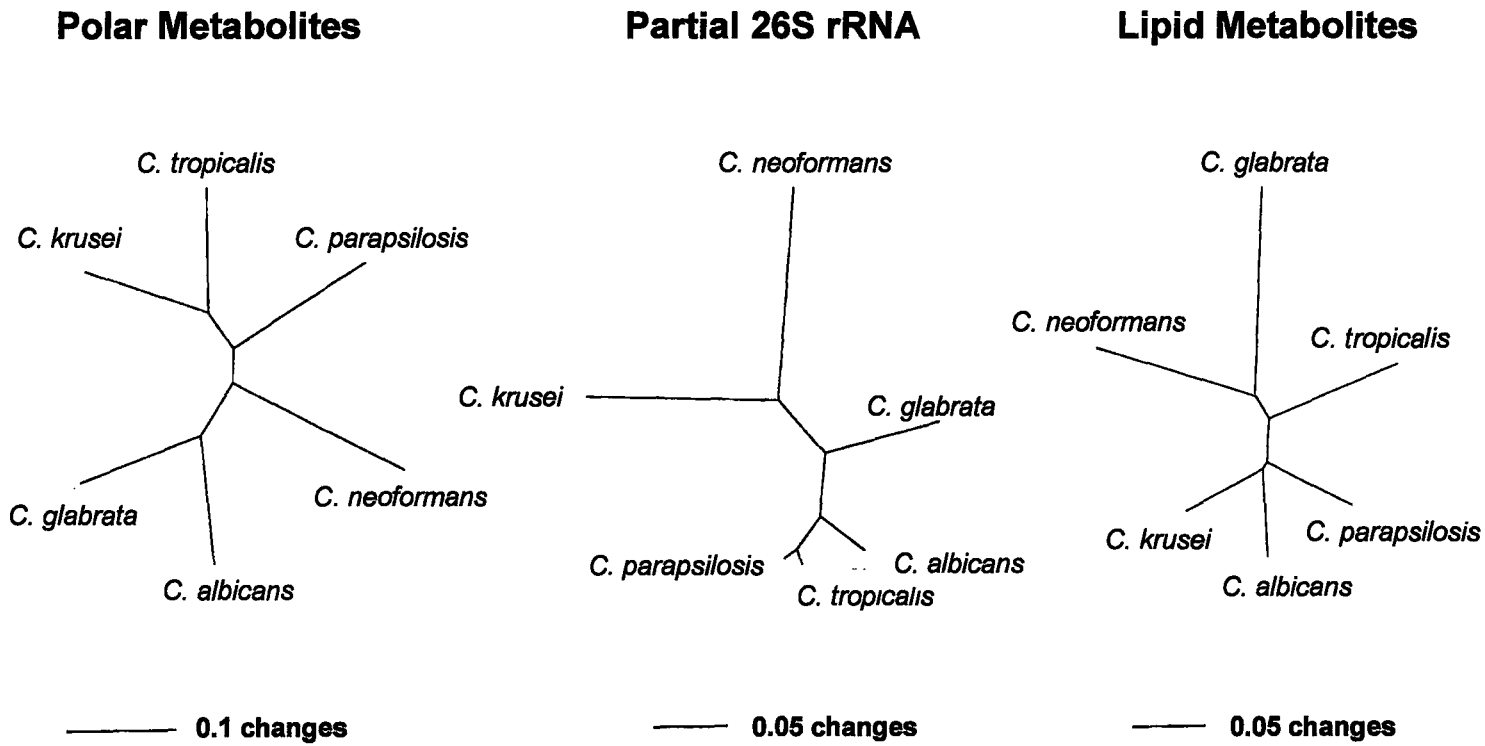

Fig. 2.8 UPGMA dendrograms reveal that lipid metabolites are better correlated to the taxonomy of these six pathogenic yeasts according to 26S rRNA sequences while polar metabolites do not reflect this taxonomical relationship.

from multiple reading frames in DNA that can lead to multiple mRNA transcripts, alternative splicing in mRNA give rise to multiple proteins (Stevens and Abelson, 2002) and post-translational modification of proteins allow for multiple functions per protein (Nevalainen, L. et al., 1989).

In this study, it was found that entire polar GC-MS metabolite profiles could not be used for the a taxonomical classification of *C. neoformans* and Candida sp. in this study due to the lack of correlation with the phylogenetic relationships among them determined from partial 26S rRNA sequences. There was large variation within the polar metabolite profiles of different strains of *C. neoformans* itself, which may be explained because they are of different varieties of the same species. Similar conclusions were made in a study where fatty acid methyl esters (FAME) detected by gas-liquid chromatography were tested for their applicability in the identification and classification of 263 yeast strains representing 44 genera (Botha and Kock, 1993a) when it was found that there was a lot of variation as well as overlap of FAME among different species. Lipid metabolite data showed a better correlation than polar metabolite data to the taxonomical relationship between these yeasts according to their 26S rRNA sequences. This is because the lipid metabolites were more conserved, reflecting the conserved nature of 26S rRNA sequences. This was reinforced after the MGA hierarchical clustering analysis revealed that a greater percentage of peaks in the lipid profiles were shared among these yeast species compared to their polar profiles.

Despite the poor correlation of polar metabolite data to the taxonomical relationship of these pathogenic yeasts, polar metabolites may be a better choice when it comes to identifying and distinguishing between them. A number of unique peaks were present in the polar profiles of all the yeast species in this study. There were also a number of peaks in the polar metabolite profile that were at elevated levels in *C. glabrata* compared to the other five pathogenic yeasts and a different set of peaks that were elevated only in *C. parapsilosis*. There were species-specific peaks in the lipid profiles but only for *C. glabrata, C. tropicalis* and *C. neoformans var. grubii*. The majority of these unique peaks are currently unknown but it would be worthwhile to identify them as they may correspond to metabolites or classes of compounds that would be valuable for distinguishing between these pathogenic yeasts species and can therefore serve as biomarkers. Glucose was putatively identified as a species-specific polar metabolite in *C. neoformans var. neoformans*. There are two possibilities that can explain this; either glucose was synthesized at higher levels than other species or glucose was not used up to the same extent in *C. neoformans var. neoformans* as it was in the other yeast species. Glucose may still be present in other yeast species but at undetectable levels under the GC-MS conditions used in this study. It is also possible that glucose was used up more in the other yeast species.

It has been previously reported that arachidonic acid metabolites were useful for distinguishing between other yeasts in the division Ascomycota. These

metabolites were detected in Lipomycetacetes while they were undetected in Dipodascacetes (Botha and Kock, 1993b). Among Candida sp., FAME was good for differentiating between *C. gilliermondii, C. krusei, C. lusitaniae, C. parapsilosis, C. tropicalis, C. utilis* and *C. valida* (Menyawi, I. et al., 2000) and between *C. albicans* and *C. dubliniensis* (Petroche-Llacsahuanga, H. et al. 2000b) but poor for distinguishing between *C. albicans, C. kefyr* and *C. glabrata* (Menyawi, I. et al., 2000; Crist, A. et al., 1996). Likewise, phospholipids were found to have chemotaxonomic significance when discriminating between eight Candida sp. (Abdi, M. et al., 1999).

Alternatively, using shorter regions of the gas chromatogram rather than the full metabolite profile may be better for distinguishing between these yeasts or may better reflect their taxonomical relationship. The region in the polar phase gas chromatograms from RT 23 - 31 mins showed peak differentiation between the six pathogenic yeasts (Fig. 2.4). However, it is not known what polar metabolites these peaks corresponded to. There was a similar region in the lipid phase gas chromatogram between RT 41 - 52 mins (Fig. 2.7) and this region included sterols. It has been shown that there is considerable variation in the sterol composition of other fungal species (Weete and Gandhi, 1997). The sterol composition in *C. neoformans* is also different from Candida sp. as it was previously reported that obtusifoliol was the major sterol in the basidiomycete (Ghannoum, M. et al., 1994). Therefore it is possible that the distribution and abundance of sterols in pathogenic yeasts may be reflective of their phylogenetic

relationship. Otherwise, these regions of the gas chromatogram can potentially be used for a quick identification of yeast species by visual inspection, especially in combination with detecting species-specific peaks in the complete metabolite profile.

CHAPTER 3

Using gas chromatography-mass spectrometry (GC-MS) to determine the extent of contribution of the metabolite phenotypes from two parents to their hybrid offspring of *Cryptococcus neoformans*

3.1 ABSTRACT

Cryptococcus neoformans is an encapsulated basidiomycete yeast that can cause a number of life-threatening infections in humans. There are three varieties or four haploid serotypes of *C. neoformans* that can be found in nature. Strains of serotypes A are of the variety *grubii*, strains of serotypes B and C belong to the variety *gattii* while serotype D strains are of the variety *neoformans*. While *C. neoformans* predominantly reproduces asexually, some of these haploid serotype strains are also able to mate and produce diploid offspring. In this study, the objective was to determine the extent of contribution of the metabolite phenotypes from a serotype A and serotype D parent strains to their hybrid

serotype AD offspring. The results from this study indicated that the polar metabolite phenotype of the hybrid offspring was dominated by that of the serotype A parent but not the serotype D parent, while the lipid metabolite phenotypes for all three strains of *C. neoformans* resembled each other.

3.2 INTRODUCTION

3.2.1 *Cryptococcus neoformans* and its serotypes

Cryptococcus neoformans is an encapsulated basidiomycete yeast that can be classified according to three varieties or four haploid serotypes that are readily found in nature. Strains of serotypes A are of the variety *grubii*, strains of serotypes B and C belong to the variety *gattii* while serotype D strains are of the variety *neoformans*. All three varieties of *C. neoformans* differ from each other based on their ecological and geographical distributions as well as genetic, biochemical and physiological characteristics. *C. neoformans var. gattii* (serotypes B and C) is known to inhabit the Eucalyptus and other trees in regions where the climate is tropical or sub-tropical (Ellis and Pfeiffer, 1990). Recently, *C. neoformans var. gattii* was isolated from several native tree species from Vancouver Island, Canada (Fraser, J. et al., 2003). On the other hand, *C. neoformans var. grubii* (serotype A) *and var. neoformans* (serotype D) are associated with bird droppings worldwide (Swine-Desgain, D., 1974; Garcia-Hermoso, D. et al., 1997).

C. neoformans is a medically significant yeast because it can be a primary or secondary human pathogen. As a primary pathogen, it is the most common cause of fungal meningitis that can be fatal (Gottfredsson and Perfect, 2000). Otherwise, it is responsible for a high incidence of opportunistic cryptococcal infections in immuno-compromised and AIDS patients (Tey, R. et al., 2003). *C. neoformans var. gattii* can affect both immuno-compromised and immuno-competent people. Recently, there was an outbreak of infection due to serotype B *C. neoformans* in healthy individuals (Fraser, J. et al., 2003). Strains of serotypes A and D are the opportunistic human pathogens. The serotype A strain accounts for about 95% of all *C. neoformans* infections and 99% of cryptococcosis infections in AIDS patients worldwide (Hull and Heitman, 2002; Mitchell and Perfect, 1995), except in Europe (Dromer, F. et al., 1996; Kwon-Chung and Bennett, 1984; Tortorano, A. et al., 1997) and New York city (Steenbergen and Casadevall, 2000) where infections caused by serotype D *C. neoformans* are more prevalent.

3.2.2 Mating in *C. neoformans*

Although not commonly isolated from the environment, diploid strains of *C. neoformans* also exist. It is believed that the primary mode of reproduction for *C. neoformans* is asexual but the sexual life cycle in *C. neoformans* has been well established by the pioneering research of Kwon-Chung (1975). This research led to the discovery that a haploid serotype A and a haploid serotype D strain could easily mate to form a diploid serotype AD hybrid offspring. *C. neoformans*

serotype AD hybrid strains are self-fertile but produce spores that propagate very poorly (Lengeler, K. et al., 2001). Under different conditions, laboratory-induced crosses between serotypes B and C strains were also successful at producing diploid hybrid offspring (Kwon-Chung, K., 1976). While serotype BC hybrids of *C. neoformans* were restricted to the laboratory, serotype AD hybrids have also been isolated from hospital patients in Europe (Boekhout, T. et al., 2001; Tortorano, A. et al., 1997) and San Francisco, USA (Brandt, M. et al., 1996) and pigeon droppings from China (Li, A. et al., 1993).

Mating between two haploid *C. neoformans* strains is also dependent on the mating type. In yeast, there are two mating types: MATa and MATα (Wickes, B., 2002). The MATa parent is compatible with a MATα parent but pairs of MATa/MATa or MATα/MATα strains cannot mate and give rise to offspring.

3.2.3 Objectives of this study

The objective of this study was to assess the metabolite phenotypes of three strains of *C. neoformans*, a haploid serotype A, a haploid serotype D and their diploid serotype AD hybrid. In doing so, the goal was to determine if the metabolite phenotype of the hybrid offspring resulted from equal contribution from both parents or if it was dominated by the phenotype of one parent. The polar and lipid metabolites were analyzed separately by GC-MS.

3.3 MATERIALS AND METHODS

3.3.1 Chemicals, reagents and media

All the chemicals used in this study were purchased from Sigma (Oakville, ON, Canada) and BDH (Toronto, ON, Canada) and Fisher Scientific (Whitby, ON, Canada). Organic solvents and acids were obtained from Caledon Laboratories (Georgetown, ON, Canada), EM Science (Darmstadt, Germany), BDH (Toronto, ON, Canada), ACP (Montreal, PQ, Canada) and Fisher (Whitby, ON, Canada). Ingredients to make culturing media were purchased from BD Biosciences (Mississauga, ON, Canada). N-methyl-N-trimethylsilyl-trifluoro acetamide (MSTFA) for derivatizing samples for GC-MS analysis was obtained from Pierce (Brockville, ON, Canada). Internal standards: ribitol and 5β-cholestan-3α-ol were obtained from Sigma (Oakville, ON, Canada).

3.3.2 *C. neoformans* strains, culture and storage conditions

Three *C. neoformans* strains were used in this study: a haploid serotype A, MATα strain (H99), a haploid serotype D, MATa strain (JEC20) and their diploid hybrid offspring, a serotype AD, MATa/α strain (Cn9920). All strains were cultured on yeast-extract-peptone-dextrose (YEPD) agar plates or YEPD broth and grown at 37 °C. Strains were stored at –70 °C in 20% glycerol-YEPD.

3.3.3 Preparation of yeast cells for GC-MS analysis

For strains to be analyzed by GC-MS, it was first grown to stationary phase in Erlenmeyer flask cultures at 37 °C in an incubator shaker at 200 rpm (innova 4300, New Brunswick Scientific, Edison, NJ, USA). Cells were harvested and disrupted for metabolite analysis by the same methods used in Chapters 1 and 2 (please refer to 1.3.8 for details). Sample were then phase separated by a series of extraction steps described previously in the Materials and Methods section in Chapter 2 (see 2.3.4). Detailed procedures for harvesting, bead-grinding and phase separation can also be found in Appendix A.2, A.3 and A.4 respectively.

Samples were prepared for running on the GC-MS by the same derivatization process described in Chapter 2 (see 2.3.4). Derivatized polar samples were diluted 25X with hexane in GC auto-sampler vials (Chromatographic specialties, Brockville, ON, Canada) by a robot (Gerstel MPS2 Multi-purpose sampler, Gerstel, Baltimore, MD, USA) before 1 μl was injected into the GC-MS instrument for analysis. Derivatized lipid samples were diluted 1:1 with hexane and 1 μl was injected into the GC-MS instrument for analysis. A detailed protocol for the derivatization step is also found in Appendix A.5. All *C. neoformans* strains were analyzed by GC-MS in duplicate.

3.3.4 GC-MS instrument and temperature program

The GC-MS instrument and temperature program in this study was the same as that used in Chapters 1 and 2. Please refer to the Materials and

Methods section (1.3.9) for details on GC-MS instrument and temperature program. In summary, the gas chromatography-mass spectrometry (GC-MS) system was composed of a Gerstel Multipurpose sampler (MPS2) (Gerstel Inc., Baltimore, MD, USA), a Trace GC gas chromatograph, and a Trace DSQ quadrupole mass spectrometer (Thermo-Finnigan, Mississauga, ON, Canada). The temperature program was as follows: the oven temperature was isocratic at 50 °C for 2.5 min and was increased to 70 °C at a rate of 7.5 °C min^{-1}. The oven temperature was increased at 5 °C min^{-1} to 310 °C, and was held for 1 min at 310 °C. It was then cooled down to 50 °C before injection of the next sample. Peaks were tentatively identified by comparisons of their mass spectra with the National Institute of Standards and Technology (NIST) MS search library version 2.0 and Fiehn library (www.mpimp-golm.mpg.de/mms-library/index-e.html) (Fiehn, O. et al., 2000).

3.3.5 GC-MS data analysis

Peak areas from each gas chromatogram were extracted from the Xcalibur program and then exported to Microsoft Excel. Peak areas were normalized with the internal standard to generate the normalized peak area (NPA) for every peak (described further in 1.3.10). Individual peaks in all metabolite profiles were then manually aligned according to their retention times (RT) and mass spectra (MS) so that comparisons could be made between different *C. neoformans* strains.

3.4 RESULTS

3.4.1 Polar metabolite profiles of the *C. neoformans* strains

By visual inspection, the polar metabolite phenotype of the serotype AD hybrid was more similar to the polar metabolite phenotype of its serotype A parent, H99 rather than its serotype D parent, JEC20 (refer to Fig. 3.1). For a more extensive analysis, the peak abundances from the polar metabolite profiles of the serotype AD hybrid strain were categorized by their similarities and differences to respective peaks in the serotype A and D parent strains (Table 3.1). This analysis of the data showed that 57% of the peaks in the serotype AD hybrid strain were at levels that were either identical or closer to the serotype A parent than the serotype D parent. Only 10% of the peaks in the hybrid strain were identical or more similar to the serotype D parent. About 16% of the peaks in the hybrid were not significantly different from either parent. Altogether, 21 out of 93 total peaks detected were identified using the NIST and Fiehn libraries (Table 3.1). The polar metabolites in the serotype AD hybrid strain that were similar to the serotype A parent included components of the citric acid cycle, various amino acids and sugar alcohols. Two out of nine polar metabolites in the hybrid that were similar to the serotype D parent were identified as serine and phenylalanine. Although there were 9 peaks in the serotype AD hybrid strain that were at levels that were different from both parents, all peaks in the polar metabolite profile of the hybrid were present in either the serotype A or the serotype D parent. In other words, there were no peaks that were unique to the

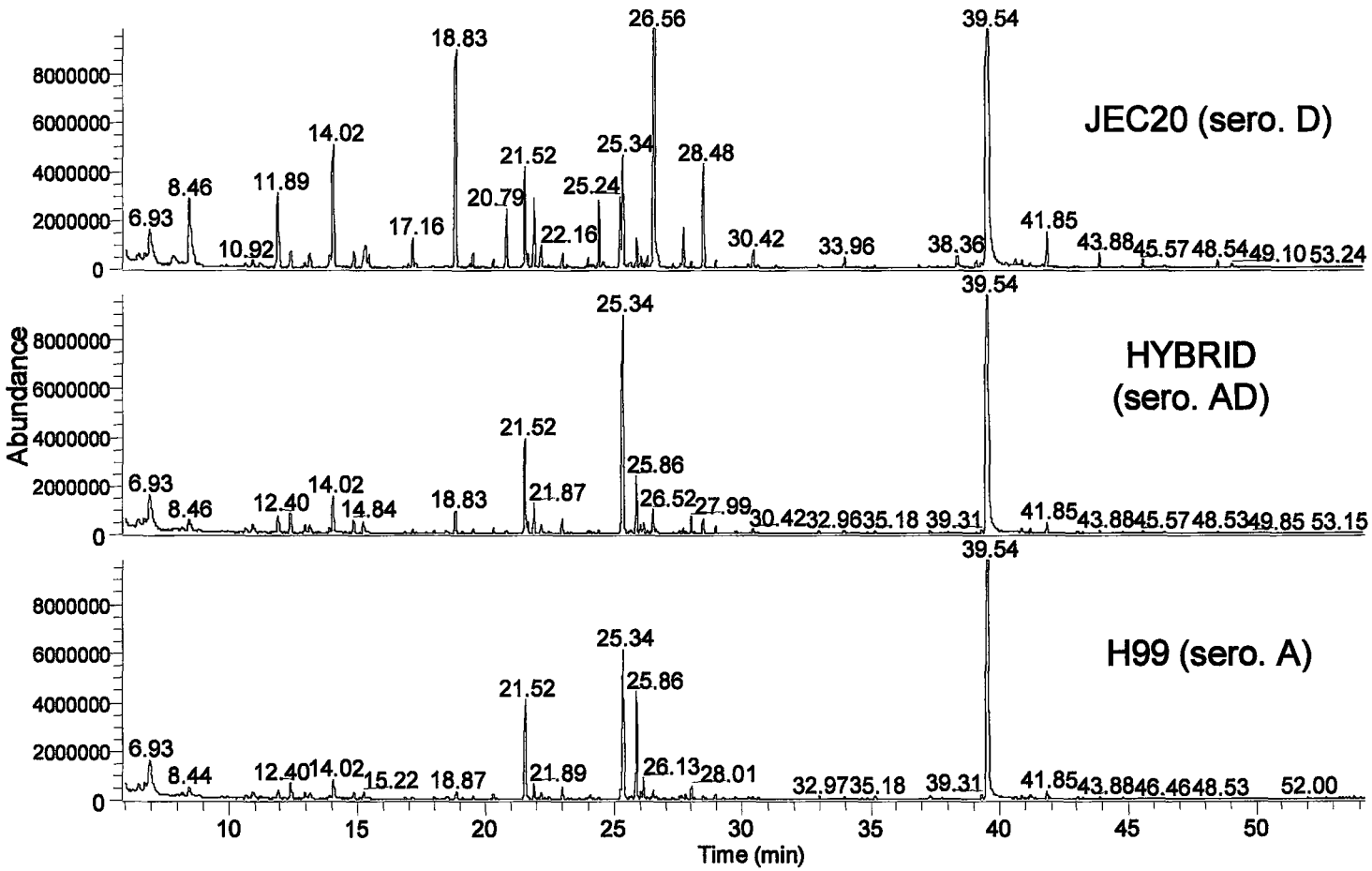

Fig. 3.1 Polar metabolite profiles of the 3 *Cryptococcus neoformans* strains reveal that the hybrid serotype AD strain resembles the H99 serotype A parent more than the JEC20 serotype D parent.

Table 3.1 Summary of peaks from the polar phase of the *C. neoformans* hybrid serotype AD strain in comparison to respective peaks from the two parent strains.

Peak abundances in the serotype AD hybrid	No. Peaks in Hybrid	% Peaks in Hybrid	Peaks Identified[a]
Identical to H99 (sero. A)	29	31	fumaric acid, succinic acid
Closer to H99 than JEC20	24	26	alanine, proline, aspartic acid, glutamic acid, glutamine, lysine, myo-inositol, glycerol, phosphate, malic acid
Median of both parents	7	8	methionine, ornithine, glucose
Closer to JEC20 than H99	3	3	serine, phenylalanine
Identical to JEC20 (sero. D)	6	6	none
Not significantly different from either parent	15	16	valine, leucine, iso-leucine, citric acid
Significantly different from both parents (unique)	9	10	none

[a] Putative identifications made from NIST and Fiehn libraries

hybrid strain. The complete list of aligned peaks in the polar metabolite profiles of all three *C. neoformans* strains can be found in Appendix B.5.

3.4.2 Lipid metabolite profiles of the *C. neoformans* strains

By visual inspection, the lipid metabolite profiles of all three strains were very similar to each other (Fig. 3.2). The peaks in the lipid profiles of the serotype AD hybrid strain were also characterized according to their similarities and differences to respective peaks in both parent strains and it was summarized in Table 3.2. However, unlike the polar metabolites, the majority (66%) of peaks in the lipid profile of the serotype AD hybrid strain were not significantly different from either parent. From the lipid profiles, 8% of peaks in the serotype AD hybrid strain were at levels that were either identical or closer to the serotype A parent than the serotype D parent and 18% of the peaks in the hybrid strain were more similar to the serotype D parent. There were no peaks that were unique to the hybrid strain. The complete list of aligned peaks in the lipid metabolite profiles of all three *C. neoformans* strains can be found in Appendix B.6.

3.5 DISCUSSION AND CONCLUSIONS

The lipid metabolite profiles were not very different among all three *C. neoformans* strains. This was not surprising since the lipid profiles were found to be fairly conserved across many different yeast species (Ch. 2) and therefore should also be expected to be very similar across members of the same species.

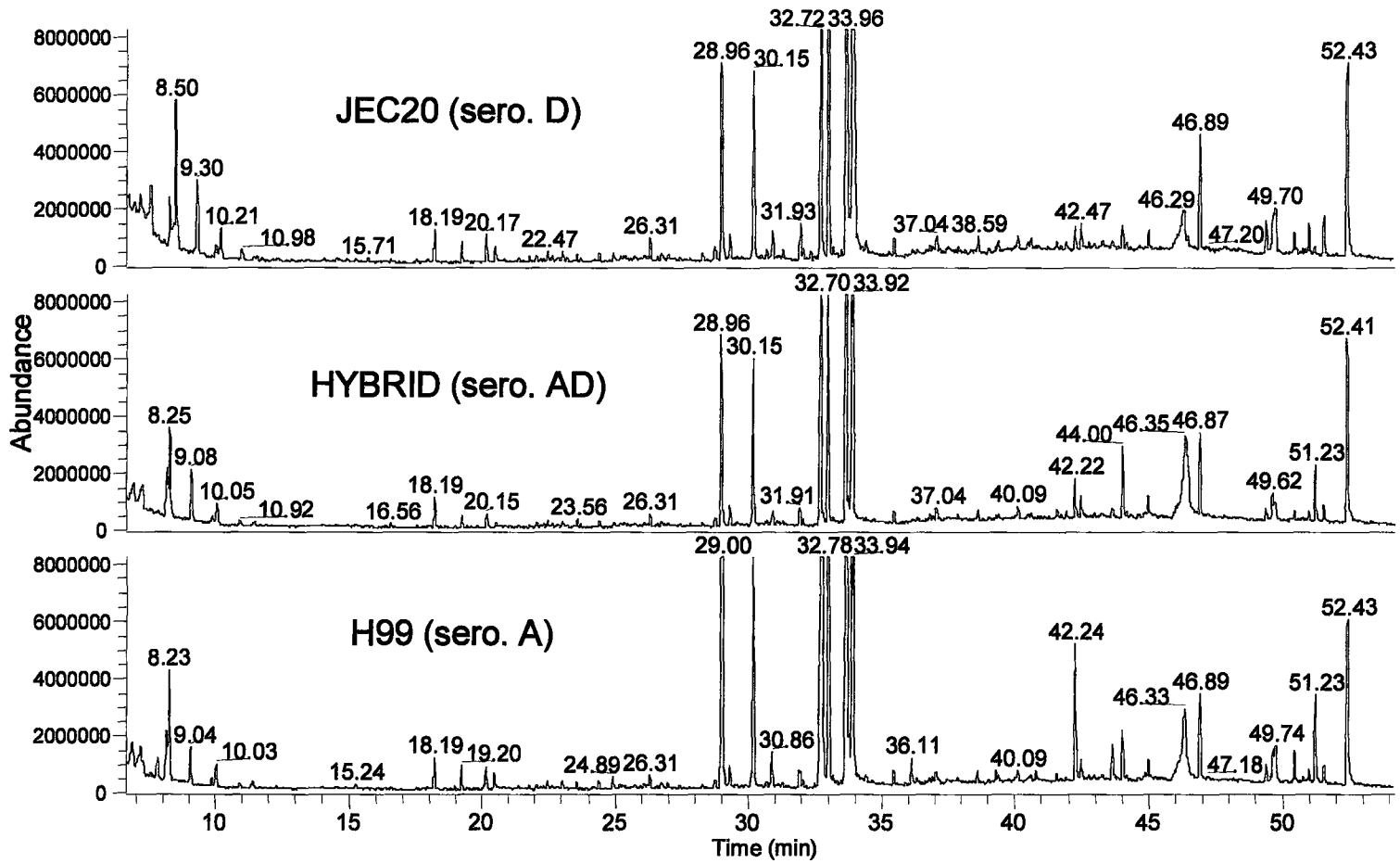

Fig. 3.2 Lipid metabolite profiles of the 3 *Cryptococcus neoformans* strains of serotypes A, D and AD are all very similar.

Table 3.2 Summary of peaks from the lipid phase of the *C. neoformans* hybrid serotype AD strain in comparison to respective peaks from the two parent strains.

Peak abundances in the serotype AD hybrid	No. Peaks in Hybrid	% Peaks in Hybrid
Identical to H99 (sero. A)	10	6
Closer to H99 than JEC20	3	2
Median of both parents	11	7
Closer to JEC20 than H99	18	11
Identical to JEC20 (sero. D)	11	7
Not significantly different from either parent	107	66
Significantly different from both parents (unique)	3	2

On the other hand, the polar metabolite phenotype of the serotype AD hybrid strain was strikingly more similar to its serotype A parent rather than its serotype D parent. This result was consistent with other laboratory analysis done on these same *C. neoformans* strains where it was found that this serotype AD hybrid strain was more similar to the serotype A parent than the serotype D parent, for example, in their colony morphologies (Yan, Z., personal communication).

The majority of polar metabolites that are detected in a typical GC-MS profile are compounds involved in primary metabolism. However, secondary metabolites may also be present in those profiles. There may also be several characteristic metabolites that may appear not to be present due to the following reason. These metabolites might be depleted through biochemical reactions in the organism such that they could be occurring at levels that are below the detection capabilities of the GC-MS instrument.

It is not known if the dominance of the serotype A phenotype for the polar metabolites in the serotype AD hybrid is dependent on the mating type of the parents. In this study, the parents were a serotype A, MATα strain and a serotype D, MATa strain. The majority of serotype A strains are of MATα and it is the α mating type that is associated with the majority of human infections (Casadevall and Perfect, 1998). According to studies done on infective mouse models, the α mating type is more virulent than the a mating type in serotype D strains of *C. neoformans* (Kwon-Chung, K. et al., 1992). This is in contrast to the findings of a similar study conducted with serotype A strains where it was found

that there was no difference in virulence between MATa and MATα strains (Nielsen, K. et al., 2003). However, it is well known that the serotype A strains and especially the common laboratory strain H99 is more virulent than serotype D strains of *C. neoformans* (Nielsen, K. et al., 2003). The MAT locus in *C. neoformans* contains several genes that encode virulence factors (Lengeler, K. et al., 2002). Virulence and mating are also controlled by the same regulatory factors in this organism (Alspaugh, J. et al., 1997). Therefore, it would be interesting to determine if the phenotype transmitted to the hybrid offspring is one that promotes greater virulence. In future work, the effect of the parents' mating type on the metabolite phenotype of the hybrid offspring of *C. neoformans* should be tested by examining the polar metabolite profiles of a MATa serotype A and MATα serotype D parents with their corresponding serotype AD hybrid.

PERSPECTIVE AND FINAL CONCLUSIONS

Metabolomics is a powerful area of science that can provide a wealth of information on a biological system in a short period of time. In this thesis, GC-MS was demonstrated to be a good technique to study various aspects of metabolomics in pathogenic yeasts. The targeted analysis of the ergosterol pathway in drug-resistant *C. albicans* clearly showed that different mutants had a different composition of sterols (Chapter 1). A double drug-resistant mutant to Fluconazole and Amphotericin B with a severe deficit in fitness was drastically altered in its sterol composition compared to the wild-type. However, Fluconazole-resistant mutants were similar to the wild-type in their relative fitness and sterol composition. The comprehensive analysis of the metabolites in six pathogenic yeasts (Chapter 2) revealed that lipid profiles were more conserved than polar profiles and better correlated to their taxonomical relationship by 26S rRNA sequences. Differential regions in the metabolite profiles in combination with the detection of species-specific peaks suggested that GC-MS could also be a valuable tool or technique for yeast identification. The comprehensive analysis of metabolite profiles in *C. neoformans* (Chapter 3) demonstrated how entire metabolite profiles could be regarded as the phenotype of a strain. While lipid metabolite phenotypes of all three *C. neoformans* strains were similar, it was

found that the polar metabolite phenotype of the hybrid offspring resembled the serotype A parent but not the serotype D parent.

LIST OF REFERENCES

1. **Abdi, M., D. Drucker, V. Boote, M. Korachi and E. Theaker.** 1999. Phospholipid molecular species distribution of some medically important Candida species analysed by fast atom bombardment mass spectroscopy. J. Appl. Microbiol. **87:**332-338.

2. **Albertson, G., M. Niimi, R. Cannon and H. Jenkinson.** 1996. Multiple efflux mechanisms are involved in *Candida albicans* fluconazole resistance. Antimicrob. Agents Chemother. **40:**2835-2841.

3. **Alspaugh, J., J. Perfect and J. Heitman.** 1997. *Cryptococcus neoformans* mating and virulence are regulated by the G-protein α subunit GPA1 and cAMP. Genes Develop. **11:**3206-3217.

4. **Arthington-Skaggs, B., H. Jradi, T. Desai, C. Morrison.** 1999. Quantitation of ergosterol content: novel method for determination of fluconazole susceptibility of *Candida albicans*. J. Clin. Microbiol. **37:**3332-3337.

5. **Boekhout, T., B. Theelen, M. Diaz, J. Fell, W. Hop, E. Abeln, F. Dromer and W. Meyer.** 2001. Hybrid genotypes in the pathogenic yeast *Cryptococcus neoformans*. Microbiology. **147:**891-907.

6. **(a) Botha, A. and J. Kock.** 1993. The distribution and taxonomic value of fatty acids and eicosanoids in the Lipomycetaceae and Dipodascaceae. Anton. Leeuwen. **63:**111-123.

7. **(b) Botha, A. and J. Kock.** 1993. Application of fatty acid profiles in the identification of yeasts. Int. J. Food Microbiol. **19:**39-51.

8. **Brajtburg, J., W. Powderly, G. Kobayashi and G. Medoff.** 1990. Amphotericin B: Current understanding of mechanisms of action. Antimicrob. Agents Chemother. **34:**183-188.

9. **Brandt, M., L. Huntwagner, L. Klug, W. Baughman, D. Rimland, E. Graviss, R. Hamill, C. Thomas, P. Pappas, A. Reingold, R. Pinner and the Cryptococcal Disease Active Surveillance Group.** 1996. Molecular subtype distribution of *Cryptococcus neoformans* in four areas of the United States. J. Clin. Microbiol. **34:**912-917.

10. **Casadevall, A. and J. Perfect.** 1998. *Cryptococcus neoformans*. ASM Press, Washington, DC, USA.

11. **Coleman, D., D. Bennett, D. Sullivan, P. Gallagher, M. Henman, D. Shanley and R. Russell.** 1993. Oral *Candida* in HIV infection and AIDS: New perspectives/new approaches. Crit. Rev. Microbiol. **19:**61-82.

12. **Cowan, L., D. Sanglard, D. Calabrese, C. Sirjusingh, J. Anderson and L. Kohn.** 2000. Evolution of drug resistance in experimental populations of *Candida albicans*. J. Bacteriol. **182:**1515-1522.

13. **Crist, A., L. Johnson and P. Burke.** 1996. Evaluation of the Microbial Identification System for identification of clinically isolated yeasts. J. Clin. Microbiol. **34**:2408-2410.

14. **Daub, C., S. Kloska and J. Selbig.** 2003. MetaGeneAlyse: analysis of integrated transcriptional and metabolite data. Bioinformatics. **19**:2332-2333.

15. **Davies, A., O. Billington, B. Bannister, W. Weir, T. McHugh and S. Gillespie.** 2000. Comparison of fitness of two isolates of *Mycobacterium tuberculosis*, one of which has developed multi-drug resistance during the course of treatment. J. Infect. **41**:184-187.

16. **Dromer, F., S. Mathoulin, B. Dupont, A. Laporte.** 1996. Epidemiology of Cryptococcosis in France: a 9-year survey (1985-1993). Clin. Infect. Dis. **23**:82-90.

17. **Dunn, B. and C. Wobbe.** 1997. Preparation of protein extracts from yeast. In: Current Protocols in Molecular Biology (F. Asubel, R. Brent, R. Kingston, D. Moore, J. Seidman, J. Smith and K. Struhl, eds) pp. 13.13.4. John Wiley & Sons, NY, USA.

18. **Ellis, D. and T. Pfeiffer.** 1990. Natural habitat of *Cryptococcus neoformans var. gattii*. J. Clin. Microbiol. **28**:1642-1644.

19. **Ellis, D., G. Harrigan and R. Goodacre.** 2003. Metabolic fingerprinting with fourier transform infrared spectroscopy. In: Metabolomic Profiling: Its role in biomarker discovery and gene function analysis. (G. Harrigan and R. Goodacre, eds) pp. 9-38. Kluwer Academic Publishers. Norwell, MA, USA.

20. **Fiehn, O., J. Kopka, R. Trethewey and L. Willmitzer.** 2000. Identification of uncommon plant metabolites based on calculation of elemental compositions using gas chromatography and quadrupole mass spectrometry. Anal. Chem. **72**:3573-3580.

21. **Fiehn, O.** 2001. Combining genomics, metabolome analysis and biochemical modeling to understand metabolic networks. Comp. Funct. Genomics. **2**:155-168.

22. **Fraser, J., R. Subaran, C. Nichols and J. Heitman.** 2003. Recapitulation of the sexual cycle of the primary fungal pathogen *C. neoformans var. gattii*: implications for an outbreak on Vancouver Island, Canada. Eukaryot. Cell. **2**:1036-1045.

23. **Garcia-Hermoso, D., S. Mathoulin-Pelissier, B. Couprie, O. Ronin, B. Dupont and F. Dromer.** 1997. DNA typing suggests pigeon droppings as a source of pathogenic *Cryptococcus neoformans* serotype D. J. Clin. Microbiol. **35**:2683-2685.

24. **Georgopapadakou, N. and T. Walsh.** 1996. Anti-fungal Agents: Chemotherapeutic targets and immunologic strategies. Antimicrob. Agents Chemother. **40**:279-291.

25. **Ghannoum, M., B. Spellberg, A. Ibrahim, J. Ritchie, B. Currie, E. Spitzer, J. Edwards and A. Casadevall.** 1994. Sterol Composition of *Cryptococcus neoformans* in the presence and absence of Fluconazole. Antimicrob. Agents and Chemother. **38**:2029-2033.

26. **Gottfredsson, M. and J. Perfect.** 2000. Fungal meningitis. Semin. Neurol. **20**:307-322.

27. **Halket, J.** 1993. Derivatives for gas-chromatography-mass spectrometry. In: Handbook of derivatives for chromatography. (J. Halket and K. Blau, 2nd ed.) John Wiley & Sons Ltd. Chichester, UK.

28. **Hartmann, M.** 1998. Plant sterols and the membrane environment. Trends Plant Sci. **3:**170-175.

29. **Heimark, L., P. Shipkova, J. Greene, H. Munayyer, T. Yarosh-Tomaine, B. DiDomenico, R. Hare and B. Pramanik.** 2002. Mechanism of azole antifungal activity as determined by liquid chromatographic/mass spectrometric monitoring of ergosterol biosynthesis. J. Mass Spectrom. **37:**265-269.

30. **Hendriks, L., A. Goris, Y. van de Peer, J. Neefs, M. Vancanneyt, K. Kersters, G. Hennebert and R. de Wachter.** 1991. Phylogenetic analysis of five medically important Candida species as deduced on the basis of small ribosomal subunit RNA sequences. J. Gen. Microbiol. **137:**1223-1230.

31. **Himmelreich, U., R. Somorjai, B. Dolenko, O. Lee, H. Daniel, R. Murray, C. Mountford and T. Sorrell.** Rapid identification of Candida sp. by using nuclear magnetic resonance spectroscopy and a statistical classification strategy. Appl. Environ. Microbiol. **69:**4566-4574.

32. **Howell, S., A. Mallet and W. Nobel.** 1990. A comparison of the sterol content of multiple isolates of the *Candida albicans* Darlington strain with other clinically azole-sensitive and –resistant strains. J. Appl. Bacteriol. **69:**696-696.

33. **Hull, C., R. Raisner and A. Johnson.** 2000. Evidence for mating of the "asexual" yeast *Candida albicans* in a mammalian host. Science. **14:**307-310.

34. **Hull, C. and J. Heitman.** 2002. Genetics of *Cryptococcus neoformans*. Annu. Rev. Genet. **36:**557-615.

35. **Kelly, S., D. Lamb, D. Kelly, N. Manning, J. Loeffler, H. Hebart, U. Schumacher and H. Einsele.** 1997. Resistance to fluconazole and cross-resistance to amphotericin B in *Candida albicans* from AIDS patients caused by defective sterol delta (5,6) desaturation. FEBS Lett. **400:**80-82.

36. **Klepser, M.** 2001. Antifungal resistance among Candida species. Pharmacotherapy. **21:**124S-132S.

37. **Kurtzman, C. and C. Robnett.** 1998. Identification and phylogeny of ascomyceteous yeasts from analysis of nuclear large subunit (26S) ribosomal DNA partial sequences. Anton. Leewen. **73:**331-371.

38. **Kwon-Chung, K.** 1975. A new genus, *Filobasidiella*, the perfect state of *Cryptococcus neoformans*. Mycologia. **67:**1197-1200.

39. **Kwon-Chung, K.** 1976. A new species of *Filobaidiella*, the sexual state of *Cryptococcus neoformans* B and C serotypes. Mycologia. **68:**943-946.

40. **Kwon-Chung, K. and J. Bennett.** 1984. Epidemiologic differences between the two varieties of *Cryptococcus neoformans*. Am. J. Epidemiol. **120:**123-130.

41. **Kwon-Chung, K., J. Edman and B. Wickes.** 1992. Genetic association of mating types and virulence in *Cryptococcus neoformans*. Infect. Immun. **60:**602-605.

42. **Lamb, D., D. Kelly, W. Schunck, A. Shyadehi, M. Akhtar, D. Lowe, B. Baldwin and S. Kelly.** 1997. The mutation T315A in *Candida albicans* sterol 14 alpha-demethylase causes reduced enzyme activity and fluconazole resistance through reduced affinity. J. Biol. Chem. **272:**5682-5688.

43. **Larone, D.** 1995. Medically important fungi: a guide to identification. 3rd ed. ASM Press: Washinton, DC, USA.

44. **Le Fur, Y., G. Maume, M. Feuillat and B. Maume.** 1999. Characterization by gas chromatography-mass spectrometry of sterols in *Saccharomyces cerevisiae* during autolysis. J. Agric. Food Chem. **47:**2860-2864.

45. **Lengeler, K., G. Cox. and J. Heitman.** 2001. Serotype AD strains of *Cryptococcus neoformans* are diploid or aneuploid and are heterozygous at the mating-type locus. Infect. Immun. **69:**115-122.

46. **Lengeler, K., D. Fox, J. Fraser, A. Allen, K. Forrester, F. Dietrich and J. Heitman.** 2002. Mating-type locus of *Cryptococcus neoformans*: a step in the evolution of sex chromosomes. Eukary. Cell. **1:**704-718.

47. **Lewis, R., B. Lund, M. Klepser, E. Ernst and M. Pfaller.** 1998. Assessment of antifungal activities of Fluconazole and Amphotericin B administered alone and in combination against *Candida albicans* by using a dynamic in vitro mycotic infection model. Antimicrob. Agents. Chemother. **42:**1382-1386.

48. **Li, A., K. Nishimura, H. Taguchi, R. Tanaka, S. Wu and M. Miyaji.** 1993. The isolation of *Cryptococcus neoformans* from pigeon droppings and serotyping of naturally and clinically sourced isolates in China. Mycopathologia. **124:**1-5.

49. **Loeffler, J., S. Kelly, H. Hebart, U. Schumacher, C. LassFlori and H. Einsele.** 1997. Molecular analysis of cyp51 from fluconazole-resistant *Candida albicans* strains. FEMS Microbiol. Lett. **151:**263-268.

50. **Louie, A., P. Kaw, P. Banerjee, W. Liu, G. Chen and M. Miller.** 2001. Impact of the order of initiation of Fluconazole and Amphotericin B in sequential or combination therapy on killing of *Candida albicans* in vitro and in a rabbit model of endocarditis and pyelonephritis. Antimicrob. Agents Chemother. **45:**485-494.

51. **Magee, B. and P. Magee.** 2000. Induction of mating in *Candida albicans* by construction of MTLa and MTLalpha strains. Science. **14:**310-313.

52. **Menyawi, I., M. Wogerbauer, H. Sigmund, H. Burgmann and W. Graninger.** 2000. Identification of yeast species by fatty acid profiling as measured by gas-liquid chromatography. J. Chrom. B. **742:**13-24.

53. **Meyer, W., G. Latouche, H. Daniel, M. Thanos, T. Mitchell, D. Yarrow, G. Schonian and T. Sorrell.** 1997. Identification of pathogenic yeasts of the imperfect genus Candida by polymerase chain reaction fingerprinting. Electrophoresis. **18:**1548-1559.

54. **Mishra, P. and R. Prasad.** 1990. An overview of lipids of *Candida albicans*. Prog. Lipid Res. **29:**65-85.

55. **Mishra, P., J. Bolard and R. Prasad.** 1992. Emerging role of lipids of *Candida albicans*, a pathogenic dimorphic yeast. Biochim. Biophys. Acta. **1127:**1-14.

56. **Mitchell, T. and J. Perfect.** 1995. Cryptococcosis in the era of AIDS - 100 years after the discovery of *Cryptococcus neoformans*. Clin. Microbiol. Rev. **8:**515-548.

57. **Monod, M, Porchet S, Baudraz-Rosselet F, Frenk E.** 1990. The identification of pathogenic yeast strains by electrophoretic analysis of their chromosomes. J Med Microbiol. **32:**123-129.

58. **Munoz, P., C. Fernandez-Turegano, L. Alcala, M. Rodriguez-Creixems, T. Pelaez, E. Bouza.** 2002. Frequency and clinical significance of bloodstream infections caused by *C. albicans* strains with reduced susceptibility to fluconazole. Diagn. Microbiol. Infect. Dis. **44:**163-167.

59. **National Committee for Clinical Laboratory Standards.** 1997. Reference method for broth dilution antifungal susceptibility testing of yeast. Approved standard. NCCLS document M27-A. National Committee for Clinical Laboratory Standards, Wayne, Pa.

60. **Neely, M. N. and M. A. Ghannoum.** 2000. The Exciting Future of Antifungal Therapy. Eur. J. Clin. Microbiol. Infect. Dis. **19:**897-914.

61. **Nielsen, K., G. Cox, P. Wang, D. Toffaletti, J. Perfect and J. Heitman.** 2003. Sexual cycle of *Cryptococcus neoformans var. grubii* and virulence of congenic a and α isolates. Infect. Immun. **71:**4831-4841.

62. **Nevalainen, L., J. Louhelainen and M. Makarow.** 1989. Post-translational modifications in mitotoic yeast cells. Eur. J. Biochem. **184:**165-172.

63. **Nolte, F., T. Parkinson, D. Falconer, S. Dix, J. Williams, C. Gilmore, R. Geller and J. Wingard.** 1997. Isolation and characterization of fluconazole and amphotericin B-resistant *Candida albicans* from blood of two patients with leukemia. Antimicrob. Agents Chemother. **41:**196-199.

64. **Oliver, S.** 2002. Functional genomics: lessons from yeast. Phil. Trans. R. Soc. Lond. B. **357:**17-23.

65. **Petroche-Ilacsahuanga, H., S. Schmidt, M. Seibold, R. Lutticken and G. Haase.** 2000. Differentiation between Candida dubliniensis and Candida albicans by fatty acid methyl ester analysis using gas-liquid chromatography. J. Clin. Microbiol. **38:**3696-3704.

66. **Raamsdonk, L., B. Teusink, D. Broadhurst, N. Zhang, A. Hayes, M. Walsh, J. Berden, K. Brindle, D. Kell, J. Rowland, H. Westerhoff, K. van Dam and S. Oliver.** 2001. A functional genomics strategy that uses metabolome data to reveal the phenotype of silent mutations. Nature Biotechnol. **19:**45-50.

67. **Ratledge, C. and C. Evans.** 1989. Lipids and their metabolism. In: The Yeasts Vol. 3 Metabolism and Physiology of Yeasts (A. Rose and J. Harrison, 2nd ed.) Academic Press Inc., UK.

68. **Redding, S., J. Smith, G. Farinacci, M. Rinaldi, A. Fothergill, J. Rhine-Chalberg and M. Pfaller.** 1994. Resistance of *Candida albicans* to fluconazole during treatment of oropharyngeal candidiasis in a patient with AIDS: documentation by in vitro susceptibility testing and DNA subtype analysis. Clin. Infect. Dis. **18:**240-242.

69. **Rex, J., M. Pfaller, J. Galgiani, M. Bartlett, A. Espinel-Ingroff, M. Ghannoum, M. Lancaster, F. Odds, M. Rinaldi, T. Walsh, A. Barry.** 1997. Development of interpretive breakpoints for antifungal susceptibility testing: conceptual framework and analysis of in vitro-in vivo correlation data for fluconazole, itraconazole and Candida infections. Clin. Infect. Dis. **24:**235-247.

70. **Sanglard, D., K. Kuchler, F. Ischer, J. Pagani, M. Monod and J. Bille.** 1995. Mechanisms of resistance to azole antifungal agents in *Candida albicans* isolates from AIDS patients involve specific multidrug transporters. Antimicrob. Agents Chemother. **39:**2378-2386.

71. **Sanglard, D., F. Ischer, M. Monod and J. Bille.** 1997. Cloning of *Candida albicans* genes conferring resistance to azole antifungal agents: characterization of CDR2, a new multidrug ABC transporter gene. Microbiology. **143:**405-416.

72. **Sanglard, D., F. Isher, T. Parkinson, D. Falconer and J. Bille.** 2003. *Candida albicans* mutations in the ergosterol biosynthesis pathway and resistance to several anti-fungal agents. Antimicrob. Agents Chemother. **47:**2404-2412.

73. **Scheven, M. and F. Schwegler.** 1995. Antagonistic interactions between azoles and Amphotericin B with yeasts depend on azole lipophilia for special test conditions in vitro. Antimicrob. Agents Chemother. **39:**1779-1783.

74. **Schwab, W.** 2003. Metabolome diversity: too few genes, too many metabolites? Phytochem. **62:**837-849.

75. **Sobel, J.** 2000. Practice guidelines for the treatment of fungal infections. Clin. Infect. Dis. **30:**652.

76. **Sokol-Anderson, M., J. Brajtburg and G. Medoff.** 1986. Amphotericin B induced oxidative damage and killing of *Candida albicans*. J. Infect. Dis. **154:**76-83.

77. **Steenbergen, J. and A. Casedevall.** 2000. Prevalence of *Cryptococcus neoformans var. neoformans* (serotype D) and *Cryptococcus neoformans var. grubii* (serotype A) isolates in New York City. J. Clin. Microbiol. **38:**1974-76.

78. **Stevens, S. and J. Abelson.** 2002. Yeast pre-mRNA splicing: methods, mechanisms and machinery. Methods Enzymol. **351:**200-220.

79. **Sugar, A., C. Hitchcock, P. Troke and M. Picard.** 1995. Combination therapy of murine invasive candidiasis with Fluconazole and Amphotericin B. Antimicrob. Agents Chemother. **39:**598-601.

80. **Swine-Desgain, D.** 1974. The pigeon as a reservoir for *Cryptoccus neoformans*. Lancet. **2:**842-843.

81. **Swofford, D.** 2001. PAUP4.0: Phylogenetic analysis using parsimonty (test version). Smithsonian Institute National Museum of Natural History, Washington, DC, USA.

82. **Tey, R., Z. Yan, S. Han, X. Li, K. Lazazzera, S. Sheng and J. Xu.** 2003. Ecology and epidemiology of drug resistance in human pathogenic yeasts. In: Research Advances in Microbiology. (R. Mohan, 3rd ed.). pp. 67-85. Global Research Network, Kerala, India.

83. **Tortorano, A., M. Viviani, A. Rigoni, M. Cogliati, A. Roverselli and A. Pagano.** 1997. Prevalence of serotype D in *Cryptococcus neoformans* isolates from HIV positive and HIV negative patients in Italy. Mycoses. **40:**297-302.

84. **Treco, D. and F. Winston.** 1997. Growth and manipulation of yeasts. In: Current Protocols in Molecular Biology (F. Asubel, R. Brent, R. Kingston, D. Moore, J. Seidman, J. Smith and K. Struhl, eds) pp. 13.2.1. John Wiley & Sons, NY, USA.

85. **Vaidyanathan, S. and R. Goodacre.** 2003. Metabolome and proteome profiling for microbial characterization. In: Metabolomic Profiling: Its role in biomarker discovery and gene function analysis. (G. Harrigan and R. Goodacre, eds) pp. 9-38. Kluwer Academic Publishers. Norwell, MA, USA.

86. **Valente, P., J. Ramos and O. Leoncini.** 1999. Sequencing as a tool in yeast molecular taxonomy. Can. J. Microbiol. **45:**949-958.

87. **Vazquez, J., M. Arganoza, D. Boikov, S. Yoon, J. Sobel and R. Akins.** 1998. Stable phenotypic resistance of Candida species to Amphotericin B conferred by pre-exposure to subinhibitory levels of azoles. J. Clin. Microbiol. **36:**2690-2695.

88. **Virioni, G. and Matsiota-Bernard, P.** 2001. Molecular typing of Candida isolates from patients hospitalized in an intensive care unit. J Infect. **42:**50-56.

89. **Weckwerth, W. and O. Fiehn.** 2002. Can we discover novel pathways using metabolomic analysis? Curr. Opin. Biotechnol. **13:**156-160.

90. **Weckwerth, W.** 2003. Metabolomics in systems biology. Annu. Rev. Plant Physiol. Plant Mol. Biol. **54:**669-689.

91. **Weete, J. and S. Gandhi.** 1997. Sterols of the phylum zygomycota: phylogenetic implications. Lipids. **32:**1309-1316.

92. **Wickes, B.** 2002. The role of mating type and morphology in *Cryptococcus neoformans* pathogenesis. Int. J. Med. Microbiol. **292:**313-329.

93. **Wong, S., M. Fares, W. Zimmermann, G. Butler and K. Wolfe.** 2003. Evidence from comparative genomics for a complete sexual cycle in the 'asexual' pathogenic yeast *Candida glabrata*. Genome Biol. **4:**R10.

94. **(a) White, T.** 1997. Increased mRNA levels of *erg16, CDR* and *MDR1* correlate with increases in azole resistance in *Candida albicans* isolates from an HIV-infected patient. Antimicrob. Agents Chemother. **41:**1482-1487.

95. **(b) White, T.** 1997. The presence of an R467K amino acid substitution and loss of alleleic variation correlate with an azole resistance in *Candida albicans* isolates from an HIV-infeted patient. Antimicrob. Agents Chemother. **41:**1488-1494.

96. **Xu, J., R. Vilgalys and T. Mitchell.** 1998. Colony size can be used to determine the MIC of fluconazole for pathogenic yeasts. J. Clin. Microbiol. **36:**2383-2385.

97. **Xu, J., A. Ramos, R. Vilgalys and T. Mitchell.** 2000. Clonal and spontaneous origins of Fluconazole resistance in *Candida albicans*. J. Clin. Microbiol. **38**:1214-1220.

APPENDIX A – DETAILED EXPERIMENTAL PROCEDURES

A.1 Yeast mini-prep protocol for DNA extraction

1. Collect a large loop of cells from a YEPD-agar culture plate and shake into 0.5 ml sterile ddH_2O in a 1.5 ml micro-fuge tube. Vortex.

2. Centrifuge tubes at 13000 rpm for 2 min to collect cells. Discard supernatant.

3. Re-suspend cells in 0.5 ml Protoplasting buffer. Incubate at 37 °C for 2 hrs.

4. Collect protoplast by centrifuging at 5000 rpm for 5 mins. Discard supernatant into chemical waste.

5. Add 0.5 ml Lysing buffer to each sample. Vortex. Incubate at 65 °C for 30 mins.

6. Add 125 µl of 7.5 M ammonium acetate. In fume hood, add 500 µl of chloroform: iso-amyl alcohol (24:1) to each sample. Close tubes well and vortex.

7. Centrifuge at 13000 rpm for 10 mins or until upper layer is clear.

8. Prepare a new set of micro-fuge tubes. Put approximately 550 µl ice cold iso-propanol in each tube. Carefully transfer supernatant (upper layer) to new tube. Mix gently by inversion. Samples can now be left at –20 °C overnight if necessary. Discard lower liquid layer into chemical waste.

9. Centrifuge at 13000 rpm for 2 mins and discard supernatant down sink.

10. Cover pellet with 70% ethanol. Let sit for 2 mins. Discard ethanol and air dry tubes overnight.

11. Re-suspend pellet in 60 µl 1X TE (10mM Tris-Cl, 1mM EDTA) buffer or ddH_2O. Then check 5 µl on a 1% agarose gel.

Protoplasting Buffer (40 samples)

β-mercaptoethanol	1%
Lysing enzyme	0.25mg/ml
Lyticase	0.25mg/ml
1M Sorbitol	fill up to 20ml

Lysing Buffer (40 samples)

EDTA	50mM
SDS	1% w/v
ddH_2O	fill up to 20ml

A.2 Growth and harvesting protocol for metabolite analysis

1. Inoculate cells from a YEPD-agar plate into a 14 ml polypropylene culture tube filled with 6 ml of YEPD liquid and grow overnight at 37 °C (30 °C for *C. neoformans var. gattii*) on a roller drum (speed setting 6; about 40 rpm).

2. Subculture cells at 0.05% of total volume of media in a 1 L Erlenmeyer flask.

3. Grow cells at 37 °C (30 °C for *C. neoformans var. gattii*) in an incubator shaker (200 rpm) until cells reach stationary phase.

4. When harvesting cells, set aside 1 ml of cell culture in a micro-fuge tube to measure the absorbance at OD 600. Try to keep the rest of cells on ice at all times.

5. Pour cell culture into a sterile 250 ml centrifuge bottle and centrifuge at 10000 rpm for 15 mins in a refrigerator centrifuge set at 4 °C. Discard supernatant.

6. Wash cell pellet by re-suspending cells in 1X PBS buffer (pH 7.3) to a total volume of 30 ml. Pipet 10 ml each into three 14 ml round bottomed polypropylene tubes and centrifuge at 4000 rpm for 5 mins. Discard supernatant. Repeat washing step 2 more times with 8 ml of 1X PBS buffer in each tube.

7. Then wash cells 3 times each with 8 ml of sterile ddH_2O per tube as in step 6.

8. Then re-suspend cells in sterile ddH_2O to a total volume that is two times the volume of the cell pellet (use increments on tube to help make an estimation on this) and transfer 1.2 ml of cell suspension to a pre-weighed sterile 2 ml screw-capped polypropylene tube.

9. Centrifuge cells in a micro-centrifuge at 13000 rpm for 2 mins. Remove supernatant with a micro-pipet. Weigh tube plus pellet to obtain a fresh weight of 600 mg cells. Adjust weight by scraping out excess cells with a sterile pipet tip.

10. Finally re-suspend cells in 600 µl sterile ddH_2O.

11. Flash freeze cells by dropping tubes into liquid nitrogen (–196 °C) and store samples at –70 °C until ready for cell disruption.

1X PBS Buffer (pH 7.3)

NaCl	137mM
KCl	2.7mM
$Na_2HPO_4 \cdot 7H_2O$	4.3mM
KH_2PO_4	1.4mM
(dissolved in ddH_2O)	

A.3 Bead-grinding protocol for yeast cell disruption

1. Let sample tubes thaw on ice before grinding. Meanwhile fill 15 ml Falcon screw-capped polypropylene tubes with glass beads (diameter 0.45 - 0.55 mm) to the 2.5 ml mark and keep on ice.

2. Transfer cells from the storage tube to the 15 ml polypropylene tube. Rinse storage tube with another 1200 µl of sterile ddH_2O and transfer to the 15 ml tube. Keep tubes on ice.

3. Grind cells by vortexing at the maximum speed for 1 min and then allowing sample tube to rest on ice for at least 2 mins. Repeat this step 5 times.

4. Incubate tubes in a 70 °C water bath for 15 mins to denature proteins and kill enzymes.

5. Allow the glass beads to settle and transfer supernatant into a new 50 ml screw-capped Nalgene® centrifuge tube.

6. Rinse beads with 1200 µl of sterile ddH_2O and vortex for 30 secs. Allow beads to re-settle and pool supernatant with that from step 5 into the Nalgene® centrifuge tube. Repeat this step. Keep polypropylene tubes with glass beads for a later step.

7. Centrifuge Nalgene® tubes containing cell lysate at 14000 rpm for 15 mins. Transfer supernatant to a new 50 ml Nalgene® centrifuge tube (water, polar phase). Keep original centrifuge tube with cell pellet.

8. As quickly as possible, rinse beads in polypropylene tube from step 6 with 1200 µl of chloroform by mixing gently for 30 secs. When beads have re-settled, transfer supernatant to the original Nalgene® centrifuge tube (chloroform, lipid phase) containing the cell pellet from step 8.

9. Proceed to the phase separation protocol in Appendix A.4.

A.4 Phase separation protocol after bead-grinding

1. After bead-grinding, there should be two Nalgene® centrifuge tubes per cell sample, one containing the chloroform (lipid) phase and one containing the water (polar) phase.

Water (polar) phase

2. Add 4 ml of ice-cold methanol to each polar phase tube and vortex to mix well. Keep tubes on ice for about 15 mins.

3. Centrifuge at 14000 rpm for 10 mins. Transfer supernatant into 2 disposable borosilicate glass test tubes, 4000 µl in each tube.

4. In each test tube, extract the polar phase with 1000 µl of chloroform by vortexing, then centrifuging at 4000 rpm for 15 mins.

5. Transfer bottom chloroform lipid phase to a new disposable borosilicate glass test tube. Lipid phases from both extractions (from both tubes) of the polar phase can be pooled into the same glass test tube. Set aside the lipid phase glass test tube for the extraction of the cell pellet (step 7 onwards).

6. Pool the top polar phase from both glass test tubes into a new 15 ml screw-capped polypropylene tube. Samples can then be stored at –20 °C until ready to derivatize for GC-MS analysis.

Chloroform (lipid) phase

7. Vortex at high speed the centrifuge tube (from step 1) containing chloroform and the cell pellet for at least 2 mins.

8. Centrifuge the tube at 14000 rpm for 10 mins. Transfer supernatant below the floating pellet into the lipid phase borosilicate glass test tube that had been set aside from step 5.

9. Re-extract the cell pellet with 1000 µl of chloroform by vortexing and then centrifuging at 14000 rpm for 10 mins. Pool supernatant together with the rest of the lipid phase in the glass test tube. Shake at a low setting to mix.

Saponification of the lipid phase

10. Divide the lipid phase extract into 2 equal volumes by transferring 2 ml into a new borosilicate glass test tube.

11. Add 2 ml of 33% methanolic KOH to each lipid phase glass test tube, cover tubes with Teflon® tape and shake at a low setting to mix. Incubate at 45 °C in a dry bath incubator for 2.5 hrs, shaking tubes periodically.

12. Add 2 ml of ddH_2O to each tube and shake at a low setting. Then centrifuge at 4000 rpm for 15 mins. Discard the top water phase. Repeat this step 2 more times or until there is no trace of precipitation left.

13. Transfer the lower saponified lipid phase into a 4 ml glass Kimble® vial with a screw cap lined with a Teflon® septum. Samples can then be stored at –20 °C until ready to derivatize for GC-MS analysis.

A.5 Derivatization of samples for GC-MS analysis

1. Before derivatizing samples, take them out of the –20 °C freezer and let them equilibrate to room temperature.

Polar Phase

2. Transfer 230 µl of the polar extract plus 4.31 µl of 2 mg/ml ribitol (dissolved in ddH_2O) into a thick-walled conical glass reaction vial and evaporate to dryness under N_2 gas.

3. Add 50 µl of 20 mg/ml methoxyamine (dissolved in pyridine) into the reaction vial and incubate at 30 °C in a dry bath incubator for 1.5 hrs.

4. Then add 80 µl of MSTFA and incubate at 37 °C in a dry bath incubator for 30 mins to derivatize the polar extract.

5. Transfer the entire portion of the derivatized lipid extract into a 250 µl GC auto-sampler vial. The derivatized polar extract was then diluted 25X in hexane with the aid of a robot attached to the GC-MS, afterwhich 1 µl of the diluted derivatized polar extract was injected into the GC-MS for analysis.

Lipid Phase

1. Transfer 500 μl of the saponified lipid extract plus 5 μl of 0.1 mg/ml 5β-cholestan-3α-ol (dissolved in chloroform) into a reaction vial. Evaporate to dryness under a stream of N_2 gas.

2. Dissolve the dried down extract in 20 μl pyridine by flicking the bottom of the vial. Then add 30 μl of MSTFA and incubate at 37 °C for 30 mins to derivatize the lipid extract.

3. Transfer the entire portion of the derivatized lipid extract into a 250 μl GC auto-sampler vial. With the aid of a robot attached to the GC-MS, the derivatized lipid extract was diluted 1:1 in hexane. 1 μl of the diluted derivatized lipid extract was then injected into the GC-MS for analysis.

APPENDIX B – METABOLITE DATA TABLES

B.1 Peaks detected in the sterol containing region of the lipid phase in *C. albicans* from RT 40 - 53 mins

	Mean NPA Values							
RT (mins)	TW1	TWAF	TW12	TW13	TW16	TWF3	TWF4	TWF5
25.92	0.175	0.211	0.091	0.028	0.023	0.046	0.023	0.053
40.01	0.244	0.135	0.103	0.096	0.067	0.031	0.179	0.084
40.30	ND	ND	0.086	0.178	0.145	0.107	0.136	0.132
40.84	ND	ND	0.046	0.107	0.205	0.130	0.096	0.174
41.06	0.116	0.114	ND	ND	ND	ND	ND	ND
41.46	0.097	0.108	0.049	0.087	0.076	0.057	0.107	0.078
41.83	0.100	0.104	0.048	0.077	0.076	0.108	0.109	0.191
42.39	0.177	0.095	0.218	0.136	0.060	0.189	0.155	0.241
42.74	0.167	0.114	0.233	0.117	0.098	0.201	0.201	0.266
42.88	0.159	0.150	0.058	0.078	0.130	0.075	0.117	0.148
43.09	0.152	0.111	0.038	0.057	0.037	0.022	0.064	0.097
43.56	ND	0.102	ND	ND	ND	ND	ND	ND
43.94	0.096	0.085	0.246	0.108	0.369	0.039	0.075	0.052
45.88	ND	1.601	ND	ND	ND	ND	ND	ND
46.37	0.098	0.086	0.077	0.117	0.073	0.070	0.087	0.105
47.42	0.080	0.028	0.039	0.127	0.053	0.035	0.083	0.107
48.19	ND	0.102	ND	ND	ND	ND	ND	ND
48.38	ND	0.103	ND	ND	ND	ND	ND	ND
49.29	0.084	ND	0.059	0.104	0.065	0.050	0.060	0.063
49.54	ND	0.197	ND	ND	ND	ND	ND	ND
49.58	0.695	ND	0.334	0.326	0.344	0.226	0.112	0.187
49.62	0.973	ND	0.553	0.961	0.387	0.169	0.168	0.415
49.78	ND	0.272	ND	ND	ND	ND	ND	ND
50.67	0.094	1.279	0.050	0.095	0.067	0.038	0.035	0.044
50.97	0.074	0.112	0.053	0.075	0.030	0.027	0.044	0.058
51.21	ND	4.643	ND	ND	ND	ND	ND	ND
52.39	9.582	7.075	1.868	1.639	1.393	2.049	2.592	2.595

B.2 Qualitative differences in the polar metabolites of the six pathogenic yeasts (1 = peak present; 0 = peak absent)

RT (mins)	Peak	CA	CG	CP	CT	CK	CN-A	CN-D
7.75	p1	1	0	1	1	0	0	1
8.37	p2	1	1	1	1	1	1	1
8.71	p3	1	1	1	1	1	1	1
9.55	p4	0	0	1	1	1	0	1
9.90	p5	0	1	1	1	1	1	1
9.92	p6	1	1	0	0	0	0	0
10.57	p7	1	1	1	1	1	1	1
10.81	p8	1	1	1	1	1	1	1
11.12	p9	1	1	1	1	1	1	1
11.39	p10	0	0	0	1	1	0	0
11.76	p11	1	1	1	1	1	1	1
11.99	p12	1	0	0	0	0	0	0
12.09	p13	0	0	1	1	0	0	0
12.26	p14	1	1	1	1	1	1	1
12.82	p15	1	1	1	1	1	1	1
13.02	p16	1	1	1	1	1	1	1
13.29	p17	1	1	1	1	0	0	0
13.56	p18	1	1	1	1	0	0	0
13.75	p19	1	1	1	1	1	1	1
13.91	p20	1	1	1	1	1	1	1
14.24	p21	0	1	0	1	1	0	0
14.47	p22	0	0	1	1	0	0	0
14.68	p23	1	1	1	1	1	1	1
15.07	p24	1	1	1	1	1	1	1
15.20	p25	0	1	0	0	1	0	1
15.30	p26	0	0	0	0	1	1	0
15.34	p27	1	1	1	1	0	1	1
15.69	p28	0	0	0	0	0	0	1
16.08	p29	1	0	1	1	1	0	0
16.23	p30	0	0	0	0	0	0	1
16.29	p31	0	0	0	1	0	0	0
16.35	p32	0	0	1	0	0	0	0
16.83	p33	0	0	0	0	0	1	1
16.87	p34	1	0	1	1	1	0	1
17.03	p35	1	0	1	0	0	1	1
17.14	p36	1	0	1	0	0	0	1
17.74	p37	1	0	0	0	0	0	0
17.84	p38	1	1	1	1	1	1	1
18.21	p39	0	0	0	0	1	0	0
18.31	p40	1	1	1	1	1	1	1
18.40	p41	1	1	1	1	1	1	1
18.56	p42	0	1	0	0	0	0	0
18.67	p43	1	1	1	1	1	1	1
18.87	p44	0	0	0	0	0	1	0
18.95	p45	1	1	0	1	1	1	1
19.24	p46	1	0	1	1	1	0	1
19.35	p47	1	1	1	1	1	1	1
19.68	p48	0	1	0	0	0	0	0
19.78	p49	0	0	1	0	0	0	0
20.13	p50	1	1	1	1	1	1	1
20.32	p51	1	0	1	0	1	0	0
20.65	p52	1	1	1	1	1	1	1
20.88	p53	0	1	1	0	1	0	0
21.13	p54	0	0	1	1	0	0	0
21.19	p55	1	0	1	0	1	0	0
21.48	p56	1	0	1	1	1	1	1
21.76	p57	1	1	1	1	1	1	1
22.01	p58	1	1	1	1	1	1	1
22.28	p59	1	1	0	0	0	0	0
22.45	p60	0	0	1	1	1	1	1
22.67	p61	1	0	1	0	0	0	0
22.82	p62	1	1	1	1	1	1	1
23.05	p63	1	1	0	0	1	0	1
23.11	p64	0	0	1	0	0	0	0
23.21	p65	0	0	1	1	1	1	1
23.36	p66	0	0	1	0	0	0	0
23.40	p67	0	1	0	1	0	0	0
23.46	p68	0	0	1	0	0	0	0
23.75	p69	1	1	1	1	1	0	0
23.89	p70	1	1	1	1	1	1	1
23.93	p71	1	1	1	1	0	1	1
23.98	p72	0	0	0	0	1	0	0
24.04	p73	1	0	1	0	0	0	0
24.14	p74	1	0	0	0	1	0	0
24.22	p75	0	0	0	0	0	0	1
24.25	p76	1	1	1	1	1	1	1
24.41	p77	1	0	1	1	1	0	1
24.64	p78	0	0	0	1	0	0	0
24.72	p79	0	1	0	1	1	0	0
24.88	p80	1	1	0	0	0	0	0
25.11	p81	1	1	1	1	1	0	1
25.17	p82	1	1	1	0	0	1	1
25.24	p83	1	0	0	1	1	0	0
25.38	p84	1	0	0	0	0	0	0

B.2 Continued

RT (mins)	Peak	CA	CG	CP	CT	CK	CN-A	CN-D
25.48	p85	0	0	0	0	1	0	0
25.50	p86	1	1	1	1	0	1	1
25.69	p87	1	1	1	1	0	0	0
25.77	p88	0	0	0	0	1	0	0
25.86	p89	0	0	0	0	0	1	1
25.86	p90	1	1	1	1	1	1	1
25.98	p91	1	1	0	0	0	1	1
26.08	p92	0	0	1	1	0	0	0
26.13	p93	1	1	1	1	1	0	1
26.19	p94	0	1	0	0	0	0	0
26.35	p95	1	1	1	1	1	1	1
26.44	p96	1	1	1	1	1	1	0
26.74	p97	1	1	0	0	1	0	0
26.85	p98	0	0	1	0	0	0	0
27.12	p99	1	1	1	1	0	1	1
27.43	p100	0	0	1	0	0	1	1
27.45	p101	1	1	1	1	1	1	0
27.63	p102	0	1	0	0	0	0	0
27.70	p103	0	0	0	0	0	1	1
27.78	p104	0	0	0	0	0	1	0
28.00	p105	0	0	0	0	0	1	1
28.07	p106	1	1	1	1	1	1	1
28.30	p107	1	1	1	1	1	1	1
28.77	p108	0	1	0	0	0	0	0
28.79	p109	1	1	1	1	1	1	1
29.08	p110	0	1	0	0	0	0	0
29.14	p111	0	0	1	0	0	0	0
29.49	p112	1	1	0	0	0	0	0
29.50	p113	0	0	0	1	1	0	0
29.54	p114	0	1	0	0	0	0	0
29.56	p115	1	0	1	1	1	1	0
29.60	p116	0	1	1	0	0	0	0
30.07	p117	0	0	1	0	0	0	0
30.11	p118	0	0	0	0	1	0	1
30.15	p119	1	1	1	0	0	0	0
30.28	p120	1	1	1	1	1	1	1
30.40	p121	1	1	1	1	0	1	1
30.53	p122	0	0	0	0	1	0	0
30.65	p123	0	0	1	0	0	0	0
30.84	p124	1	0	0	0	0	0	0
31.08	p125	1	1	0	0	0	0	0
31.13	p126	0	0	1	0	0	0	0
31.32	p127	0	1	0	0	0	0	1

RT (mins)	Peak	CA	CG	CP	CT	CK	CN-A	CN-D
31.42	p128	1	1	1	0	1	0	0
32.45	p129	0	0	0	0	0	0	1
32.72	p130	1	1	1	1	1	1	1
32.99	p131	0	0	1	1	0	0	0
33.07	p132	0	0	0	0	0	0	1
33.42	p133	1	1	0	0	0	0	0
33.81	p134	1	1	1	1	1	1	1
34.23	p135	1	1	0	0	0	0	0
34.31	p136	0	0	1	0	0	0	0
34.35	p137	1	1	1	1	0	0	0
34.51	p138	1	1	1	1	0	0	0
34.68	p139	1	1	1	1	0	0	0
34.85	p140	0	0	0	0	0	0	1
34.95	p141	0	0	1	1	0	0	0
35.15	p142	1	1	1	1	1	1	1
35.22	p143	0	1	0	1	1	0	0
35.92	p144	1	1	0	0	0	0	0
36.08	p145	1	1	1	0	0	0	0
36.89	p146	0	0	0	0	0	0	1
37.04	p147	1	1	0	0	0	0	0
37.12	p148	0	0	1	1	1	0	0
37.27	p149	0	0	0	1	1	1	1
37.64	p150	0	0	1	1	1	0	0
37.90	p151	1	1	1	0	0	0	0
38.26	p152	0	1	0	0	0	0	0
38.36	p153	0	0	0	0	0	0	1
38.44	p154	0	0	0	0	0	0	1
38.46	p155	0	0	1	0	0	0	0
38.92	p156	1	1	0	0	0	0	1
38.94	p157	0	0	0	1	0	0	0
38.95	p158	0	0	0	0	1	0	0
38.96	p159	0	0	1	0	0	0	0
39.04	p160	1	1	0	1	1	1	1
39.19	p161	0	0	1	0	0	0	0
39.45	p162	1	1	1	1	1	1	1
40.14	p163	0	0	0	0	1	0	0
40.15	p164	0	0	1	0	0	0	0
40.43	p165	0	1	0	0	0	0	0
40.53	p166	0	0	1	0	1	0	0
40.67	p167	0	1	1	1	1	1	1
40.84	p168	0	1	1	0	1	0	0
40.94	p169	1	1	0	0	0	1	1
41.17	p170	0	0	1	1	1	0	0

B.2 Continued

RT (mins)	Peak	CA	CG	CP	CT	CK	CN-A	CN-D
41.68	p171	1	1	1	1	1	1	1
42.82	p172	0	0	1	1	1	0	0
42.74	p173	1	1	1	1	1	1	1
43.88	p174	0	0	0	0	0	1	1
44.47	p175	1	1	1	0	1	1	0
45.40	p176	1	1	0	0	1	0	1
45.51	p177	1	0	0	0	0	0	0
46.11	p178	1	1	0	0	0	1	1
46.29	p179	0	1	0	0	0	0	0
46.39	p180	0	0	1	0	0	0	0
46.64	p181	0	0	1	1	0	0	0
47.70	p182	0	1	0	0	0	0	0
48.34	p183	1	1	0	1	1	0	1
49.10	p184	0	0	0	0	0	0	1
49.87	p185	1	0	1	0	0	0	0

B.3 Quantitative differences in the polar metabolites of the six pathogenic yeasts (Mean NPA values are presented)

RT (mins)	Peak	CA	CG	CP	CT	CK	CN-A	CN-D	$Mean_{row}$ NPA
7.75	p1	0.154	0	0.218	0.093	0	0	0.200	0.095
8.37	p2	2.751	2.289	5.172	2.112	1.269	0.195	1.626	2.202
8.71	p3	0.010	0.047	0.060	0.021	0.048	0.030	0.008	0.032
9.55	p4	0	0	0.022	0.020	0.015	0	0.007	0.009
9.90	p5	0	0.018	0.015	0.012	0.027	0.018	0.017	0.015
9.92	p6	0.023	0.024	0	0	0	0	0	0.007
10.57	p7	0.048	0.075	0.092	0.089	0.129	0.046	0.048	0.075
10.81	p8	0.212	0.235	0.445	0.436	0.214	0.123	0.118	0.255
11.12	p9	0.134	0.070	0.198	0.159	0.371	0.019	0.071	0.146
11.39	p10	0	0	0	0.016	0.017	0	0	0.005
11.76	p11	0.369	0.374	3.555	0.582	1.079	0.122	1.034	1.016
11.99	p12	0.023	0	0	0	0	0	0	0.003
12.09	p13	0	0	0.022	0.013	0	0	0	0.005
12.26	p14	0.105	0.131	0.469	0.437	0.234	0.262	0.226	0.266
12.82	p15	0.060	0.113	0.282	0.251	0.090	0.088	0.070	0.136
13.02	p16	0.484	0.194	0.291	0.446	0.385	0.063	0.227	0.299
13.29	p17	0.045	0.047	0.027	0.028	0	0	0	0.021
13.56	p18	0.018	0.009	0.023	0.015	0	0	0	0.009
13.75	p19	0.169	0.700	0.318	0.726	0.274	0.028	0.139	0.336
13.91	p20	2.178	1.435	4.067	2.882	2.813	0.293	1.608	2.182
14.24	p21	0	0.014	0	0.014	0.063	0	0	0.013
14.47	p22	0	0	0.125	0.037	0	0	0	0.023
14.68	p23	1.529	0.357	0.479	0.507	0.211	0.068	0.203	0.479
15.07	p24	0.764	0.154	0.876	0.574	0.140	0.079	0.136	0.389
15.20	p25	0	0.097	0	0	0.074	0	0.268	0.063
15.30	p26	0	0	0	0	0.048	0.015	0	0.009
15.34	p27	0.086	0.182	0.127	0.192	0	0.014	0.154	0.108
15.69	p28	0	0	0	0	0	0	0.011	0.002
16.08	p29	0.014	0	0.022	0.011	0.020	0	0	0.010
16.23	p30	0	0	0	0	0	0	0.014	0.002
16.29	p31	0	0	0	0.016	0	0	0	0.002
16.35	p32	0	0	0.027	0	0	0	0	0.004
16.83	p33	0	0	0	0	0	0.006	0.015	0.003
16.87	p34	0.027	0	0.021	0.021	0.026	0	0.029	0.018
17.03	p35	0.013	0	0.068	0	0	0.019	0.297	0.057
17.14	p36	0.022	0	0.016	0	0	0	0.047	0.012
17.74	p37	0.012	0	0	0	0	0	0	0.002
17.84	p38	0.015	0.025	0.056	0.023	0.024	0.025	0.027	0.028
18.21	p39	0	0	0	0	0.013	0	0	0.002
18.31	p40	0.013	0.023	0.029	0.018	0.024	0.019	0.016	0.020
18.40	p41	0.010	0.016	0.016	0.012	0.015	0.007	0.008	0.012
18.56	p42	0	0.009	0	0	0	0	0	0.001
18.67	p43	0.330	1.667	0.480	0.753	0.387	0.038	1.970	0.804
18.87	p44	0	0	0	0	0	0.061	0	0.009

B.3 Continued

RT (mins)	Peak	CA	CG	CP	CT	CK	CN-A	CN-D	$Mean_{row}$ NPA
18.95	p45	0.017	0.026	0	0.012	0.014	0.015	0.011	0.014
19.24	p46	0.006	0	0.059	0.021	0.010	0	0.031	0.018
19.35	p47	0.196	0.174	0.273	0.207	0.143	0.027	0.132	0.165
19.68	p48	0	0.013	0	0	0	0	0	0.002
19.78	p49	0	0	0.028	0	0	0	0	0.004
20.13	p50	0.074	0.03	0.061	0.061	0.068	0.030	0.069	0.056
20.32	p51	0.007	0	0.013	0	0.009	0	0	0.004
20.65	p52	0.119	0.081	0.530	0.184	0.013	0.008	0.484	0.203
20.88	p53	0	0.014	0.014	0	0.027	0	0	0.008
21.13	p54	0	0	0.021	0.020	0	0	0	0.006
21.19	p55	0.015	0	0.010	0	0.010	0	0	0.005
21.48	p56	4.029	0	24.36	0.326	0.103	0.041	0.145	4.144
21.76	p57	2.782	4.085	5.233	1.443	1.504	0.123	0.512	2.240
22.01	p58	0.923	1.487	1.847	0.565	0.668	0.058	0.219	0.824
22.28	p59	0.021	0.041	0	0	0	0	0	0.009
22.45	p60	0	0	0.023	0.010	0.016	0.016	0.014	0.011
22.67	p61	0.014	0	0.023	0	0	0	0	0.005
22.82	p62	0.078	0.055	0.269	0.229	0.128	0.086	0.117	0.137
23.05	p63	0.011	0.031	0	0	0.015	0	0.021	0.011
23.11	p64	0	0	0.036	0	0	0	0	0.005
23.21	p65	0	0	0.012	0.009	0.012	0.009	0.009	0.007
23.36	p66	0	0	0.013	0	0	0	0	0.002
23.40	p67	0	0.010	0	0.010	0	0	0	0.003
23.46	p68	0	0	0.014	0	0	0	0	0.002
23.75	p69	0.049	0.012	0.010	0.108	0.167	0	0	0.049
23.89	p70	0.430	0.129	0.303	0.059	0.077	0.014	0.081	0.156
23.93	p71	0.045	0.020	0.034	0.045	0	0.033	0.014	0.027
23.98	p72	0	0	0	0	0.054	0	0	0.008
24.04	p73	0.064	0	0.757	0	0	0	0	0.117
24.14	p74	0.062	0	0	0	0.017	0	0	0.011
24.22	p75	0	0	0	0	0	0	0.028	0.004
24.25	p76	0.230	0.106	0.896	0.231	0.090	0.017	0.581	0.307
24.41	p77	0.052	0	0.175	0.084	0.033	0	0.077	0.060
24.64	p78	0	0	0	0.015	0	0	0	0.002
24.72	p79	0	0.023	0	0.020	0.007	0	0	0.007
24.88	p80	0.004	0.012	0	0	0	0	0	0.002
25.11	p81	1.430	0.709	0.968	1.084	0.186	0	0.555	0.705
25.17	p82	0.173	0.246	0.546	0	0	1.548	1.176	0.527
25.24	p83	0.080	0	0	0.222	0.209	0	0	0.073
25.38	p84	0.029	0	0	0	0	0	0	0.004
25.48	p85	0	0	0	0	0.021	0	0	0.003
25.50	p86	0.030	0.120	0.114	0.027	0	0.034	0.068	0.056
25.69	p87	0.077	22.51	1.034	0.531	0	0	0	3.450
25.77	p88	0	0	0	0	0.042	0	0	0.006
25.86	p89	0	0	0	0	0	0.998	0.259	0.180

B.3 Continued

RT (mins)	Peak	CA	CG	CP	CT	CK	CN-A	CN-D	$Mean_{row}$ NPA
25.86	p90	0.082	2.417	0.409	0.052	0.010	0.065	0.065	0.443
25.98	p91	0.016	6.424	0	0	0	0.171	0.039	0.950
26.08	p92	0	0	0.161	0.091	0	0	0	0.036
26.13	p93	0.387	0.779	0.222	0.037	0.009	0	0.077	0.216
26.19	p94	0	0.054	0	0	0	0	0	0.008
26.35	p95	0.406	0.363	1.795	1.125	0.308	0.049	3.956	1.143
26.44	p96	0.111	0.134	0.589	0.371	0.262	0.019	0	0.212
26.74	p97	0.011	0.120	0	0	0.034	0	0	0.024
26.85	p98	0	0	0.019	0	0	0	0	0.003
27.12	p99	0.028	0.015	0.243	0.079	0	0.014	0.032	0.059
27.43	p100	0	0	0.017	0	0	0.022	0.010	0.007
27.45	p101	0.021	2.168	0.063	0.060	0.010	0.029	0	0.336
27.63	p102	0	0.032	0	0	0	0	0	0.005
27.70	p103	0	0	0	0	0	0.014	0.328	0.049
27.78	p104	0	0	0	0	0	0.037	0	0.005
28.00	p105	0	0	0	0	0	0.097	0.058	0.022
28.07	p106	0.021	0.029	0.012	0.010	0.015	0.014	0.018	0.017
28.30	p107	0.522	0.212	0.548	0.031	0.371	0.031	1.059	0.396
28.77	p108	0	0.030	0	0	0	0	0	0.004
28.79	p109	0.034	0.245	0.133	0.123	0.029	0.033	0.055	0.093
29.08	p110	0	0.227	0	0	0	0	0	0.032
29.14	p111	0	0	0.013	0	0	0	0	0.002
29.49	p112	0.007	0.015	0	0	0	0	0	0.003
29.50	p113	0	0	0	0.011	0.006	0	0	0.002
29.54	p114	0	0.016	0	0	0	0	0	0.002
29.56	p115	0.014	0	0.089	0.035	0.029	0.012	0	0.026
29.60	p116	0	0.044	0.059	0	0	0	0	0.015
30.07	p117	0	0	0.07	0	0	0	0	0.010
30.11	p118	0	0	0	0	0.022	0	0.003	0.004
30.15	p119	0.394	0.152	0.172	0	0	0	0	0.103
30.28	p120	0.181	0.182	0.181	0.158	0.065	0.019	0.149	0.134
30.40	p121	0.075	0.041	0.053	0.022	0	0.022	0.022	0.034
30.53	p122	0	0	0	0	0.013	0	0	0.002
30.65	p123	0	0	0.024	0	0	0	0	0.003
30.84	p124	0.019	0	0	0	0	0	0	0.003
31.08	p125	0.027	0.013	0	0	0	0	0	0.006
31.13	p126	0	0	0.026	0	0	0	0	0.004
31.32	p127	0	0.048	0	0	0	0	0.029	0.011
31.42	p128	0.010	0.037	0.008	0	0.015	0	0	0.010
32.45	p129	0	0	0	0	0	0	0.013	0.002
32.72	p130	0.026	0.039	0.014	0.014	0.018	0.024	0.022	0.022
32.99	p131	0	0	0.017	0.008	0	0	0	0.004
33.07	p132	0	0	0	0	0	0	0.023	0.003
33.42	p133	0.019	0.008	0	0	0	0	0	0.004
33.81	p134	0.445	0.416	0.094	0.201	0.023	0.018	0.102	0.186

B.3 Continued

RT (mins)	Peak	CA	CG	CP	CT	CK	CN-A	CN-D	$Mean_{row}$ NPA
34.23	p135	0.061	0.179	0	0	0	0	0	0.034
34.31	p136	0	0	0.064	0	0	0	0	0.009
34.35	p137	0.062	0.133	0.077	0.011	0	0	0	0.040
34.51	p138	0.040	0.079	0.042	0.011	0	0	0	0.025
34.68	p139	0.224	0.635	0.299	0.053	0	0	0	0.173
34.85	p140	0	0	0	0	0	0	0.022	0.003
34.95	p141	0	0	0.101	0.014	0	0	0	0.016
35.15	p142	0.103	0.187	0.019	0.015	0.02	0.028	0.025	0.057
35.22	p143	0	0.028	0	0.012	0.023	0	0	0.009
35.92	p144	0.021	0.017	0	0	0	0	0	0.005
36.08	p145	0.074	0.072	0.029	0	0	0	0	0.025
36.89	p146	0	0	0	0	0	0	0.018	0.003
37.04	p147	0.040	0.051	0	0	0	0	0	0.013
37.12	p148	0	0	0.032	0.016	0.011	0	0	0.008
37.27	p149	0	0	0	0.015	0.021	0.027	0.034	0.014
37.64	p150	0	0	0.021	0.008	0.019	0	0	0.007
37.90	p151	0.034	0.185	0.090	0	0	0	0	0.044
38.26	p152	0	0.039	0	0	0	0	0	0.006
38.36	p153	0	0	0	0	0	0	0.109	0.016
38.44	p154	0	0	0	0	0	0	0.036	0.005
38.46	p155	0	0	0.037	0	0	0	0	0.005
38.92	p156	0.022	0.027	0	0	0	0	0.062	0.016
38.94	p157	0	0	0	0.022	0	0	0	0.003
38.95	p158	0	0	0	0	0.028	0	0	0.004
38.96	p159	0	0	0.011	0	0	0	0	0.002
39.04	p160	0.032	0.045	0	0.014	0.021	0.040	0.027	0.026
39.19	p161	0	0	0.044	0	0	0	0	0.006
39.45	p162	0.071	2.412	21.55	0.501	0.214	7.544	15.56	6.836
40.14	p163	0	0	0	0	0.012	0	0	0.002
40.15	p164	0	0	0.166	0	0	0	0	0.024
40.43	p165	0	0.019	0	0	0	0	0	0.003
40.53	p166	0	0	0.021	0	0.055	0	0	0.011
40.67	p167	0	0.038	0.027	0.023	0.315	0.016	0.054	0.068
40.84	p168	0	0.015	0.010	0	0.022	0	0	0.007
40.94	p169	0.026	0.052	0	0	0	0.031	0.03	0.020
41.17	p170	0	0	0.017	0.012	0.013	0	0	0.006
41.68	p171	0.021	0.098	0.185	0.023	0.084	0.055	0.247	0.102
42.82	p172	0	0	0.107	0.034	0.013	0	0	0.022
42.74	p173	0.023	0.029	0.012	0.006	0.014	0.014	0.012	0.016
43.88	p174	0	0	0	0	0	0.014	0.124	0.020
44.47	p175	0.013	0.019	0.009	0	0.009	0.008	0	0.008
45.40	p176	0.030	0.020	0	0	0.026	0	0.053	0.018
45.51	p177	0.026	0	0	0	0	0	0	0.004
46.11	p178	0.007	0.010	0	0	0	0.008	0.007	0.005
46.29	p179	0	0.047	0	0	0	0	0	0.007

B.3 Continued

RT (mins)	Peak	CA	CG	CP	CT	CK	CN-A	CN-D	$Mean_{row}$ NPA
46.39	p180	0	0	0.018	0	0	0	0	0.003
46.64	p181	0	0	0.017	0.011	0	0	0	0.004
47.70	p182	0	0.009	0	0	0	0	0	0.001
48.34	p183	0.075	0.089	0	0.020	0.016	0	0.054	0.036
49.10	p184	0	0	0	0	0	0	0.016	0.002
49.87	p185	0.010	0	0.017	0	0	0	0	0.004

B.4 Qualitative differences in the lipid metabolites of the six pathogenic yeasts (1 = peak present; 0 = peak absent)

RT (mins)	Peak	CA	CG	CP	CT	CK	CN-A
6.89	L1	1	1	1	1	1	1
7.16	L2	1	1	1	1	1	1
7.26	L3	1	1	1	1	1	1
7.98	L4	0	0	0	0	0	1
8.15	L5	1	1	1	1	1	1
8.25	L6	1	1	1	1	1	1
9.08	L7	1	1	1	1	1	1
9.86	L8	1	1	1	1	1	1
10.05	L9	1	1	1	1	1	1
10.86	L10	1	1	1	1	1	1
11.37	L11	1	1	0	0	1	1
11.43	L12	1	1	1	1	1	1
11.50	L13	0	0	0	1	0	0
11.68	L14	1	1	1	0	1	1
11.85	L15	1	1	1	1	1	1
12.05	L16	1	0	1	1	0	0
12.12	L17	1	1	1	1	1	1
12.22	L18	0	0	0	1	0	1
12.24	L19	1	1	1	1	1	0
13.03	L20	1	1	1	1	1	1
13.23	L21	1	1	1	1	1	0
14.00	L22	0	1	0	0	0	0
14.10	L23	1	1	1	1	1	1
14.45	L24	1	1	1	1	1	1
14.55	L25	1	1	1	1	1	1
14.89	L26	1	1	1	0	1	0
15.11	L27	0	1	0	1	0	1
15.22	L28	1	0	1	1	1	1
15.36	L29	1	1	1	1	1	1
15.65	L30	1	1	1	1	1	1
15.82	L31	1	0	1	1	1	1
16.00	L32	1	1	0	1	1	1
16.08	L33	1	1	1	1	1	1
16.23	L34	1	1	1	1	1	1
16.43	L35	1	1	1	1	0	0
16.52	L36	1	1	1	1	1	1
16.76	L37	0	1	1	1	1	1
17.22	L38	1	0	0	1	0	1
17.38	L39	0	0	1	1	0	0
17.47	L40	1	1	1	1	1	1
17.67	L41	1	1	1	1	1	1
17.74	L42	1	1	1	1	1	1

RT (mins)	Peak	CA	CG	CP	CT	CK	CN-A
17.88	L43	1	1	1	1	1	1
18.09	L44	1	1	1	1	1	1
18.13	L45	1	1	1	1	1	1
18.23	L46	1	1	1	1	1	1
18.46	L47	1	1	1	1	1	1
18.94	L48	1	1	1	0	1	1
19.14	L49	0	1	0	1	0	1
19.39	L50	1	1	1	1	1	1
19.64	L51	1	1	1	1	1	1
19.72	L52	1	1	1	1	1	1
20.07	L53	1	1	1	1	1	1
20.09	L54	1	1	1	1	1	1
20.42	L55	1	1	1	1	1	1
20.55	L56	0	0	0	1	0	0
20.79	L57	1	1	1	1	1	1
20.94	L58	1	1	1	1	1	1
21.08	L59	0	0	0	1	1	0
21.21	L60	1	1	1	1	1	1
21.31	L61	1	1	1	1	1	1
21.77	L62	0	1	0	0	0	0
21.87	L63	1	0	0	1	1	1
22.07	L64	0	1	0	0	0	0
22.05	L65	1	1	1	1	1	1
22.10	L66	1	1	1	1	1	1
22.30	L67	1	1	1	1	1	1
22.39	L68	1	1	1	1	1	1
22.47	L69	1	0	1	1	1	0
22.57	L70	1	1	1	1	1	1
22.81	L71	1	1	1	1	1	1
22.97	L72	1	1	1	1	1	1
23.11	L73	1	1	1	1	1	1
23.48	L74	1	1	0	1	1	1
23.63	L75	1	1	1	1	1	1
23.75	L76	1	0	0	1	0	0
23.90	L77	1	0	1	1	1	0
24.12	L78	1	0	0	1	0	0
24.24	L79	0	0	0	0	0	1
24.35	L80	0	1	1	0	1	0
24.37	L81	0	0	0	0	0	1
24.41	L82	0	1	0	0	0	0
24.47	L83	1	0	1	1	1	0
24.70	L84	0	1	0	0	0	0

B.4 Continued

RT (mins)	Peak	CA	CG	CP	CT	CK	CN-A
24.80	L85	1	1	0	1	1	1
24.85	L86	1	1	1	1	1	1
25.13	L87	0	1	0	0	0	0
25.17	L88	1	1	1	1	1	1
25.24	L89	1	0	1	1	1	1
25.61	L90	0	1	1	0	1	0
25.67	L91	1	1	1	1	1	1
25.92	L92	1	1	1	1	1	1
26.02	L93	1	1	1	1	1	1
26.15	L94	1	1	1	1	1	1
26.25	L95	1	1	1	1	1	1
26.50	L96	1	1	1	1	1	1
26.66	L97	1	1	1	1	1	1
26.91	L98	1	1	1	1	1	1
27.31	L99	1	1	0	1	1	1
27.51	L100	0	0	0	1	0	1
27.95	L101	1	0	1	0	0	0
28.19	L102	1	1	1	1	1	1
28.40	L103	1	1	1	1	1	1
28.63	L104	1	1	1	1	1	1
28.90	L105	1	1	1	1	1	1
28.98	L106	1	1	1	1	1	0
29.25	L107	1	1	1	1	1	1
29.53	L108	0	0	0	0	0	1
29.62	L109	1	1	1	1	1	1
29.80	L110	1	1	0	0	0	0
29.85	L111	1	1	0	1	1	0
30.09	L112	1	1	1	1	1	1
30.12	L113	1	1	1	1	1	0
30.45	L114	1	1	1	1	1	1
30.59	L115	1	1	1	1	1	1
30.80	L116	1	1	1	1	1	1
30.96	L117	1	1	1	1	1	1
31.13	L118	0	0	0	0	0	1
31.15	L119	1	1	1	1	1	1
31.66	L120	0	1	0	0	0	0
31.74	L121	0	1	0	0	0	0
31.85	L122	1	1	1	1	1	1
31.99	L123	0	0	0	0	0	1
32.06	L124	1	1	1	1	1	1
32.18	L125	1	1	1	1	1	1
32.39	L126	0	1	0	1	1	1
32.60	L127	1	1	1	1	1	1

RT (mins)	Peak	CA	CG	CP	CT	CK	CN-A
32.71	L128	1	1	1	1	1	1
32.90	L129	1	1	1	1	1	1
33.11	L130	1	1	1	1	1	1
33.26	L131	1	1	1	1	1	1
33.40	L132	1	0	1	1	1	1
33.57	L133	1	1	1	1	1	1
33.69	L134	1	1	1	1	1	1
33.81	L135	1	1	1	1	1	1
33.85	L136	1	0	0	1	0	1
34.06	L137	1	1	1	1	1	1
34.15	L138	1	1	1	0	1	1
34.31	L139	1	0	1	1	1	1
34.54	L140	1	1	0	0	1	0
35.03	L141	1	0	1	1	1	1
35.48	L142	0	1	0	0	0	0
35.36	L143	1	1	1	1	1	1
36.13	L144	1	1	1	1	1	1
36.58	L145	1	1	1	1	1	1
36.71	L146	1	1	1	1	1	1
36.83	L147	0	1	0	1	0	1
36.87	L148	1	1	1	1	1	1
36.96	L149	1	1	1	1	1	1
37.14	L150	1	0	1	0	0	1
37.57	L151	0	0	0	1	0	0
38.07	L152	0	0	1	1	0	0
38.27	L153	0	0	1	1	0	0
38.69	L154	0	1	0	0	0	0
38.81	L155	1	1	1	1	1	1
38.94	L156	0	1	0	0	0	0
39.02	L157	0	1	0	0	0	0
39.18	L158	1	1	1	1	1	1
39.20	L159	1	0	1	1	1	1
39.29	L160	1	0	1	1	0	1
40.13	L161	0	1	0	0	0	0
40.30	L162	1	1	1	1	1	1
40.34	L163	0	1	1	1	1	1
40.49	L164	0	1	1	1	1	1
40.78	L165	0	0	0	0	0	1
41.07	L166	0	1	1	1	1	1
41.54	L167	0	0	0	0	0	1
41.62	L168	1	1	1	1	1	1
42.00	L169	1	1	1	1	1	1
42.16	L170	0	0	1	1	0	1

B.4 Continued

RT (mins)	Peak	CA	CG	CP	CT	CK	CN-A
42.39	L171	1	1	1	0	0	1
42.76	L172	1	1	0	1	0	0
42.87	L173	1	1	1	1	0	1
43.09	L174	1	1	1	0	1	1
43.17	L175	1	1	1	0	1	1
43.63	L176	0	0	0	0	0	1
43.94	L177	1	1	1	1	1	1
44.21	L178	1	1	1	1	1	1
44.42	L179	1	1	1	1	1	1
44.91	L180	1	1	1	1	1	1
45.88	L181	0	0	0	1	0	0
46.38	L182	1	1	1	1	1	1
46.47	L183	1	1	0	1	1	1
46.79	L184	1	1	1	1	1	1
47.18	L185	0	0	0	0	0	1
48.36	L186	0	0	1	0	1	0
49.29	L187	1	1	1	1	1	1
49.58	L188	1	1	1	1	1	1
49.62	L189	1	1	1	1	1	1
50.36	L190	0	0	0	1	0	0
50.45	L191	0	0	0	0	0	1
50.90	L192	0	1	0	0	0	0
51.00	L193	1	1	1	1	1	1
51.29	L194	1	1	1	1	1	1
51.15	L195	0	0	0	1	0	1
51.56	L196	0	0	0	0	0	1
52.37	L197	1	1	1	1	1	1

B.5 List of peaks in the polar metabolite profiles of *C. neoformans* strains, H99 (serotype A), JEC20 (serotype D) and Cn9920 (serotype AD hybrid)

	Mean NPA values		
RT (mins)	H99	J20	hybrid
7.84	0	0.200	0
8.44	0.195	1.626	0.283
8.85	0.030	0.008	0.030
9.62	0	0.007	0.028
9.95	0.018	0.017	0.023
10.67	0.046	0.048	0.070
10.92	0.123	0.118	0.169
11.23	0.019	0.071	0.038
11.91	0.122	1.034	0.262
12.40	0.262	0.226	0.172
12.96	0.088	0.070	0.123
13.15	0.063	0.227	0.130
13.89	0.028	0.139	0.064
14.02	0.293	1.608	0.476
14.84	0.068	0.203	0.165
15.22	0.079	0.136	0.144
15.28	0	0.268	0
15.34	0.015	0	0.024
15.44	0.014	0.154	0.015
15.71	0	0.011	0
16.23	0	0.014	0
16.83	0.006	0.015	0.016
17.01	0	0.029	0
17.18	0.019	0.297	0.044
17.28	0	0.047	0
18.00	0.025	0.027	0.023
18.46	0.019	0.016	0.019
18.52	0.007	0.008	0.008
18.83	0.038	1.970	0.233
18.87	0.061	0	0
19.12	0.015	0.011	0.013
19.39	0	0.031	0
19.53	0.027	0.132	0.034
20.28	0.030	0.069	0.053
20.80	0.008	0.484	0.024
21.64	0.041	0.145	0.130
21.89	0.123	0.512	0.255
22.18	0.058	0.219	0.087
22.47	0.016	0.014	0.014
22.99	0.086	0.117	0.125
23.19	0	0.021	0
23.32	0.009	0.009	0

	Mean NPA values		
RT (mins)	H99	J20	hybrid
24.00	0.014	0.081	0.024
24.10	0.033	0.014	0.021
24.22	0	0.028	0
24.41	0.017	0.581	0.041
24.58	0	0.077	0
25.24	0	0.555	0
25.34	1.548	1.176	2.807
25.67	0.034	0.068	0.054
25.86	0.998	0.259	0.580
26.04	0.065	0.065	0.056
26.13	0.171	0.039	0.092
26.27	0	0.077	0.016
26.52	0.049	3.956	0.194
26.64	0.019	0	0.036
27.30	0.014	0.032	0.011
27.55	0.022	0.010	0.028
27.63	0.029	0	0
27.68	0.014	0.328	0.057
27.78	0.037	0	0.016
28.01	0.097	0.058	0.151
28.11	0.014	0.018	0.022
28.46	0.031	1.059	0.158
28.96	0.033	0.055	0.060
29.76	0.012	0	0.011
30.24	0	0.003	0
30.42	0.019	0.149	0.051
30.63	0.022	0.022	0.025
31.32	0	0.029	0
32.45	0	0.013	0
32.97	0.024	0.022	0.029
33.07	0	0.023	0
33.98	0.018	0.102	0.034
34.85	0	0.022	0.012
35.18	0.028	0.025	0.034
36.89	0	0.018	0
37.29	0.027	0.034	0.035
38.36	0	0.109	0
38.44	0	0.036	0
39.10	0	0.062	0
39.31	0.040	0.027	0.029
39.54	7.544	15.557	10.032
40.86	0.016	0.054	0.030

B.5 Continued

	Mean NPA values		
RT (mins)	H99	J20	hybrid
41.23	0.031	0.030	0.033
41.85	0.055	0.247	0.084
43.03	0.014	0.012	0.017
43.88	0.014	0.124	0.027
44.75	0.008	0	0.013
45.57	0	0.053	0.015
46.42	0.008	0.007	0.007
48.53	0	0.054	0.008
49.10	0	0.016	0

B.6 List of peaks in the lipid metabolite profiles of *C. neoformans* strains, H99 (serotype A), JEC20 (serotype D) and Cn9920 (serotype AD hybrid)

	Mean NPA values		
RT (mins)	H99	J20	hybrid
7.03	0.524	0.483	0.546
7.30	0.504	0.283	0.351
7.44	0.332	0.772	0.440
7.98	0.361	0.128	0.165
8.23	0.751	0.661	0.759
8.40	1.290	1.528	1.388
9.20	0.531	0.750	0.843
9.97	0.118	0.151	0.115
10.15	0.341	0.439	0.390
10.98	0.104	0.141	0.114
11.43	0.145	0.052	0.068
11.52	0.042	0.089	0.083
11.76	0.028	0.038	0.034
11.95	0.023	0.014	0.031
12.32	0.048	0.031	0.028
14.02	0.038	0.032	0.031
14.49	0.024	0.057	0.030
14.60	0.024	0.049	0.036
14.99	0.084	0.051	0.060
15.24	0.098	0.068	0.073
15.42	0.014	0.016	0.016
15.69	0.040	0.065	0.058
15.86	0.026	0.021	0.029
16.14	0.058	0.025	0.044
16.58	0.049	0.036	0.048
17.51	0.032	0.049	0.038
17.72	0.046	0.019	0.022
17.80	0.029	0.013	0.022
17.94	0.049	0.031	0.035
18.11	0.121	0.083	0.136
18.19	0.281	0.314	0.263
18.56	0.029	0.026	0.044
18.96	0.046	0.037	0.048
19.22	0.422	0.122	0.318
19.45	0.033	0.019	0.030
19.70	0.020	0.018	0.018
20.09	0.201	0	0.102
20.15	0.332	0.240	0.281
20.46	0.356	0.178	0.354
20.84	0.059	0.020	0.023
21.00	0.034	0.026	0.033
21.27	0.032	0.021	0.018

	Mean NPA values		
RT (mins)	H99	J20	hybrid
21.37	0.055	0.039	0.038
21.56	0.024	0.020	0.025
21.77	0.065	0.057	0.068
22.05	0.069	0.051	0.059
22.18	0.041	0.044	0.061
22.32	0.051	0.030	0.054
22.47	0.131	0.087	0.110
22.65	0.064	0.052	0.062
22.82	0.046	0.052	0.072
23.03	0.110	0.074	0.111
23.19	0.052	0.055	0.042
23.54	0.057	0.063	0.090
23.67	0.048	0.042	0.048
24.16	0.020	0.021	0.041
24.24	0.031	0.042	0.042
24.37	0.108	0.084	0.089
24.60	0.017	0.019	0.021
24.89	0.229	0.079	0.135
25.17	0.057	0.052	0.070
25.28	0.066	0.052	0.071
25.77	0.048	0.050	0.048
25.98	0.035	0.011	0.026
26.10	0.065	0.054	0.062
26.23	0.048	0.039	0.034
26.31	0.140	0.148	0.138
26.58	0.059	0.043	0.051
26.74	0.113	0.086	0.087
26.97	0.090	0.050	0.068
27.45	0.030	0.037	0.041
27.57	0.026	0.011	0.020
27.82	0.014	0.028	0.023
28.29	0.064	0.093	0.060
28.42	0.028	0.021	0.019
28.69	0.042	0.083	0.090
28.73	0.101	0.102	0.098
29.00	7.826	1.218	3.380
29.04	0	0.102	0.255
29.29	0.240	0.234	0.272
29.53	0.078	0.048	0.065
29.78	0.051	0.032	0.050
29.89	0.031	0.030	0.045
30.17	3.336	1.496	2.166

B.6 Continued

	Mean NPA values		
RT (mins)	H99	J20	hybrid
30.48	0.029	0.021	0.028
30.67	0.046	0.033	0.033
30.71	0.061	0.063	0.072
30.86	0.713	0.223	0.363
31.04	0.044	0.031	0.059
31.13	0.069	0	0.068
31.27	0.094	0.087	0.091
31.91	0.184	0.076	0.101
31.99	0.203	0.206	0.196
32.10	0.143	0.089	0.086
32.31	0	0.052	0.030
32.49	0.067	0.037	0.036
32.74	7.603	1.029	3.832
32.86	14.678	2.720	5.027
33.07	6.866	2.472	4.833
33.19	0.289	0.087	0.183
33.30	0.064	0.025	0.048
33.50	0.085	0.036	0.040
33.71	7.304	0.748	2.497
33.77	8.258	5.101	6.244
33.90	4.342	3.077	2.956
33.98	5.659	4.358	4.794
34.10	0.376	0.164	0.195
34.23	0.177	0.075	0.117
34.45	0.303	0.134	0.122
34.64	0.064	0.030	0.063
35.44	0.204	0.147	0.159
35.88	0.042	0.031	0.027
36.11	0.437	0	0.095
36.33	0.063	0.047	0.065
36.66	0.030	0.027	0.021
36.79	0.094	0.072	0.067
36.89	0.140	0.039	0.064
37.04	0.181	0.175	0.157
37.14	0.076	0.048	0.069
37.47	0.119	0.095	0.129
37.84	0.076	0.069	0.059
38.59	0.151	0.125	0.128
38.81	0.033	0.028	0.060
39.00	0.074	0.056	0.067
39.27	0.203	0.045	0.087
39.37	0.111	0.094	0.090
39.99	0.071	0.055	0.051
40.09	0.154	0.156	0.151

	Mean NPA values		
RT (mins)	H99	J20	hybrid
40.47	0.093	0.091	0.063
40.59	0.165	0.108	0.098
40.78	0.205	0.028	0.042
41.54	0.126	0.099	0.106
41.71	0.033	0.048	0.042
41.91	0.101	0.084	0.085
42.26	2.027	0.161	0.855
42.47	0.370	0.212	0.304
42.74	0.113	0.070	0.081
42.94	0.049	0.062	0.082
43.17	0.031	0.034	0.032
43.26	0.110	0.081	0.100
43.48	0.029	0.014	0.032
43.63	0.623	0.095	0.258
44.02	0.874	0.164	1.617
44.14	0.084	0.070	0.079
44.29	0.057	0.023	0.046
44.60	0.029	0.024	0.038
44.64	0.043	0.042	0.035
44.83	0.052	0.033	0.061
44.99	0.327	0.141	0.411
46.07	0.066	0.237	0.264
46.15	0.204	0.207	0.229
46.29	1.269	1.804	2.378
46.46	0.170	0.222	0.475
47.18	0.041	0.041	0.038
49.37	0.302	0.232	0.239
49.62	0.621	0.323	0.627
49.74	1.127	0.604	0.792
50.45	0.593	0.168	0.254
50.76	0.125	0.045	0.147
50.98	0.239	0.214	0.257
51.25	1.540	0.073	1.236
51.56	0.403	0.287	0.419
52.45	3.072	2.114	2.043

APPENDIX C – MASS SPECTRA OF UNKNOWN PEAKS

C.1 *C. albicans* strain TWAF, RT 43.56 mins (peak a in Fig. 1.13)

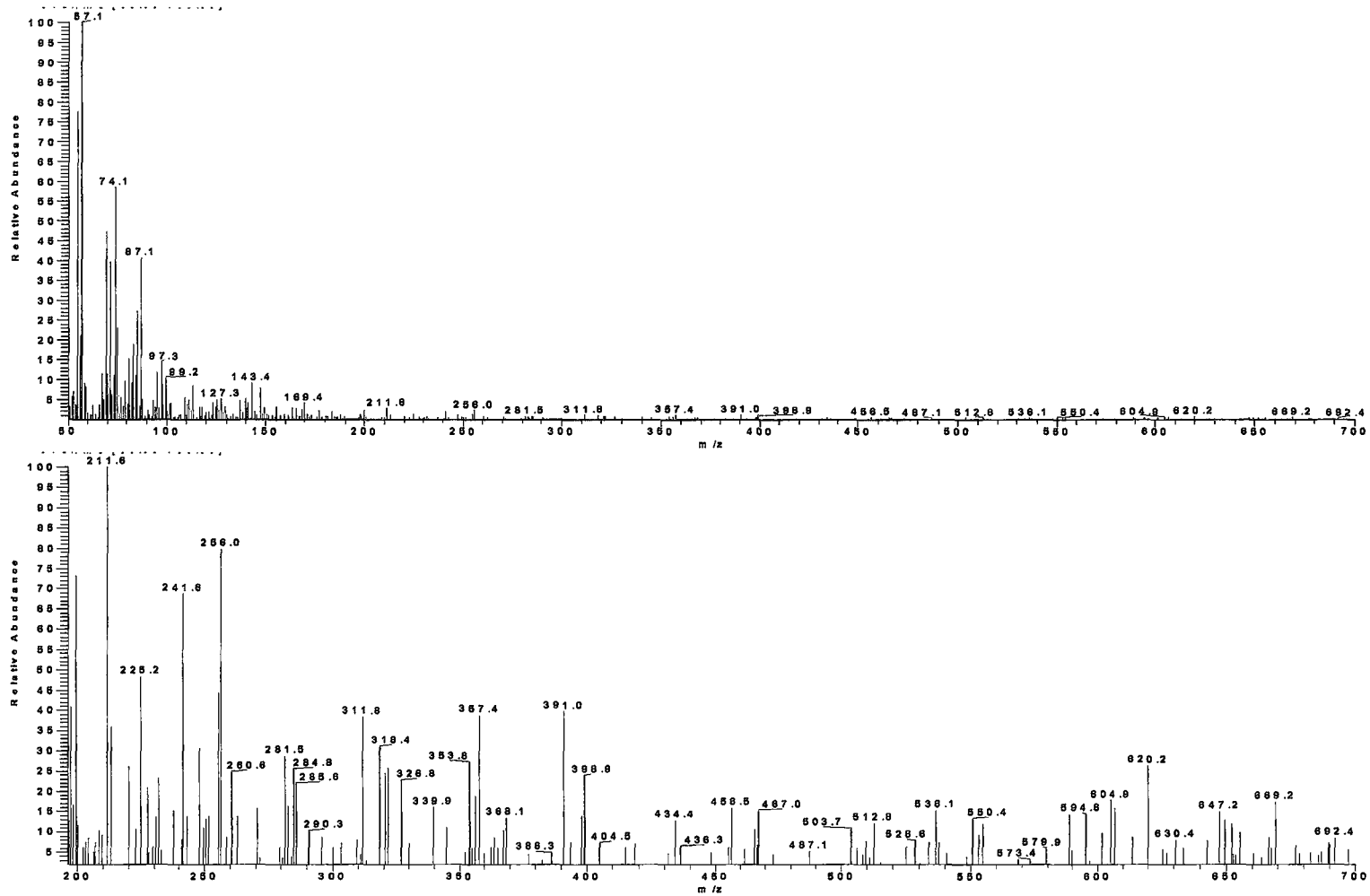

C.2 *C. albicans* strain TWAF, RT 45.88 mins (peak b in Fig. 1.13)

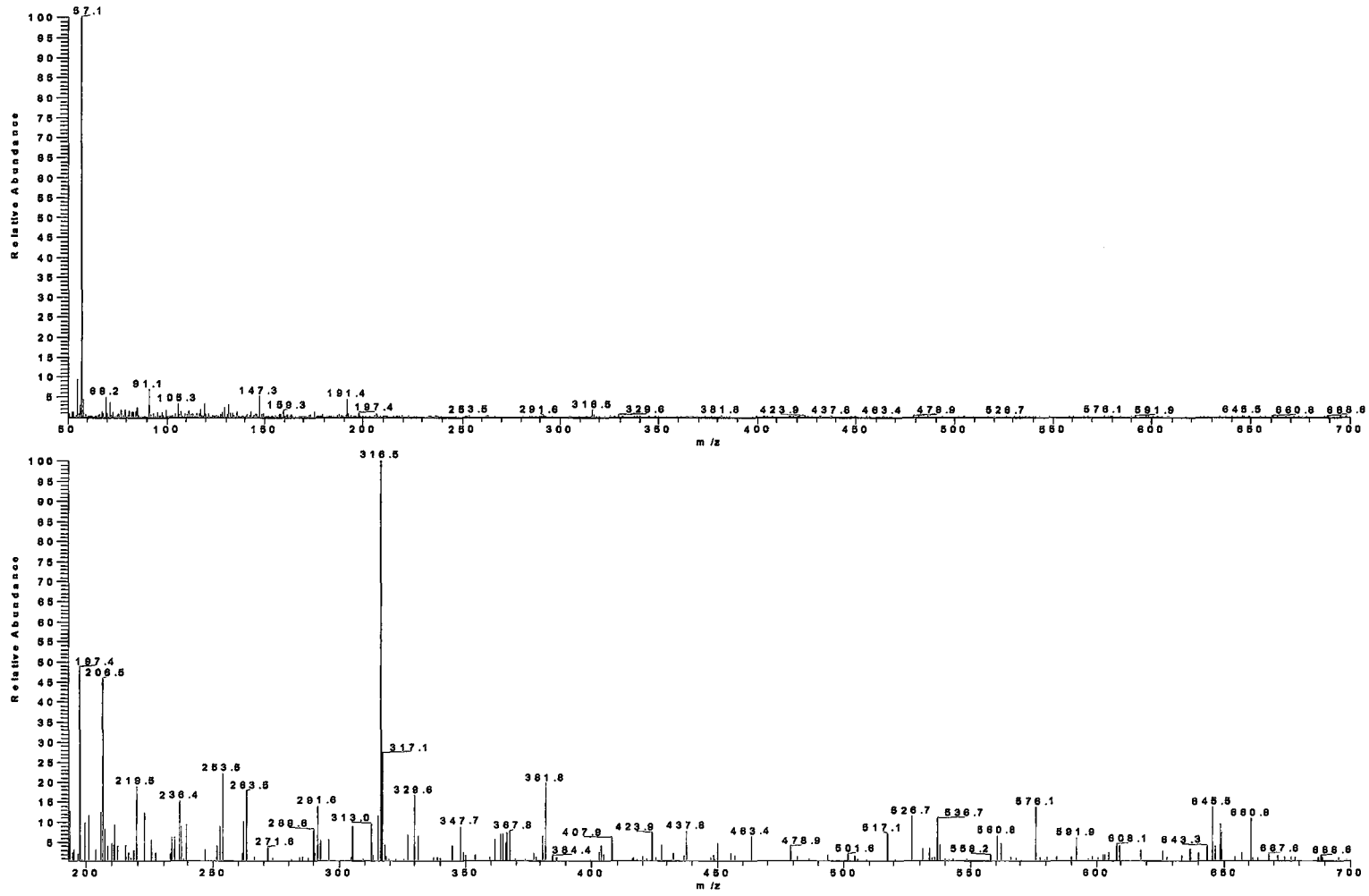

C.3 *C. albicans* strain TWAF, RT 48.19 mins (peak c in Fig. 1.13)

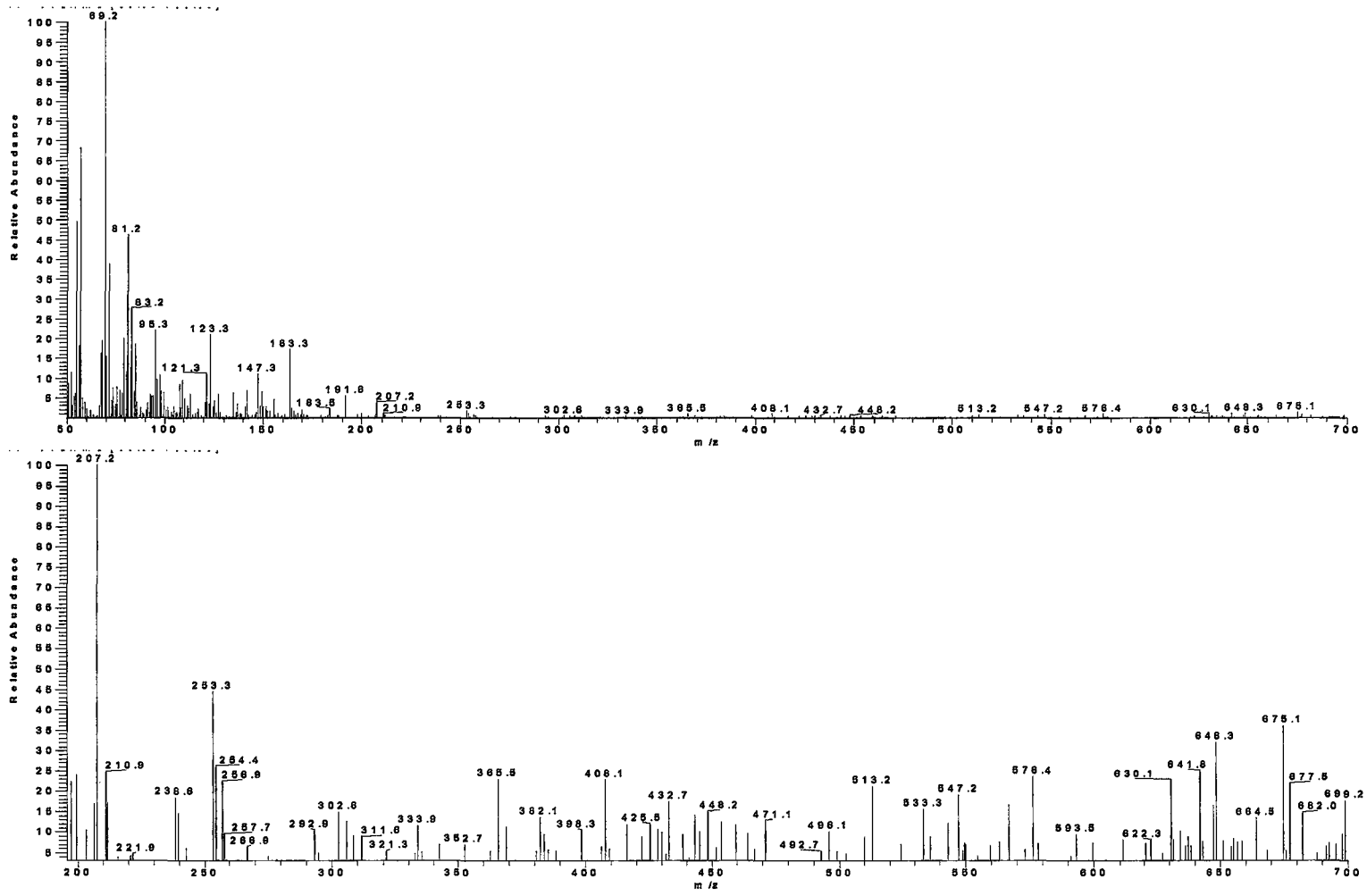

C.4 *C. albicans* strain TWAF, RT 48.38 mins (peak d in Fig. 1.13)

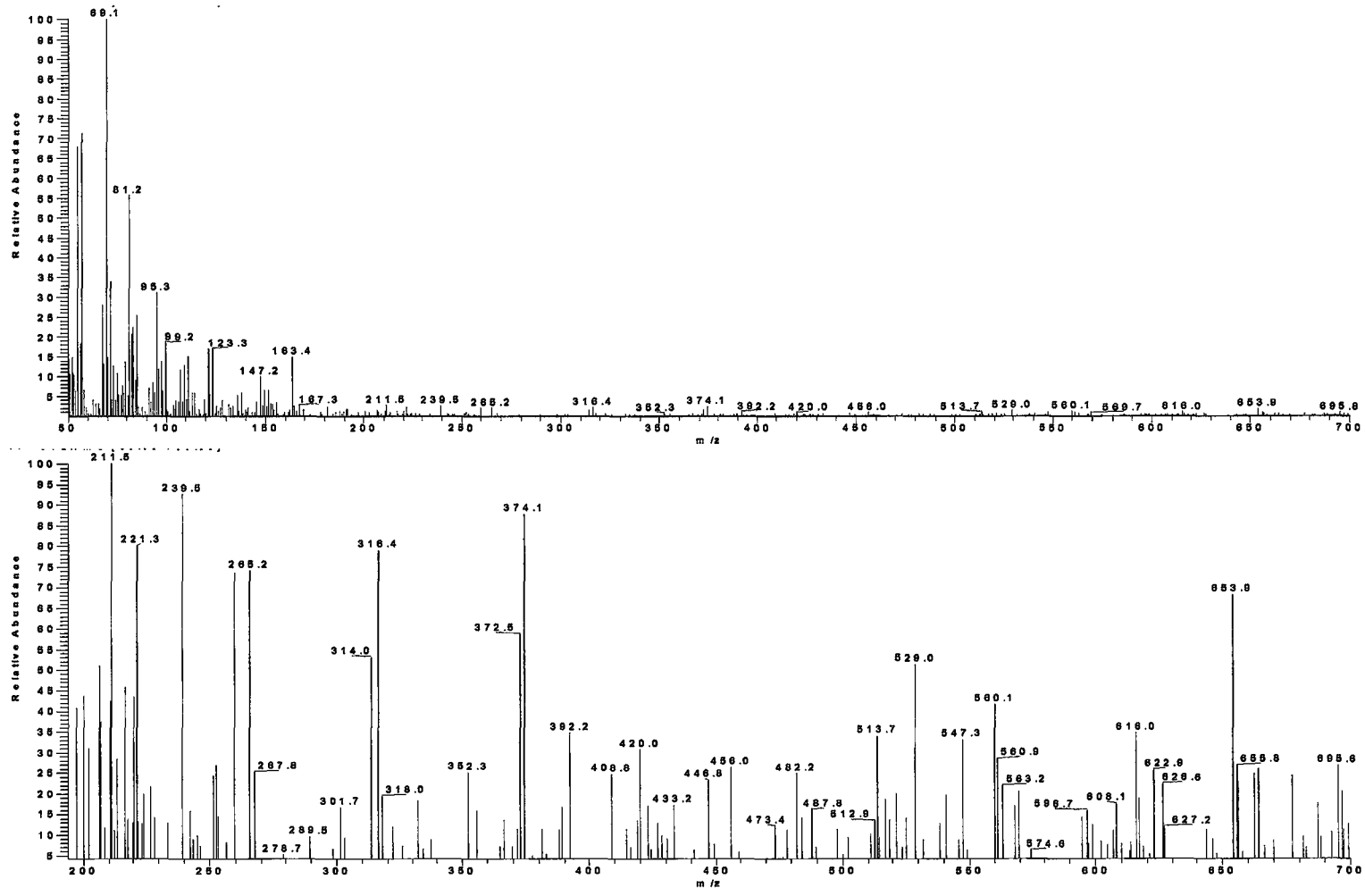

C.5 *C. albicans* strain TWAF RT 49.54 mins (peak e in Fig. 1.13)

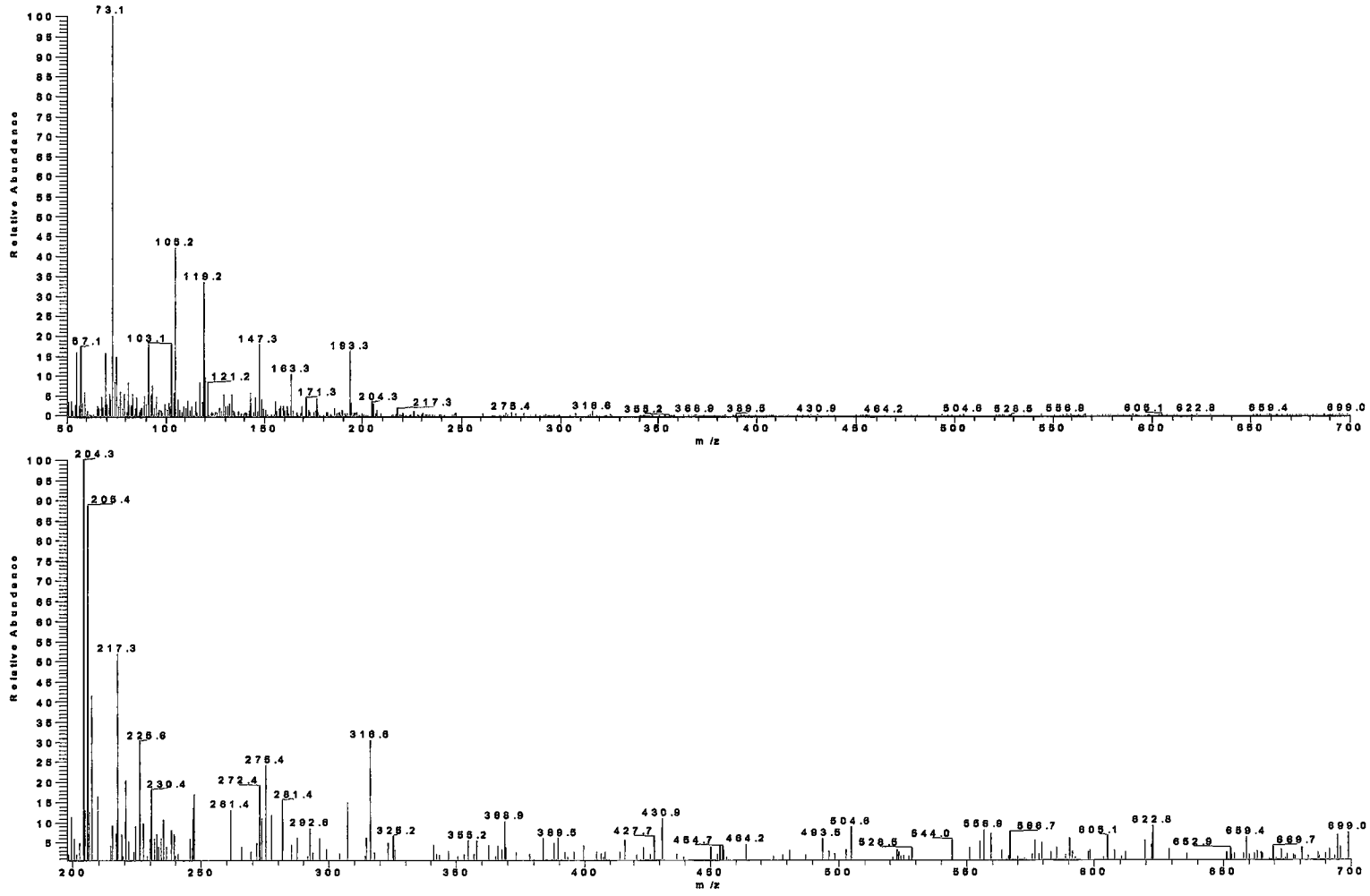

C.6 *C. albicans* strain TWAF, RT 49.78 mins (peak f in Fig. 1.13)

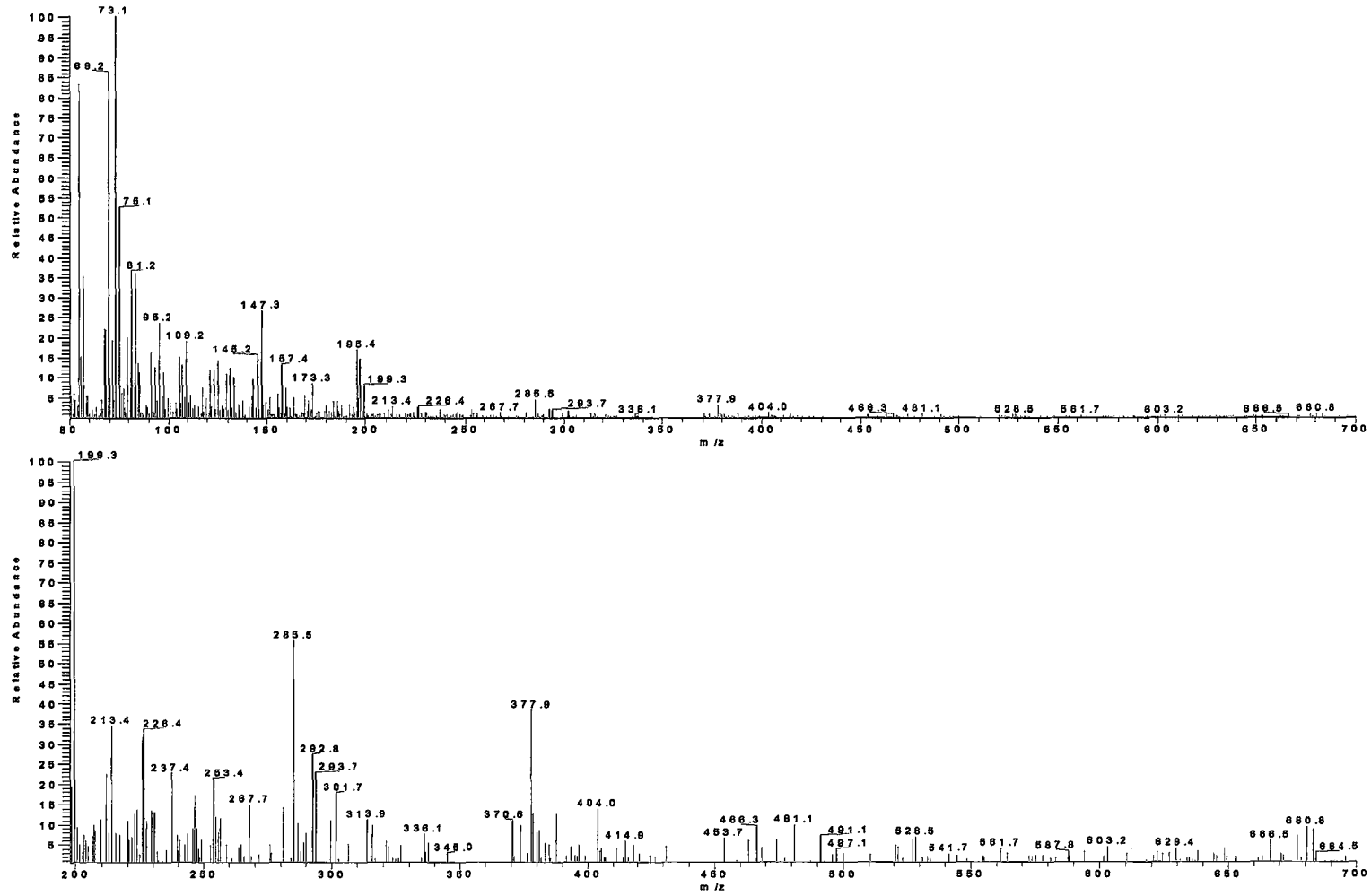

C.7 *C. albicans* strain TWAF, RT 51.19 mins (peak g in Fig. 1.13)

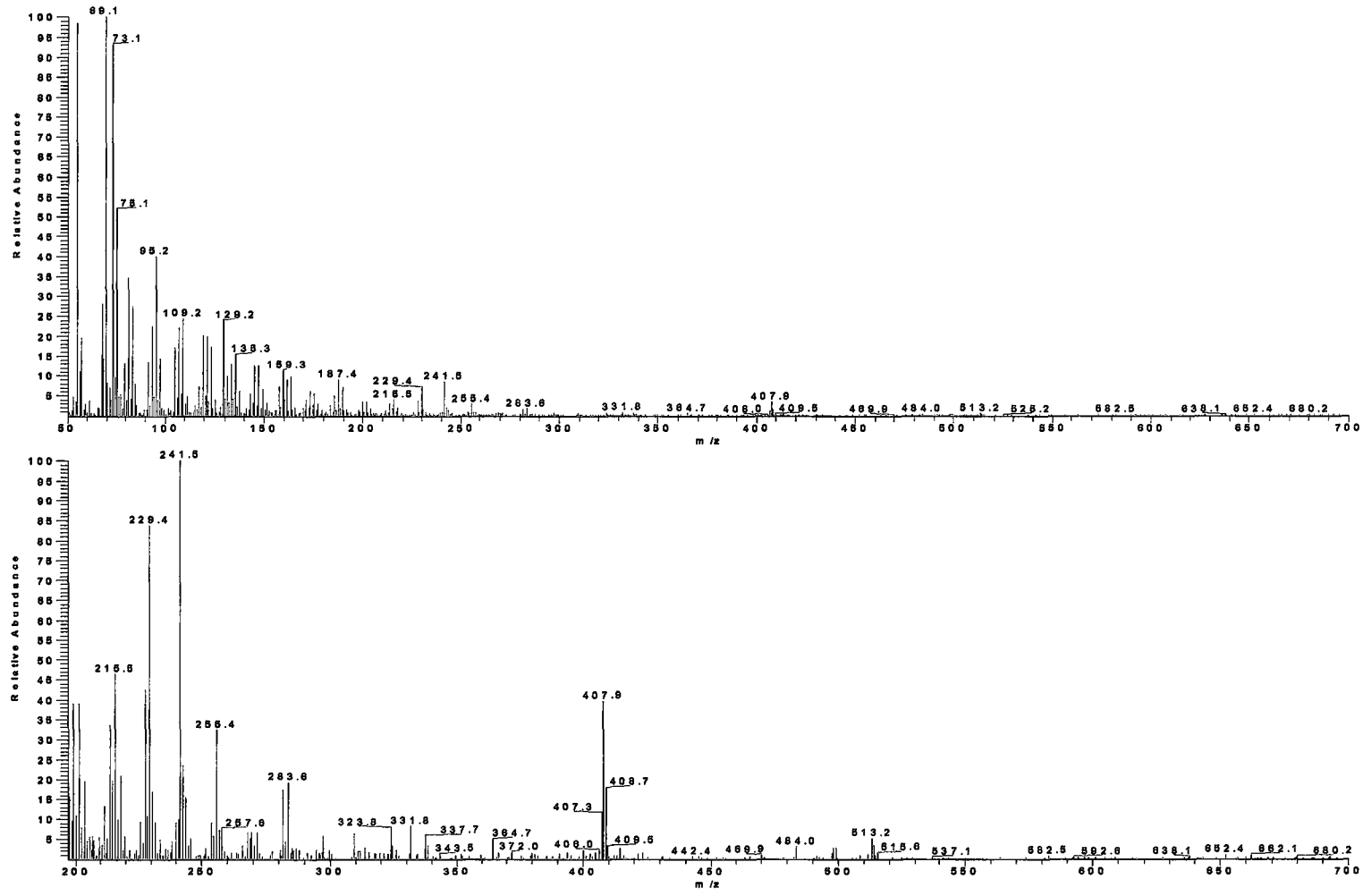

APPENDIX D – DENDROGRAMS FROM HIERARCHICAL CLUSTERING USING MGA

D.1 Hierarchical clustering of qualitative polar metabolite data for *C. albicans, C. glabrata, C. parapsilosis, C. tropicalis, C. krusei, C. neoformans* (serotype A) and *C. neoformans* (serotype D)

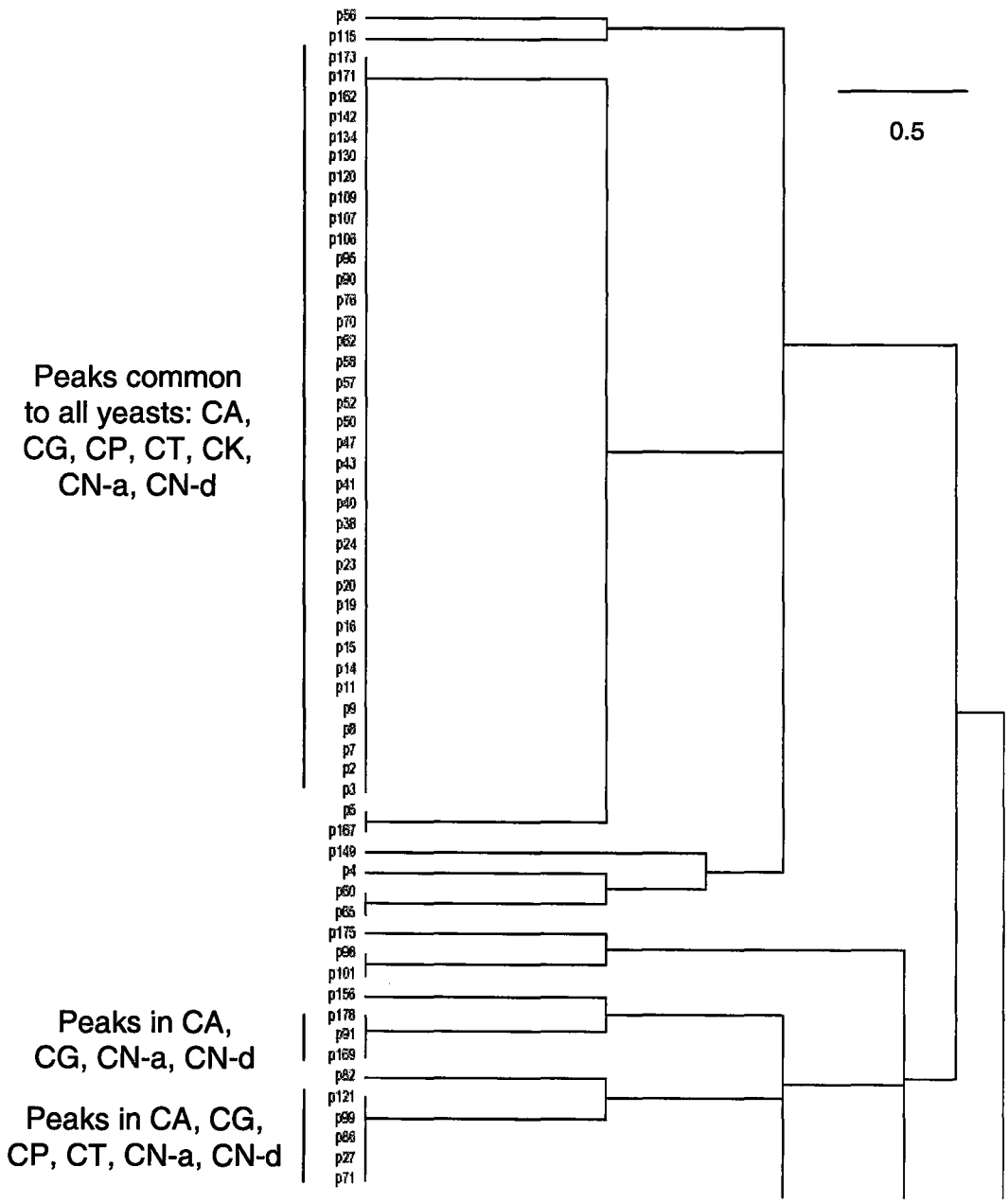

D.1 Continued

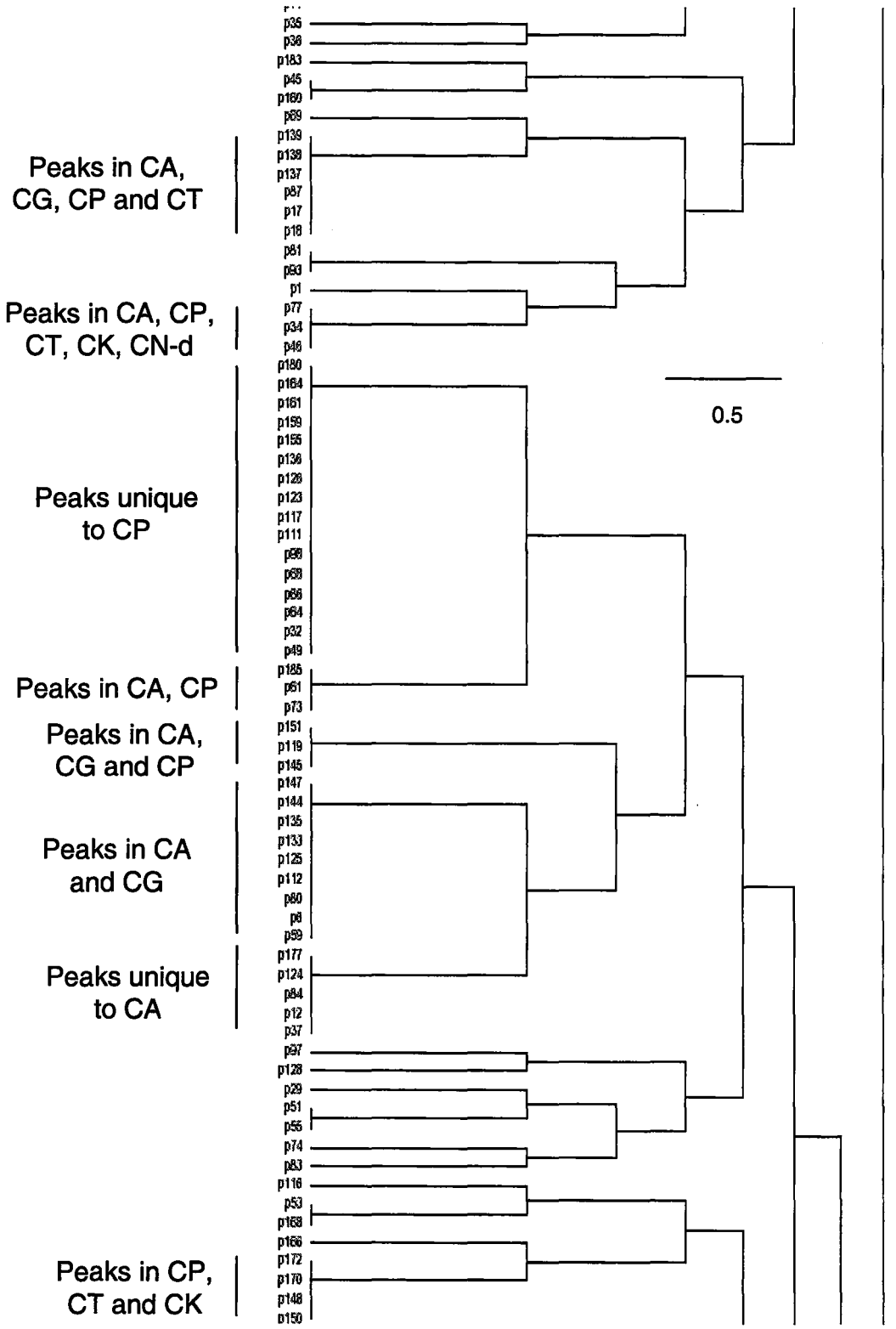

D.1 Continued

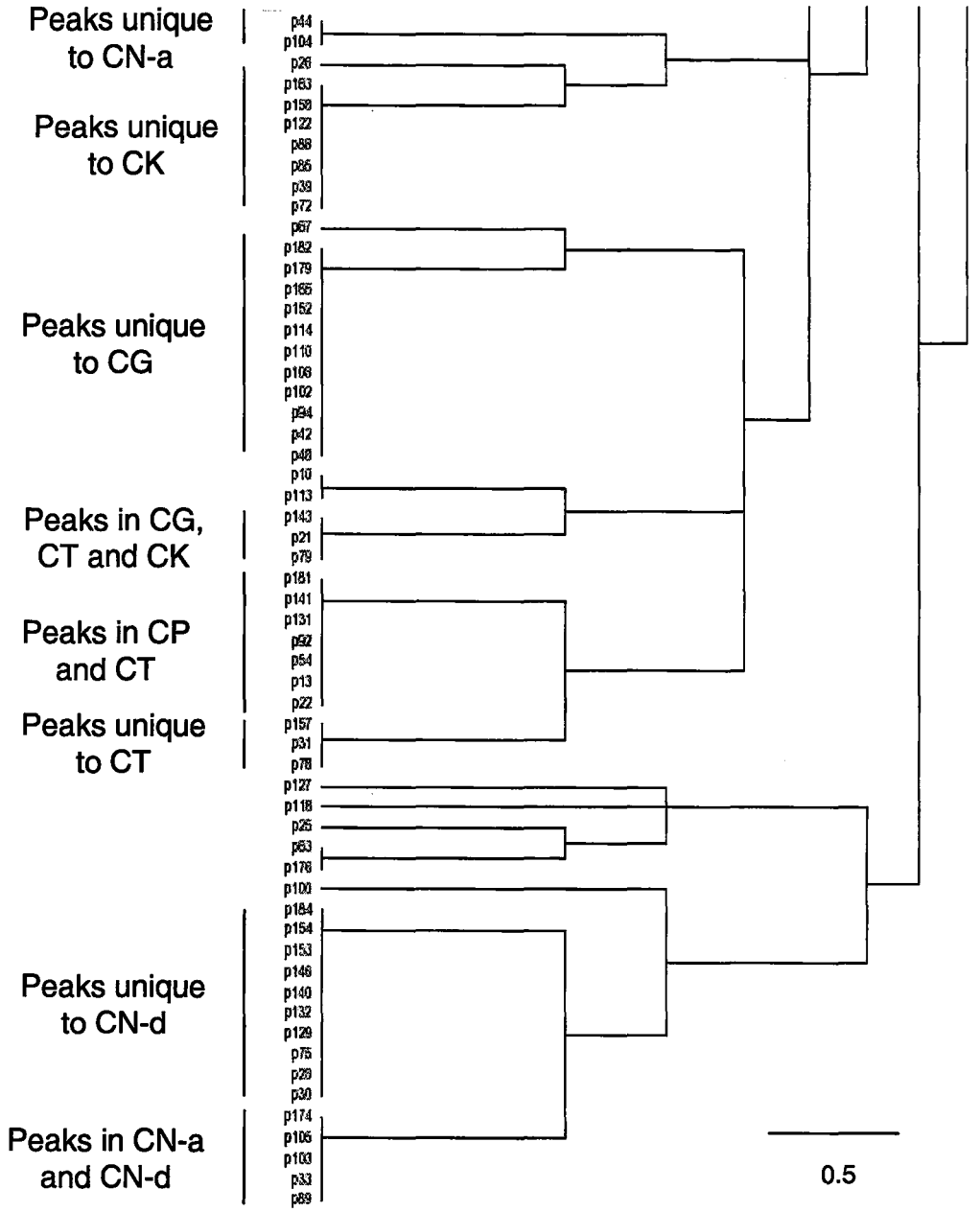

D.2 Hierarchical clustering of quantitative polar metabolite data for *C. albicans, C. glabrata, C. parapsilosis, C. tropicalis, C. krusei, C. neoformans* (serotypes A and D)

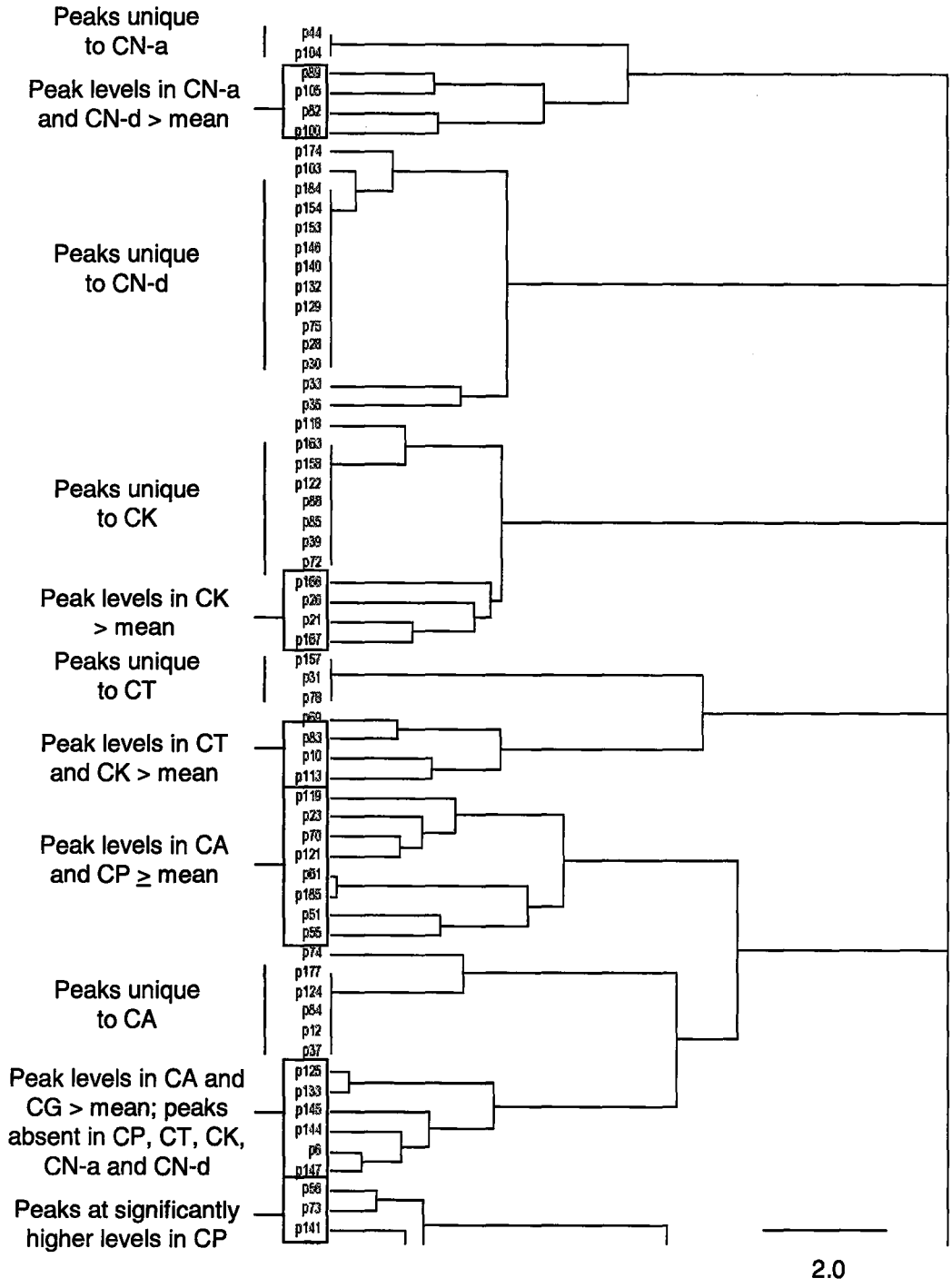

D.2 Continued

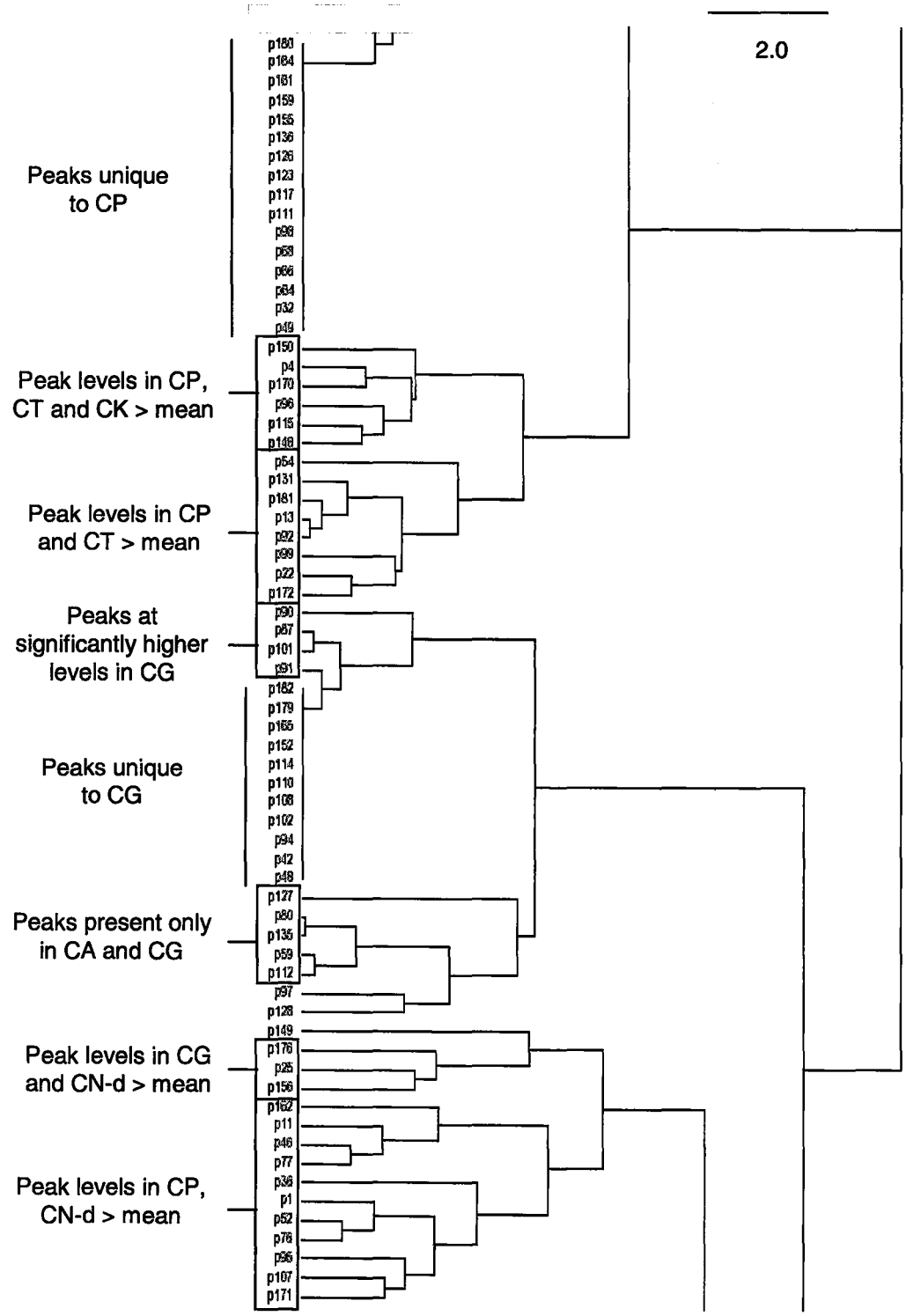

D.2 Continued

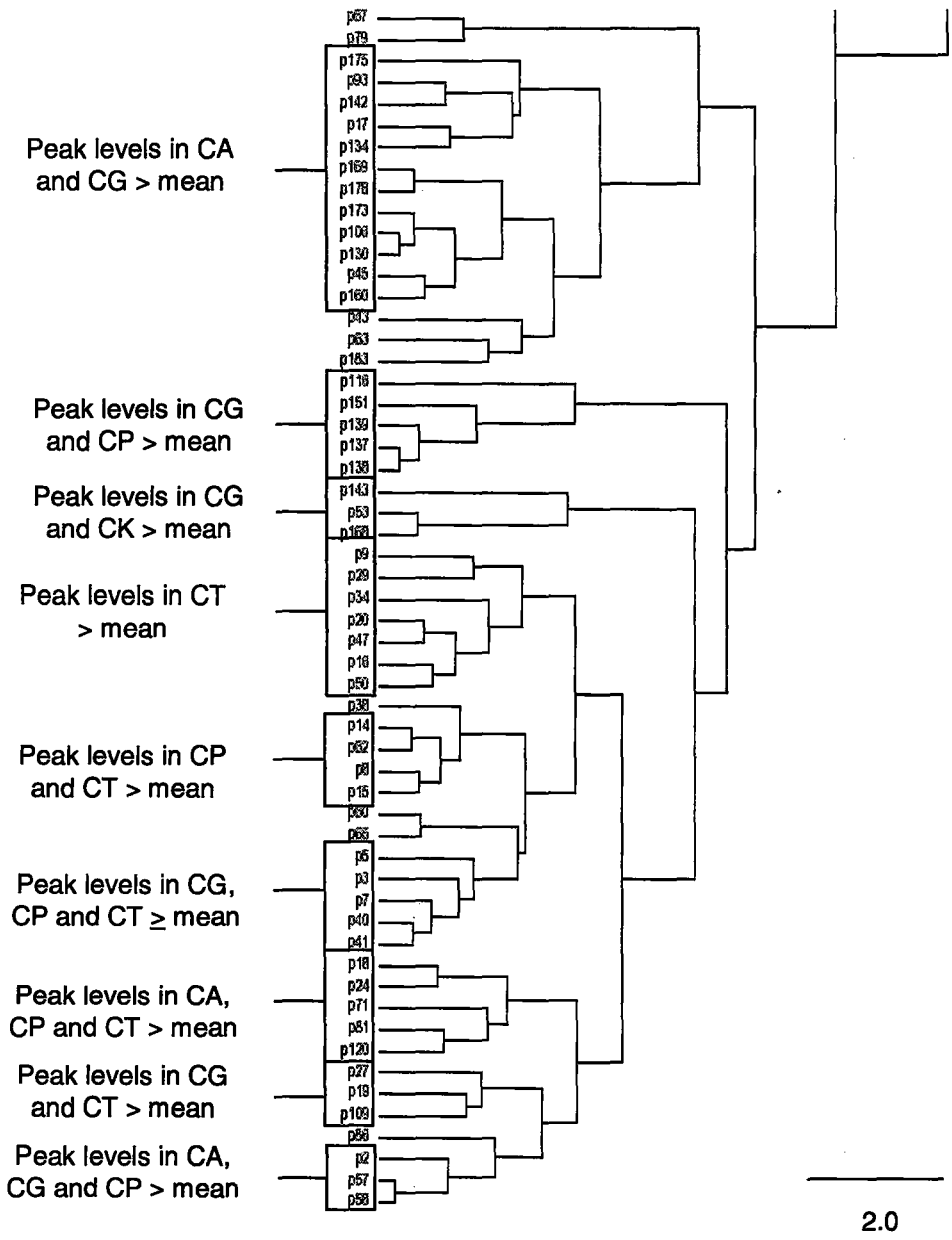

D.3 Hierarchical clustering of qualitative lipid metabolite data for *C. albicans, C. glabrata, C. parapsilosis, C. tropicalis, C. krusei* and *C. neoformans* (serotype A)

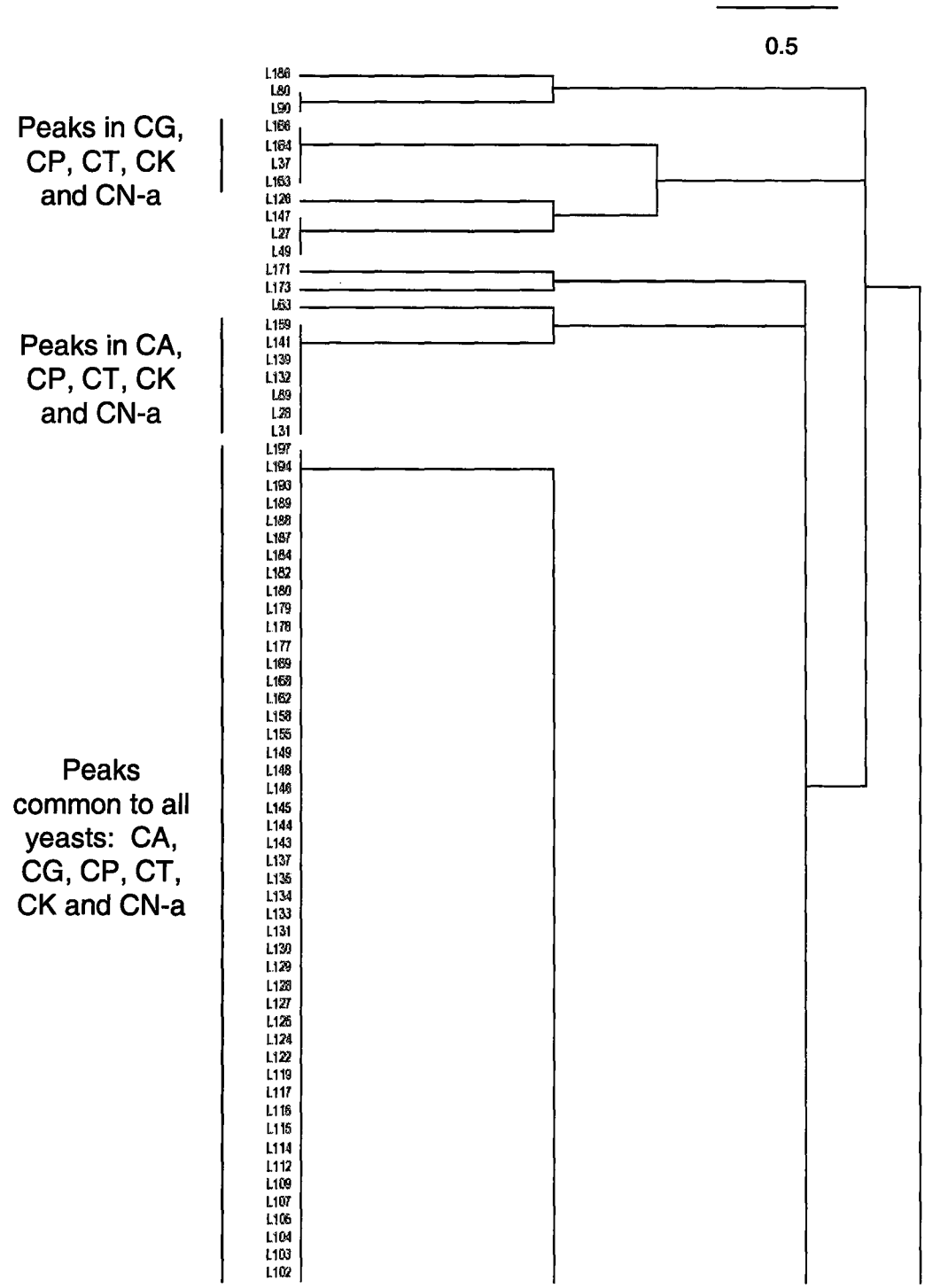

D.3 Continued

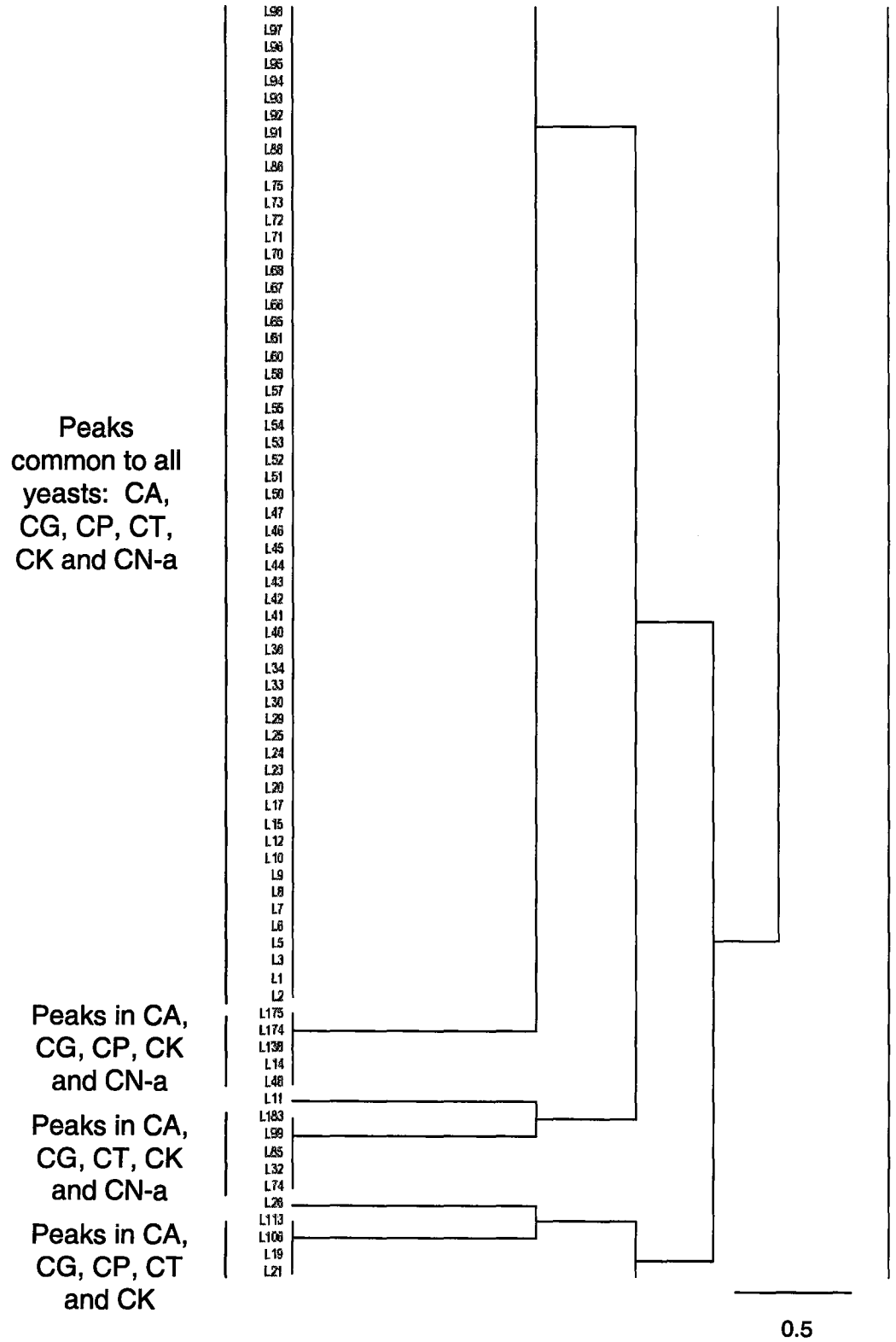

D.3 Continued